

The author(s) shown below used Federal funds provided by the U.S. Department of Justice and prepared the following final report:

**Document Title: Application of Spatial Statistics to Latent Print
Identifications: Towards Improved Forensic
Science Methodologies**

**Author(s): Stephen J. Taylor, Emma K. Dutton, Patrick R.
Aldrich, Bryan E. Dutton**

Document No.: 240590

Date Received: December 2012

Award Number: 2009-DN-BX-K228

This report has not been published by the U.S. Department of Justice. To provide better customer service, NCJRS has made this Federally-funded grant report available electronically.

**Opinions or points of view expressed are those
of the author(s) and do not necessarily reflect
the official position or policies of the U.S.
Department of Justice.**

***APPLICATION OF SPATIAL STATISTICS TO LATENT PRINT IDENTIFICATIONS:
TOWARDS IMPROVED FORENSIC SCIENCE METHODOLOGIES***

Award Number: 2009-DN-BX-K228

Final Technical Report Submitted By:

Principle Investigator: Stephen J. Taylor¹, Ph.D.
Co-Principle Investigator: Emma K. Dutton², Ph.D.
Project Director: Patrick R. Aldrich¹, M.S.
Research Analyst: Bryan E. Dutton¹, Ph.D.

¹Division of Natural Sciences and Mathematics
Western Oregon University
345 N Monmouth Ave.
Monmouth, Oregon 97361

²Oregon State Police, Forensic Services Division
255 Capitol St. N.E., 4th Floor
Salem, Oregon 97310

ABSTRACT

In 2010 we initiated a research project to address criticisms raised in a 2009 National Academy of Sciences (NAS) report regarding the presumption of fingerprint uniqueness and the reliability of latent print identifications using the ACE-V methodology (National Research Council 2009). This project addresses the question of fingerprint uniqueness (i.e., the discriminating value of the various fingerprint ridgeline features) by statistically evaluating the spatial distribution of these features. The purpose of the project was to review the latent print ACE-V comparison methodology to ascertain the fingerprint features considered during the comparison process and apply principles of spatial analyses to calculate false-match probabilities. The objectives were to spatially analyze fingerprint features (e.g., minutiae and ridge lines) using Geographic Information Systems (GIS) techniques and empirically derive probabilities to provide a quantitative measure of the discriminating value of the various ridgeline features. The resultant probabilities are applicable for subsequent qualification of latent print comparison conclusions.

Project methods included spatial pattern characterization using GIS, geometric morphometric (GM) analysis, and the calculation of false-match probabilities using Monte Carlo (MC) simulations. A data set of digitized fingerprints from the Oregon population was compiled and spatially analyzed utilizing GIS software to place minutiae and ridge line features in a common Cartesian coordinate system. The parameters of these fingerprint features, including minutiae location, direction and minutiae ridgeline configurations, were evaluated. Geometric morphometrics was used to study shape variation between and among fingerprint pattern types. GIS-based procedures were established for the selection of landmarks and semi-landmarks, the superimposition of fingerprint images, the visualization of shape change, the ordination of superimposition data, and the application of multivariate statistics. Using MC simulations, random-match probabilities were calculated to evaluate the spatial configurations of minutiae within and between pattern types to quantitatively evaluate the discriminating value of fingerprints features; that is, do two fingerprints or two regions of different fingerprints have the same spatial distribution of minutiae and ridgelines? MC simulations were performed using 3, 5, 7 and 9 minutiae with other minutiae attributes chosen for additional match criteria.

GIS results showed there was a greater density of minutiae and ridgelines below the core compared to above the core, regardless of pattern type. However, the distributions of bifurcations and ridge endings were more similar within any pattern type rather than among them. Also, pattern types with comparable ridge flow (e.g., right and left slant loops, and whorls and double loop whorls) had greater similarity between them when comparing various metrics such as axis dimensions and Thiessen polygon ratios. GM results demonstrated little shape variation among fingerprints of the same pattern type with the greatest shape variation associated with the deltas. Additional GM spatial analyses suggested a very high degree of shape consistency between left and right slant loops and between whorls and double loop whorls. MC simulations showed that the probability of random minutiae correspondence drastically decreased as the fingerprint attribute criteria (e.g., minutiae type and direction) increased. In addition, increasing the number of minutiae and fingerprint attributes applied in searches away from the core and delta regions yielded lower probabilities for a false match. However, results demonstrated that minutiae spatial distributions in regions around and below the core were not always unique.

Fingerprint characterization of ridgeline minutiae configurations and establishing random-match probabilities when using specified features quantitatively describe the discriminating value of these fingerprint ridgeline features. As such, random-match probabilities will allow the latent print examiner to qualify their comparison conclusions.

TABLE OF CONTENTS

ABSTRACT	2
TABLE OF CONTENTS	3
EXECUTIVE SUMMARY	5
CHAPTER 1 –PROJECT INTRODUCTION	14
1. INTRODUCTION	14
A. Statement of the Problem.....	14
B. Literature Review.....	14
C. Statement of Rationale.....	18
2. REFERENCES	18
CHAPTER 2 – GEOGRAPHIC INFORMATION SYSTEMS, DATA ACQUISITION AND PATTERN CHARACTERIZATION	23
1. INTRODUCTION	23
2. METHODS	23
3. RESULTS	28
4. CONCLUSIONS	32
5. REFERENCES	33
FIGURES	36
TABLES	57
CHAPTER 3 – GEOMETRIC MORPHOMETRIC ANALYSES	62
1. INTRODUCTION	62
2. METHODS	62
3. RESULTS AND CONCLUSIONS	65
4. SUMMARY	66

5. REFERENCES	67
FIGURES	68
CHAPTER 4 – FALSE-MATCH PROBABILITIES AND MONTE CARLO ANALYSES	78
1. INTRODUCTION	78
2. METHODS	80
3. RESULTS	83
4. CONCLUSIONS	84
5. REFERENCES	85
FIGURES	87
TABLES	91
CHAPTER 5 – SUMMARY	104
1. PROJECT SUMMARY	104
2. IMPLICATIONS FOR POLICY AND PRACTICE	105
3. IMPLICATIONS FOR FURTHER RESEARCH	106
4. DISSEMINATION OF RESEARCH FINDINGS	106

EXECUTIVE SUMMARY

Fingerprint comparisons used for identification of individuals based on matches of minutiae and friction ridge features between a ten-print standard and a latent print have been employed since the early 1900s (for review see: Henry 1900; Hoover 1931; Barnes 2011). Acceptance of such identifications in a court of law has been based on the premise that fingerprints do not change over the lifetime of an individual and that fingerprints are unique to every individual. Several studies have demonstrated the permanence of fingerprints (Galton 1892, Wentworth and Wilder 1932, Ashbaugh 1999, see Langenburg 2011 for a review). However, since the landmark ruling of *Daubert vs. Merrell Dow Pharmaceuticals* (1993) which set the scientific standard for the admissibility of forensic evidence, the premise of fingerprint uniqueness has had multiple challenges. Two such challenges include the *United States vs. Mitchell* (1999) and *United States vs. Brian Keith Rose* (2009), claiming that fingerprint uniqueness has not been scientifically tested or validated and that examiner accuracy (i.e., error rate) associated with latent print examiner identifications has not been determined. In addition, in February, 2009 the National Academy of Sciences (NAS) released a report, “Strengthening Forensic Science in the United States: A Path Forward” (National Research Council Committee on Identifying the Needs of the Forensic Sciences Community 2009) which was critical of the forensic science community, primarily the impression disciplines of trace, firearms and latent prints. NAS cited recommendations to improve the scientific reliability and accuracy of several forensic science methodologies, including the ACE-V procedure used for latent print comparisons. The NAS report specifically indicated, “Additionally, more research is needed regarding the discriminating value of the various ridge formations and clusters of ridge formations” (National Research Council Committee on Identifying the Needs of the Forensic Sciences Community 2009). These criticisms cited in the NAS report primarily stem from a perceived lack of statistical validation of fingerprint “uniqueness” or distinctiveness (i.e., what is the probability that fingerprint features occur in the same spatial configuration on two different fingerprints) and the subsequent lack of application of empirical statistics or probabilities to latent print comparison conclusions.

This project addresses the question of fingerprint uniqueness (i.e., the discriminating value of the various ridgeline features and sets of ridgeline features) by statistically evaluating the spatial distribution of fingerprint features and establishing probabilities that describe the spatial distribution of these fingerprint features across the whole fingerprint, as well as within regions of the fingerprint. The purpose of the project was to initially review, with latent print examiners, the latent print ACE-V comparison methodology to ascertain the fingerprint features considered during the comparison process and apply principles of spatial analyses to develop statistical certainty measures for latent print comparison conclusions. The specific objectives were to (1.) use Geographic Information Systems (GIS) spatial analysis techniques to evaluate fingerprint features or topological attributes (e.g., minutia number, type and orientation, and ridge lines), and (2.) derive probabilities that can be used for qualifying latent print comparison conclusions.

Geographic Information Systems

A Geographic Information System (GIS) is a collection of hardware and software components that integrate digital map elements with relational database functionality. GIS data are typically captured in the form of either raster grids (e.g., pixels) or vector features (i.e., points, lines, and polygons) with points referenced in space using X, Y and sometimes Z coordinate values (Price 2012). The power of a GIS is in its ability to allow users to integrate, store, edit and analyze spatial features and relationships, as well as query and display spatial information. Such systems include

traditional mapping capabilities (e.g., land surveying and aerial photography) and provide users with tools to interactively search and analyze spatial information.

GIS technology was initially developed for cartography with one of the first computerized land-management systems in Canada in 1962 (Tomlinson 1967, 1970). Since then, GIS systems have been applied in increasingly novel ways to include land use planning, environmental management, marketing, and criminology. Most recently, GIS has been used for characterizing surgical procedures (Garb et al. 2007), conducting dental EMR imaging (Wu et al. 2006) and for in neuroanatomical and anthropological research (Ungar and M'Kirera 2003, Martone et al. 2004). While GIS is widely used for crime pattern analysis and emergency management applications, (ESRI 2000, 2001; Chainey et al. 2005; Bodbyl-Mast 2009), its analytical capabilities have not been previously applied to fingerprint characterization and pattern recognition (Stanley et al. 2012).

GIS-based spatial analysis involves analyzing the positions, patterns and relationships between objects located in a defined space, similar to graph theory in discrete mathematics (Maguire et al. 2005; Smith et al. 2007). Collections of objects in a defined coordinate space may be linked or associated with one another geometrically or by functional associations. Techniques in spatial analysis include data modeling, image processing, grid algebra, surface analysis, network analysis and visualization. The GIS-based tools available for spatial analysis have grown exponentially in recent years, all driven by the practical need to understand, predict, and model relationships between objects located in space. Given that fingerprint analyses and latent print comparisons are based on spatial associations between minutiae and ridgelines (e.g., minutia patterns, ridge counts and minutiae location), GIS-based tools are a natural extension. Utilization of GIS in conducting dactylographic research is particularly appealing given that fingerprint minutiae and ridge patterns are analogous to geometries reflected in Earth surface topography, a traditional focus of GIS.

This project takes a novel approach utilizing GIS and related tools to derive spatial statistics for fingerprint patterns, with the ultimate deliverable involving the estimation of false-match probabilities that can be applied to qualify latent print comparison conclusions. The methodologies presented herein provide a framework for cataloging, characterizing and quantifying fingerprint features using custom GIS tools. An extensive set of GIS-based analytical tools were developed and have yielded valuable results that aid in the quantification of fingerprint characteristics and spatial distribution of minutiae and ridge lines in georeferenced coordinate space. The analytical tools are very robust and provide firm foundation upon which to derive probabilities which describe the discriminating value of these fingerprint features.

The primary results of the GIS-based spatial characterization component of the study are summarized as follows:

- (1) Techniques in Geographic Information Systems can be employed to spatially analyze fingerprint patterns;
- (2) The standardized georeference system developed for this study provides a standardized coordinate system that allows complex analysis of minutiae and ridgeline distributions across fingerprint space;
- (3) A wide variety of spatial analysis tools can be developed in the GIS software environment to characterize fingerprint features and statistically characterize distributions between pattern types;
- (4) A robust sample set of over 1200 fingerprints, 102,000 minutiae and 20,000 ridge lines were digitally captured from the Oregon population as part of this project effort;

- (5) The average number of minutiae per fingerprint is 85.1, with ridge endings outnumbering bifurcations by a factor of 1.4;
- (6) Minutiae and ridge lines are most densely packed in the region below the core, with the greatest ridge line-length density surrounding the core;
- (7) More complex ridge patterns with higher degrees of line curvature (e.g., whorls and double loop whorls) are associated with a greater number of minutiae as compared to more streamlined patterns (e.g., arches).

GIS methodologies and standardized georeferencing allowed for the placement of fingerprint features within a common coordinate space. Once fingers were aligned in a common coordinate space, the spatial analyses were conducted to characterize pattern types, minutiae distributions and ridge line configurations. Overall, there was a greater density of minutiae and ridgelines below the core than above, regardless of pattern type. However, the distributions of bifurcations and ridge endings were more similar within any pattern type rather than among them. Also, similar pattern types (e.g., loops and whorls) tend to have greater similarity between them when comparing various metrics such as hull axis ratios and Thiessen polygon ratios, suggesting that these patterns arise through similar biological phenomena.

As latent examiners have observed, fingerprint minutiae distributions are neither uniform nor do they appear to be random. Furthermore, when taking into account the greater number of ridges in the lower region of the fingerprint, as compared with the upper, it does not explain the differential distribution of minutiae across the fingerprint. It appears that the more complex the ridge pattern type (e.g., double loop whorls vs. arches), the greater number of minutiae present on the finger. The spatial variation between the upper and lower regions of the fingerprint also implies that this minutiae differential is influenced by complexity of pattern associated with deltas and other disruptions in ridge flow. Conversely, the upper regions of the finger have a relatively uniform flow of ridgelines with simpler line geometries. Thus, the more complex pattern types (e.g. whorls and double loop whorls) tend to be similar to each other, are associated with larger pattern dimensions, and significantly differ from all other pattern types. The less complex pattern types, as exemplified by arches, tend to display fingerprint metrics at the other end of the scale.

Geometric Morphometric Analyses

Research on the spatial relationship of fingerprint features, (e.g., minutiae and ridge lines) and the application of this information to automatic fingerprint identification systems have historically employed biometric techniques. These methods generally involve analyzing linear geometrical properties of the fingerprint physical characteristics (e.g., the distances between minutiae and the geometric pattern formed). While biometric techniques are an invaluable tool for exploring covariance among sets of geometric comparators, these techniques ignore the biomathematical aspects of the original measurements (Bookstein 1996). These biomathematical aspects include inherent biological properties (e.g., homology and embryology) of biological features (i.e., minutiae) that can be represented by their spatial arrangements. Furthermore, failure to consider these aspects when analyzing minutiae may exclude important spatial patterns that are dictated by underlying embryological and evolutionary cues.

As a biomathematical modeling method, geometric morphometrics utilizes biologically-based features (i.e., homologies) that are useful for quantitatively studying shape variation and is what distinguishes it from biometric approaches. Geometric morphometrics includes techniques from statistics, non-Euclidean geometry, multivariate biometrics and computer graphics that do not sacrifice biomathematical aspects (Bookstein 1996).

Within the forensic science community, forensic anthropology has led the way in exploring the applicability of geometric morphometric techniques. Examples include analyzing mandibular morphology (Franklin et al. 2007, Franklin et al. 2008) and craniofacial landmarks (Kimmerle et al. 2008), studying frontal sinus radiography methods for making identifications (Christensen 2005), creating a virtual 3-D reconstruction of a fragmented cranium (Benazzi et al. 2009), and estimating pediatric skeletal age (Braga and Treil 2007). However, to date, there has been very little exploration of the use of geometric morphometric techniques for the study of fingerprint shape variation.

For this project, geometric morphometric analyses were employed to study shape variation of four fingerprint pattern types in an effort to ascertain the extent and degree of variation within and among fingerprint patterns. These analyses were conducted utilizing GIS spatial analysis tools described in Chapter 2 as it minimized data manipulation and increased the overall efficiency of spatial analyses.

Tasks completed include: 1) establishing a methodology for conducting geometric morphometric analyses on fingerprints in a GIS environment in combination with Python programming language and R statistical software (version 2.15.0), and 2) completing an initial analysis of shape variation on four fingerprint patterns [(A) left slant loops (B) right slant loops, (C) whorls, and (D) double loop whorls] using generalized Procrustes analysis, thin plate spline and principle components analysis. The resulting data were used to characterize the shape of four fingerprint pattern types and describe the foundational shape variation within and among these pattern types, specifically:

- (1) Generalized Procrustes Analysis (GPA) showed that there was little shape variation in the innermost core ridgeline (a feature used in our comparison of patterns types) in left and right slant loops and whorls and double loop whorls. In addition, the greater variation in the continuous ridge line (features used in our comparison of patterns types) is due to variation in the size and possible rotational effects of each of the original fingerprint images in coordinate space.
- (2) Thin-Plate Spline (TPS) showed that the greater the deformation in any given area of the TPS grid, the more shape variation there is between the pattern types in those particular regions. These results indicate a very high degree of shape consistency between left and right slant loops with the greatest degree of shape variation in the delta region. The greatest degree of shape variation was likewise found in the two delta regions of whorls and double loop whorls.
- (3) Principle Components Analysis (PCA) showed that the direction of variation is consistent between loop patterns in the first principle component (PC) with approximately 43% and 37% of the shape variation being accounted for left and right slant loops, respectively. While variation is consistent in the following two PCs, the direction of the variation is different for left and right slant loops. The greatest amount of shape variation occurs in the delta regions. This can be seen for all three PCs. The extent and pattern of variation is also similar for whorls and double loop whorls with the greatest degree of shape variation occurring in the delta regions.

Utilizing geometric morphometrics, in conjunction with a GIS tools, represents a novel approach for evaluating and quantifying spatial relationships among friction ridgeline features (i.e., minutiae). The impacts of this work include an increase in forensic science knowledge and understanding of the

spatial patterns of friction skin minutiae. Additionally, there will be direct implications for quantifying another element of potential variance associated with estimating probabilities for describing the discriminating value of fingerprint features, especially when the probabilities are based on ten-print standards. This is the first empirical study that quantifies fingerprint shape variation utilizing geometric morphometric methods for latent print comparison purposes, which in turn, could have implications for the latent print comparison process and practice.

False-Match Probabilities and Monte Carlo Simulations

The Monte Carlo (MC) method is a computer algorithm used to repeatedly resample data from a given population to make inferences about stochastic processes. The Monte Carlo method is one of the optimal ways to quantify rare events that have correspondingly low probabilities of occurrence. Because of the rare nature of these events, it is extremely difficult to evaluate them using typical analytical means. The goal of a MC simulation is to produce an expected result, $\mu = E(X)$, where X is a random variable. The Monte Carlo simulation creates n independent samples of X , and as n increases towards infinity, the average of the n independent samples ($1/n \sum_{i=1}^n x_i$) moves towards μ (Rubinstein and Kroese 2007), thus, producing a very large number of independent samples which allows for the detection of rare events and for the estimation of the probability of occurrence.

The MC method has been used in a variety of fields to analyze rare events. Lin and Wen (2010) used MC simulations, specifically Markov Chain Monte Carlo simulations, in the analysis of natural disasters. They studied the occurrence of large debris flows such as landslides and floods, to help determine the placement of villages to reduce the destruction caused by these phenomena. The MC simulations were used to determine where disastrous debris flows would most likely occur, and help plan where villages would be built in areas of China. In community ecology, MC methods have been employed to study the robustness of species diversity indices (Ricklefs and Lau 1980; Manly 2006). In addition, it is commonly used in the estimation of phylogenies when studying evolution (Bouchard-Côté et al. 2012). The MC method has also been used to study the frequency in which airplanes pass within close proximity to each other (Paielli and Erzberger 1996). The authors used the MC probabilities to make inferences and suggestions on how to reduce the possibility of close proximity flights. While this is not an exhaustive review, it demonstrates that this statistical method has been used in a wide variety of disciplines to make inferences about phenomena that are either rare or difficult to analytically quantify.

In the case of fingerprints, for the last century Latent Print Examiners have emphatically avowed that fingerprints are unique with no two fingers, on the same individual or on different individuals, including identical twins, possessing the same fingerprint characteristics when considering all levels of detail (i.e., pattern, type, minutiae, ridgelines, pores). Biologically, there is a basis for this premise of uniqueness due to genetic and epigenetic factors that play a role in fingerprint development. However, statistically, there is always a minute chance that an exact replica of any given fingerprint could exist somewhere in the world. The probability or likelihood that an exact replica of a fingerprint exists somewhere in the world can be, and has been, theoretically and empirically calculated. For examples, see Champod and Margot 1996; Dass et al. 2005; Srihari 2009; Neumann et al., 2012. See Langenburg (2011) for a review of individuality probability models proposed from 1892 to 2001. Most latent prints, however, are typically only a portion of the entire fingerprint; thus, the question becomes, what is the likelihood or probability that an exact replica of a region of any given fingerprint exists in the world. That is, are all regions of a fingerprint unique?

The employment of the Monte Carlo method, as supported by the literature, is an efficacious method for the creation of probabilities associated with minutiae pattern similarities. The MC

method employed in this study is a naïve Monte Carlo, meaning that there are no assumptions built into the simulations, and Markov Chains were not employed in creating the distributions. Thus, this is an empirical, “brute force” approach to estimate probabilities describing fingerprint similarities. The MC method produces probabilities associated with the spatial patterns of fingerprint attributes (minutiae and ridgelines), and are foundational probabilities which quantify the discriminating value of these various ridgeline features. As such, these probabilities can be employed during the comparison process to qualify the comparison conclusion.

The probabilities of a false match generated by the Monte Carlo simulations demonstrate that even with very little information, if the number of minutiae used is sufficiently large, the probability of finding a similar minutiae pattern is quite rare. For example, in MC1, where the only information considered is the location of the minutiae in X-Y coordinate space, the probability of a false match decreases 100 fold when the number of minutiae is increased by two, such as five selected versus three selected. This demonstrates that increasing the number of minutiae selected drastically impacts that probability of finding a similar minutiae pattern. In addition, the area where the minutiae are selected also changes the probability of a false match, with the upper regions of a finger having lower probabilities of a false match than regions below or near the core. As one would expect, the greater number of minutiae below the core allows for a greater chance of having similar patterns exist in that region.

Adding multiple layers of attribute information to the MC simulation made it more restrictive and thus, more difficult to find false matches in the sample set. However, the probability of a false match is not drastically different either among pattern types or when the searches were performed within pattern type. The Monte Carlo simulations had difficulty finding any false matches with seven or nine minutiae, with only a single match identified when selecting nine minutiae and considering X-Y minutiae coordinates only. This indicates that the probability of a false match is extremely low when nine minutiae are selected. It must be stressed that zeroes do not mean that there is no probability of a false match. Because the denominators of the probabilities are inherently associated with the number of fingerprints in the database, these results suggest that the database, while large, was not of sufficient size for finding false matches using the MC parameters selected.

These analyses demonstrate that the database was not of sufficient size to produce probabilities with a greater number of minutiae. Thus, increasing the database size would allow for the finding of fingerprints with similar patterns of nine minutiae and higher. In addition, adding ridge counts as a parameter in the Monte Carlo simulations would also add one more parameter that is used by examiners in fingerprint identification. The drawback to including these parameters is that both vectorization of ridge lines (to allow for ridge counting) and the preparation of fingerprints is very time consuming. In addition, if the database is increased 10 to 100 fold, to about 100,000 fingerprints, the Monte Carlo simulations will need to be altered because the naïve Monte Carlo method employed is computationally time consuming. The employment of parallel Markov Chain Monte Carlo methods, or conditional Monte Carlo methods, would need to be implemented to allow for the production of data in a relatively quick timeframe. Also, simulations that perform a modified Markov Chain Monte Carlo associated with a nearest neighbor approach will allow the simulations to be more similar to the way latent print examiners search target groups of minutiae on fingerprints. These additional procedures will produce probabilities that are more closely associated with all the data used by examiners when performing latent print comparisons.

REFERENCES

- Ashbaugh, D. R. 1999. Quantitative-qualitative friction ridge analysis: An introduction to basic and advanced ridgeology. V. J. Geberth, editor. CRC Press LLC, Boca Raton, Florida.
- Barnes, J. G. 2011. History, *in* The Fingerprint Sourcebook. A. McRoberts, editor. National Institute of Justice, Washington D.C. Ch.1, pp. 1-22.
- Benazzi, S., E. Stansfield, C. Milani, and G. Gruppioni. 2009. Geometric morphometric methods for three-dimensional virtual reconstruction of a fragmented cranium: The case of Angelo Poliziano. *International Journal of Legal Medicine* **123**:333-344.
- Bodbyl-Mast, A. 2009. Enhancing the law enforcement workflow: Server GIS app supports analysis, resource management and communication. *ArcUser Magazine*, Winter Edition:20-21.
- Bookstein, F. L. 1996. Biometrics, biomathematics and the morphometric synthesis. *Bulletin of Mathematical Biology* **58**:313-365.
- Bouchard-Côté, A., S. Sankararaman, and M. I. Jordan. 2012. Phylogenetic Inference via Sequential Monte Carlo. *Systematic Biology*.
- Braga, J. and J. Treil. 2007. Estimation of pediatric skeletal age using geometric morphometrics and three-dimensional cranial size changes. *International Journal of Legal Medicine* **121**:439-443.
- Chainey, S. and J. Ratcliffe. 2005. *GIS and Crime Mapping*. John Wiley & Sons Ltd, Hoboken, New Jersey.
- Champod, C. and P. A. Margot. 1996. Computer assisted analysis of minutiae occurrences on fingerprints. pp. 305-318, *in* Proceedings of the International Symposium on Fingerprint Detection and Identification. J. Almog, E. Springer, M. Yisrael, eds., Israel National Police, Neurim, Israel.
- Christensen, A. M. 2005. Testing the reliability of frontal sinuses in positive identification. *Journal of Forensic Sciences* **50**:18-22.
- Dass, S. C., Y. Zhu, and A. K. Jain. 2005. Statistical models for assessing the individuality of fingerprints, *in* Fourth IEEE Workshop on Automatic Identification Advanced Technologies, Buffalo, New York, pp. 3-9, IEEE Computer Society.
- Daubert vs. Merrell Dow Pharmaceuticals. 509 US 579. 1993.
- ESRI. 2000. Risk analysis and response - GIS and public safety. *ArcUser Magazine*, January-March Edition.
- ESRI. 2001. GIS aids emergency response. *ArcUser Magazine*, July-September Edition.
- Franklin, D., P. O'Higgins, and C. E. Oxnard. 2008. Sexual dimorphism in the mandible of indigenous South Africans: A geometric morphometric approach. *South African Journal of Science* **104**:101-106.

- Franklin, D., C. E. Oxnard, P. O'Higgins, and I. Dadour. 2007. Sexual dimorphism in the subadult mandible: Quantification using geometric morphometrics. *Journal of Forensic Sciences* 52:6-10.
- Galton, F. 1892. *Fingerprints*. Macmillan and Co., London, England.
- Garb, J., S. Ganai, R. Skinner, C. S. Boyd, and R. B. Wait. 2007. Using GIS for spatial analysis of rectal lesions in the human body. *International Journal of Health Geographics* 6:11-24.
- Henry, E. R. 1900. *Classification and Uses of Fingerprints*. Routledge & Sons, London, England.
- Hoover, J. E. 1931. Criminal identification. *The American Journal of Police Science* 2:8-19.
- Kimmerle, E. H., A. Ross, and D. E. Slice. 2008. Sexual dimorphism in America: Geometric morphometric analysis of the craniofacial region. *Journal of Forensic Sciences* 53:54-57.
- Langenburg, G. 2011. Scientific research supporting the foundations of friction ridge examinations, *in* *The Fingerprint Sourcebook*. A. McRoberts, editor. National Institute of Justice, Washington D.C. Ch. 14, pp.1-31.
- Lin, Y.-C. and K.-C. Wen. 2010. A simulation assessment by using Monte Carlo method on the risk of debris flow disaster in urban areas. *Asia GIS 2010 International Conference*, Kaohsiung, Taiwan.
- Maguire, D. J., M. Batty, and M. F. Goodchild. 2005. *GIS, Spatial Analysis and Modeling*. ESRI Press, Redlands, CA.
- Manly, B. F. J. 2006. *Randomization, Bootstrap and Monte Carlo Methods in Biology*. 3rd. edition. C. Chatfield, J. Zidek, eds. Chapman & Hall/CRC, United States.
- Martone, M. E., A. Gupta, and M. H. Ellisman. 2004. e-Neuroscience: challenges and triumphs in integrating distributed data from molecules to brains. *Nature Neuroscience* 7:467-472.
- National Research Council Committee on Identifying the Needs of the Forensic Sciences Community. 2009. *Strengthening forensic science in the United States: A path forward*. The National Academies Press, Washington D.C.
- Neumann, C., I. W. Evett, and J. Skerrett. 2012. Quantifying the weight of evidence from a forensic fingerprint comparison: A new paradigm. *Journal of the Royal Statistical Society, Series A (Statistics in Society)* 175:371-415.
- Paielli, R. A. and H. Erzberger. 1996. *Conflict probability estimation for free flight*. Ames Research Center, Moffett Field, CA.
- Price, M. 2012. *Mastering ArcGIS. Fifth Edition*. McGraw Hill, Boston, Massachusetts.
- Ricklefs, R. E. and M. Lau. 1980. Bias and Dispersion of Overlap Indices: Results of Some Monte Carlo Simulations. *Ecology* 61:1019-1024.
- Rubinstein, R. and D. P. Kroese. 2007. *Simulation and the Monte Carlo Method*. Second edition. John Wiley and Sons, Inc., Hoboken, New Jersey.

- Smith, M., M. F. Goodchild, and P. A. Longley. 2007. *Geospatial Analysis - A Comprehensive Guide to Principles, Techniques and Software Tools*. Winchelsea Press, Leicester, England.
- Srihari, S. N. 2009. Quantitative assessment of the individuality of friction ridge patterns. Research report, University at Buffalo, State University of New York, Buffalo, New York.
- Stanley, R. J., E. K. Dutton, S. B. Taylor, P. Aldrich, and B. E. Dutton. 2012. Geographic information systems and spatial analysis - Part 1: Quantifying fingerprint patterns and minutiae distributions. AAFS 64th Annual Scientific Meeting, Atlanta, Georgia.
- Tomlinson, R. F. 1967. An introduction to the Geo-information system of the Canada Land Inventory. ARDA, Canada Land Inventory, Dept. of Forestry and Rural Development, Ottawa, Canada.
- Tomlinson, R. F. 1970. Computer-based Geographical Data Handling Methods. *in* *New Possibilities and Techniques for Land Use and Related Surveys*. I. H. Cox, editor. Geographical Publications Ltd., Berkhamsted, England.
- Ungar, P. S. and F. M'Kirera. 2003. A solution to the worn tooth conundrum in primate functional anatomy. *Proceedings of the National Academy of Sciences* 100:3874-3877.
- United States vs. Byron Mitchell. Criminal Action No. 96-407, US District Court for the Eastern District of Pennsylvania. 1999.
- United States vs. Brian Keith Rose. 672 F. Supp. 2d 723 - Dist. Court, D. Maryland. 2009.
- Wentworth, B. and H.H. Wilder. 1932. *Personal Identification - Methods for the Identification of Individuals Living or Dead*. 2nd edition. T. G. Cooke, editor. The Fingerprint Publishing Association, Chicago.
- Wu, M., L. Koenig, J. Lynch, and T. Wirtz. 2006. Spatially-oriented EMR for Dental Surgery. *in* *AMIA 2006 Symposium*, Washington D.C., pg. 1147.

CHAPTER 1 –PROJECT INTRODUCTION

I. INTRODUCTION

A. *Statement of the Problem*

Fingerprint comparisons used for identification of individuals based on matches of minutiae and friction ridge features between a ten-print standard and a latent print have been employed since the early 1900s (for review see: Henry 1900; Hoover 1931; Barnes 2011). Acceptance of such identifications in a court of law has been based on the premise that fingerprints do not change over the lifetime of an individual and that fingerprints are unique to every individual. Several studies have demonstrated the permanence of fingerprints (Galton 1892; Wentworth and Wilder 1932; Ashbaugh 1999; see Langenburg 2011 for a review). However, since the landmark ruling of *Daubert vs. Merrell Dow Pharmaceuticals* (1993) which set the scientific standard for the admissibility of forensic evidence, the premise of fingerprint uniqueness has had multiple challenges. Two such challenges include the *United States vs. Mitchell* (1999) and *United States vs. Brian Keith Rose* (2009), claiming that fingerprint uniqueness has not been scientifically tested or validated and that examiner accuracy (i.e., error rate) associated with latent print examiner identifications has not been determined. In addition, in February 2009 the National Academy of Sciences (NAS) released a report, “Strengthening Forensic Science in the United States: A Path Forward” (National Research Council Committee on Identifying the Needs of the Forensic Sciences Community 2009) which was critical of the forensic science community, primarily the impression disciplines of trace, firearms and latent prints. The NAS report cited recommendations to improve the scientific reliability and accuracy of several forensic science methodologies, including the ACE-V procedure used for latent print comparisons. Specifically the NAS report indicated, “Additionally, more research is needed regarding the discriminating value of the various ridge formations and clusters of ridge formations” (National Research Council Committee on Identifying the Needs of the Forensic Sciences Community 2009). These criticisms cited in the NAS report primarily stem from a perceived lack of statistical validation of fingerprint “uniqueness” or distinctiveness (i.e., what is the probability that fingerprint features occur in the same spatial configuration on two different fingerprints) and the subsequent lack of application of empirical statistics or probabilities to latent print comparison conclusions.

This project addresses the question of fingerprint uniqueness (i.e., the discriminating value of the various ridgeline features or clusters of ridgeline features) by statistically evaluating the spatial distribution of fingerprint features and establishing probabilities that describe the spatial distribution of these fingerprint features across the whole fingerprint as well as within regions of the fingerprint. The purpose of the project was to initially review, with latent print examiners, the latent print comparison practice or the ACE-V methodology to ascertain the fingerprint features utilized during the comparison process and apply principles of spatial analyses to develop statistical certainty measures for latent print comparison conclusions. The specific objectives were to (1.) use Geographic Information Systems (GIS) spatial analysis techniques to evaluate fingerprint features or topological attributes (e.g., minutia number, type and orientation, and ridge lines), and (2.) derive probabilities that can be used for qualifying latent print comparison conclusions.

B. *Literature Review*

Multiple studies, the first being Galton’s in 1892, attempted to establish statistical probabilities for fingerprint individuality (Galton 1892). These early studies evaluated fingerprint pattern types

(loops, whorls, and arches), a few minutiae and sometimes ridge counts (Galton 1892; Henry 1900; Roxburgh 1933; Gupta 1968; Osterburg et al. 1977; Sclove 1979; see Langenburg 2011 for review) to base probability estimations on untested assumptions regarding minutiae types, frequency of occurrence and distributions (Stoney and Thornton 1986, 1987; Srihari and Srinivasan 2007). In addition, many of these studies used a small sample size, evaluated single pattern types (e.g., ulnar loops), included only one gender, or a limited number of minutiae (e.g., ridge endings and bifurcations). Although Stoney and Thornton (1986) systematically evaluated all pattern types, minutiae densities, frequencies, orientation, and spatial association, the analyses were limited to the distal portion of male thumb prints only. In a more recent study, Swofford (2005) statistically analyzed pattern type and ethnicity. This work demonstrated a significant correlation between pattern type and fingers, but not pattern type and ethnicity.

Champod and Margot (1996) evaluated nine minutiae types, minutiae number, orientation, length, and ridge counts from 1000 inked fingerprints. They described minutiae configuration probabilities showing that minutiae density is higher in the core and delta regions as compared to the periphery. They also found that minutiae frequency is independent of pattern type and the number of minutiae, but that it is dependent on surface position. They found no significant difference between pattern type and gender. Gutierrez et al. (2007, 2011) performed similar studies to evaluate minutiae frequency of occurrence, distribution and association with pattern types using 200 individuals (100 males & 100 females) from a Spanish population and 14 to 20 minutiae types. Similar to Champod and Margot (1996), Gutierrez et al., (2007) found no significant difference between pattern type and gender with the exception of the right index finger and they also showed that ridge endings, followed by convergences and bifurcations, are the most frequent minutiae types with a greater density of ridge endings in the periphery and bifurcations in the central area. Other observations showed that whorl patterns contain significantly more minutiae than other pattern types, with arches having the greatest density of minutiae in the core region. Gutierrez-Redomero et al. (2008) expanded upon the above studies to include ridge density and the evaluation of gender differences using likelihood ratios. Their results indicated a lower ridge density for the thumb and index fingers, with ridge densities decreasing from the radial to ulnar side for all fingers. In addition, females typically have a higher ridge density than males. Most recently, Gutierrez-Redomero et al., (2012) compared these results to the distribution and frequency of minutiae in two Argentinian population samples. Their data showed a significant difference in the frequency of minutiae type and pattern type between the two populations. In addition, in the Argentinian populations, females had a higher frequency of ridge endings compared to males.

Several other researchers have built on these observations to employ statistical approaches for establishing probability distributions for fingerprint individuality using minutiae location, orientation, pattern type and/or ridge flow (Pankanti et al. 2002; Dass et al. 2005; Fang et al. 2007; Zhu et al. 2007; Su and Srihari 2010; Neumann et al., 2006, 2007). These studies demonstrated that the greater the number of minutiae used in the analyses, the lower the probability of random correspondence and that inclusion of ridge morphology strengthens the probability. For a review of proposed fingerprint individuality probability models see Langenburg (2011) and Stoney (2001).

The fundamental assumption for utilizing fingerprints in latent print comparisons is that fingerprints are unique to each individual and that fingerprint patterns do not change over an individual's lifetime. There are published data that support the veracity of the latter assumption (Galton 1892; Wentworth and Wilder 1932; see Langenburg 2011 for a review). In addition, in the last ten years the scientific community has accumulated a significant body of data that supports the premise and limits of the discriminating value of fingerprint ridge features which describes fingerprint uniqueness (Pankanti et al. 2002; Dass et al. 2005; Fang et al. 2007; Srihari and Srinivasan 2007; Zhu et al. 2007; Su and Srihari 2010; Neumann et al., 2006, 2007). However,

stating that fingerprints are unique and that they do not change over time does not address the accuracy of the methodology employed for performing fingerprint comparisons nor does it provide a quantitative parameter for qualifying the resultant comparison conclusion. The current practice used for comparing a latent print to a fingerprint standard is still, in large part, based on subjective pattern matching (Investigation and Justice 1990; Ashbaugh 1999; Maltoni et al. 2009) by a trained Latent Print Examiner and does not employ an objective quantitative analysis component. Historically, a numerical point standard was adopted in most countries where analysts would compare a latent print to a known fingerprint standard by identifying all common features or points (see Champod 1995 for review). If a sufficient number of features are in common, the examiner concludes “individualization”, that is, the two prints are from the same source. While the point standard is widely applied in many countries, the point system is variable and non-standardized. Different countries establish varying standards in terms of the number of points necessary for identification (e.g., 7 to 16 points), analysts arbitrarily assign more weight to some features than others and may not agree on which features to use for an identification. For example, from 1953 to 2001, a 16-point standard was used in England and Wales (Leadbetter, 2005) whereas an 8-12 point standard was used in the United States until 1973 (Champod 1995; FBI Law Enforcement Bulletin 1973).

In the United States, the International Association for Identification created a Standardization Committee to study the point-standard system and in 1973 the committee concluded that “no valid basis exists at this time for requiring that a predetermined minimum number of friction ridge characteristics must be present in two impressions in order to establish positive identification” (FBI Law Enforcement Bulletin 1973). In September 2003, the Scientific Working Group on Friction Ridge Analysis, Study and Technology (SWGFAST) adopted a similar position (Polski et al., 2011). In 1988, England and Wales followed suite with a review of the 16-point system used in the UK (Evelt and Williams 1996). Several years after these studies, multiple countries, including the United States, moved away from a strict point identification standard to a four-step method called ACE-V, which includes the following steps: (1) Analysis: the analyst examines the latent image to determine if sufficient quantity and clarity (quality) of detail is present to perform a comparison; (2) Comparison: the analyst compares the quality and quantity of features and identifies similarities and dissimilarities between the known and unknown prints; (3) Evaluation: the analyst reviews the agreement and/or disagreement in detail and formulates a conclusion; (4) Verification: a second analyst performs an independent analysis, comparison and evaluation of the two prints and the conclusions are compared. The conclusions must be in agreement for an individualization to be reported. For a review of the ACE-V methodology, see Ashbaugh 1991, Ashbaugh 1999 and Champod et al., 2004. It should be noted that while the ACE-V methodology has generally been adopted in the United States, there are other methodologies similar to the ACE-V method that also incorporate a point standard.

When employing the ACE-V process, there are three conclusions possible: (1) individualization or identification (i.e., the individual that supplied the known standard is the source of the latent), (2) inconclusive (insufficient agreement or disagreement between the standard and the latent to reach a definitive conclusion), or (3) exclusion (the individual that supplied the standard is not the source of the latent). In 1979, the International Association for Identification (IAI) published Resolution VII stating that “friction ridge identifications are positive, and [that the IAI] officially oppose any testimony or reporting of possible, probably or likely friction ridge identifications” (Identification News 1979). However, neither the accuracy of the practitioners employing the ACE-V method to make correct identifications nor the number of required fingerprint feature matches, with a defined level of certainty, had been statistically validated. Following the publication of the NAS report (2009), IAI members redacted the above statement (IAI Resolution 2010-18) on July 16, 2010 at the

International Association for Identification Conference in Spokane, WA (for review see Polski et al., 2011).

To quantitatively establish the reliability or accuracy of the ACE-V methodology, one needs to evaluate two things: (1) Accuracy of the practitioner employing the ACE-V method to make correct identifications and (2) The probabilities of a false match to fingerprint regions to establish certainty levels for comparison conclusions. Practitioner accuracy addresses the ability of Latent Print Examiners (LPE) to utilize the ACE-V method in making a correct identification within a statistically determined degree of certainty. Several measures of practitioner accuracy evaluated in the last few years include analysis of latent print proficiency test data and the IAI's certification examination. However, these two measures do not delineate error types. Wertheim et al. (2006) evaluated the accuracy of 92 LPEs with more than one year of experience. Only two out of 5861 (0.03%) identifications were erroneous or incorrect. Langenburg (2009) performed a pilot study using six examiners to evaluate the accuracy of comparisons on a set of 60 samples. The conclusions of the six examiners were consistent for identifications (mean = 44.7 ± 2.7). Although no erroneous identifications occurred, not all possible identifications were made. Thus, practitioner accuracy using the ACE-V method for identifications was not 100%.

Ulery et al. (2011) in the first large scale study, analyzed the accuracy and reliability of 169 latent print examiners' comparison decisions. Six false positives or erroneous identifications were made out of 4083 comparisons suitable for identification, thus indicating a 0.147% error. Ulery et al., went on to study the repeatability and reproducibility of these decisions (Ulery et al. 2012). Langenburg et al. (2012) performed a similar study using 176 examiners in which quality assessment software and likelihood ratio tools were utilized to assist the examiners in their comparison decisions. The resultant outcome was that these tools do increase the accuracy and consistency in fingerprint feature selection which may have a subsequent impact on the accuracy and reliability of the comparison decision.

Probabilities that describe the discriminating value of the various ridgeline features or clusters of fingerprint ridgeline features address the number and/or relationship of these features required to conclude a latent print "identification" within a statistically determined level of certainty. Therefore, it is critical to estimate the probability of a false match across spatial sub-regions of a given fingerprint. This is a critical concept for LPEs since they rarely compare a full fingerprint impression to a known standard as distorted, smudged, and/or partial impressions are common. Consequently, it is important not only to establish the baseline statistics for determining fingerprint false match probabilities, but also to evaluate how these probabilities vary across fingerprint space when only a portion of the impression is available for consideration. Hence, two key questions frame the problem as applied in the forensic laboratory: (1) What is the probability of a match between a known and unknown when comparing a subset of fingerprint features available and (2) What is the statistical minimum threshold required within a level of certainty to make an identification?

One statistical approach for evaluating these questions was presented by Neumann et al. (2006, 2007) and Egli et al. (2007) in which they calculated likelihood ratios (LR) for within- and between-finger variability. Their results showed that a calculated LR using three or more minutiae is a robust statistical measure that can be used to predict the probability limits of a latent identification. Srihari and Srinivasan (2008) evaluated LR and ROC (receiver operating characteristic) models for potential use as an automatic fingerprint verification method. Their study showed that with a large sample (40 to 60) of minutiae, a 99.8% identification accuracy is possible. However, accuracy decreased significantly when fewer minutiae were available for matching. Ross et al. (2002) also found that using a combination of minutiae and ridge patterns provided the most robust matches, compared to using either feature alone. Along these same lines, Su and Srihari (2010) developed a method for

computing fingerprint rarity using a given set of minutiae. Results showed that the probability of random correspondence increased when the number of minutiae decreased. That is, when fewer minutiae were considered, there was a higher probability that the latent print matched other fingerprints. Most recently, Neumann et al. (2012) optimized his statistical approach using likelihood ratios and developed a formal model for the application of a quantitative value to fingerprint ridgeline feature configurations which describes the discriminating weight of the resultant comparison conclusion.

C. Statement of Rationale

While there is a wealth of information available regarding fingerprint ridgeline features, (e.g., the distribution, density and frequency of minutiae per pattern type, hand, gender and ethnicity), there are few studies that have utilized this information to empirically determine the discriminating value of these ridgeline features; even fewer studies, one to date (Neumann et al., 2012), have been developed to the point of being suitable for implementation in the latent print comparison process. With recent court challenges to the admissibility of fingerprint evidence due to a lack of scientific rigor in the validation of the comparison methodology and to examiner testimony stating fingerprints are unique and an identification is to the exclusion of all others, scientific research evaluating the methodology and the discriminating value of the various fingerprints features utilized for latent print comparison is warranted.

The purpose of the project was to review, with latent print examiners, the ACE-V methodology to ascertain the fingerprint features considered during the latent print comparison process and apply principles of spatial analyses to develop statistical certainty measures for latent print comparison conclusions. The specific objectives were to (1) use Geographic Information Systems (GIS) spatial analysis techniques to evaluate fingerprint features or topological attributes (e.g., minutia number, type and orientation, and ridge flow and density), and (2) derive probabilities that describe the discriminating value of these ridgeline features and (3) utilize the derived fingerprint probabilities to establish certainty levels to qualify latent print comparison conclusions.

2. REFERENCES

Ashbaugh, D. R. 1991. Introduction to ridgeology. *Journal of Forensic Identification* **41**:16-64.

Ashbaugh, D. R. 1999. Quantitative-qualitative friction ridge analysis: An introduction to basic and advanced ridgeology. CRC Press LLC, Boca Raton, Florida.

Barnes, J. G. 2011. History, *in* The Fingerprint Sourcebook. A. McRoberts, editor. National Institute of Justice, Washington D.C. Ch.1, pp. 1-22.

Champod, C. 1995. Edmond Locard - Numerical standards and "probable" identifications. *Journal of Forensic Identification* **45**:136-163.

Champod, C. and P. A. Margot. 1996. Computer assisted analysis of minutiae occurrences on fingerprints. pp. 305-318, *in* Proceedings of the International Symposium on Fingerprint Detection and Identification. J. Almog, E. Springer, M. Yisrael, eds., Israel National Police, Neurim, Israel.

Champod, C., C. Lennard, P. Margot, and M. Stoilovic. 2004. Fingerprints and other ridge skin impressions. J. Robertson, editor. CRC Press LLC, Boca Raton, Florida.

- Dass, S. C., Y. Zhu, and A. K. Jain. 2005. Statistical models for assessing the individuality of fingerprints. pp. 3-9, *in* Fourth IEEE Workshop on Automatic Identification Advanced Technologies. IEEE Computer Society, Buffalo, New York.
- Daubert vs. Merrell Dow Pharmaceuticals. 509 US 579. 1993
- Egli, N. M., C. Champod, and P. Margot. 2007. Evidence evaluation in fingerprint comparison and automated fingerprint identification systems--Modelling within finger variability. *Forensic Science International* **167**:189-195.
- Evetts, I. W. and R. L. Williams. 1996. A review of the sixteen points fingerprint standard in England and Wales. *Journal of Forensic Identification* **46**:49-73.
- Fang, G., S. N. Srihari, and H. Srinivasan. 2007. Generative models for fingerprint individuality using ridge types. pp. 423-428, *in* Third International Symposium on Information Assurance and Security. IEEE Computer Society, Manchester, United Kingdom.
- Galton, F. 1892. *Fingerprints*. Macmillan and Co., London, England.
- Gupta, S. R. 1968. Statistical survey of ridge characteristics. *International Criminal Police Review* **218**:130-140.
- Gutierrez-Redomero, E., C. Alonso, E. Romero, and V. Galera. 2008. Variability of fingerprint ridge density in a sample of Spanish Caucasians and its application to sex determination. *Forensic Science International* **180**:17-22.
- Gutierrez, E., V. Galera, J. M. Martinez, and C. Alonso. 2007. Biological variability of the minutiae in the fingerprints of a sample of the Spanish population. *Forensic Science International* **172**:98-105.
- Gutierrez-Redomero, E., C. Alonso-Rodriguez, L. E. Hernandez-Hurtado, and J. E. Rodriguez-Villalba. 2011. Distribution of the minutiae in the fingerprints of a sample of the Spanish population. *Forensic Science International* **208**:79-90.
- Gutierrez-Redomero, E., N. Rivalderia, C. Alonso-Rodriguez, L. M. Martin, D. J. E., M. A. Fernandez-Peire, and R. Morillo. 2012. Are there population differences in minutiae frequencies? A comparative study of two Argentinian population samples and one Spanish sample. *Forensic Science International* **222**:266-276.
- Henry, E. R. 1900. *Classification and Uses of Fingerprints*. Routledge & Sons, London, England.
- Hoover, J. E. 1931. Criminal identification. *The American Journal of Police Science* **2**:8-19.
- International Association of Identification. 1973. Standardization Committee Report. *FBI Law Enforcement Bulletin* **42**:7-8.
- International Association of Identification. 1979. Resolution VII. *Identification News*, Volume **29**:8.

- Investigation, U.S.F. B. and Department of Justice. 1990. *The Science of Fingerprints: Classification and uses*. U. S. Government Printing Office, Washington D. C.
- Langenburg, G. 2009. Performance study of the ACE-V process: a pilot study to measure the accuracy, precision, reproducibility, repeatability, and biasability of conclusions resulting from the ACE-V process. *Journal of Forensic Identification* **59**:219-257.
- Langenburg, G. 2011. Scientific research supporting the foundations of friction ridge examinations, *in* *The Fingerprint Sourcebook*. A. McRoberts, editor. National Institute of Justice, Washington D.C. Ch. 14, pp.1-31.
- Langenburg, G., C. Champod, T. Genessay, and J. Jones. 2012. Informing the judgements of fingerprint analysts using quality metric and statistical assessment tools. *Forensic Science International* **219**:183-198.
- Leadbetter, M. J. 2005. Fingerprint evidence in England and Wales - The revised standard. *Medicine, Science and the Law* **45**:1-5.
- Maltoni, D., D. Maio, A. K. Jain, and S. Prabhakar. 2009. *Handbook of fingerprint recognition*. Second edition. Springer-Verlag, London, England.
- National Research Council Committee on Identifying the Needs of the Forensic Sciences Community. 2009. *Strengthening forensic science in the United States: A path forward*. The National Academies Press, Washington D.C.
- Neumann, C., C. Champod, R. Puch-Solis, N. M. Egli, A. Anthonioz, and A. Bromage-Griffiths. 2007. Computation of likelihood ratios in fingerprint identification for configurations of any number of minutiae. *Journal of Forensic Sciences* **52**:54-64.
- Neumann, C., C. Champod, R. Puch-Solis, N. M. Egli, A. Anthonioz, D. Meuwly, and A. Bromage-Griffiths. 2006. Computation of likelihood ratios in fingerprint identification for configurations of three minutiae. *Journal of Forensic Sciences* **51**:1255-1266.
- Neumann, C., I. W. Evett, and J. Skerrett. 2012. Quantifying the weight of evidence from a forensic fingerprint comparison: A new paradigm. *Journal of the Royal Statistical Society, Series A (Statistics in Society)* **175**:371-415.
- Osterburg, J. W., T. Parthasarathy, T. E. S. Raghavan, and S. L. Sclove. 1977. Development of a mathematical formula for the calculation of fingerprint probabilities based on individual characteristics. *Journal of American Statistical Association* **72**:772-778.
- Pankanti, S., S. Prabhakar, and A. K. Jain. 2002. On the individuality of fingerprints. *IEEE Transactions on Pattern Analysis and Machine Intelligence* **24**:1010-1025.
- Polski, J., R. Smith, R. Garrett, et.al. 2010. *The Report of the International Association for Identification, Standardization II Committee*.

- Ross, A., J. Reisman, and A. K. Jain. 2002. Fingerprint matching using feature space correlation. pp. 48-57, *in* Proceedings of Post-ECCV Workshop on Biometric Authentication LNCS 2359. Springer-Verlag, Copenhagen, Denmark.
- Roxburgh, T. 1933. On the evidential value of fingerprints. *Sankhya: The Indian Journal of Statistics* **1**:189-214.
- Sclove, S. L. 1979. The occurrence of fingerprint characteristics as a two-dimensional process. *Journal of American Statistical Association* **74**:588-595.
- Srihari, S. N. and H. Srinivasan. 2007. Individuality of fingerprints: comparison of models and measurements. University at Buffalo, The State University of New York, Buffalo, New York.
- Srihari, S. N. and H. Srinivasan. 2008. Comparison of ROC and likelihood decision methods in automatic fingerprint verification. *International Journal of Pattern Recognition and Artificial Intelligence* **22**:535-553.
- Stoney, D. A. and J. I. Thornton. 1986. A critical analysis of quantitative fingerprint individuality models. *Journal of Forensic Sciences* **31**:1187-1216.
- Stoney, D. A. and J. I. Thornton. 1987. A systematic study of epidermal ridge minutiae. *Journal of Forensic Sciences* **32**:1182-1203.
- Stoney, D. A. 2001. Measurement of Fingerprint Individuality. pp. 327-387, *in* Advances in Fingerprint Technology. H. C. Lee and R. E. Gaensslen, eds., CRC Press LLC, Washington D.C.
- Su, C. and S. N. Srihari. 2010. Evaluation of rarity of fingerprints in forensics. *Advances in Neural Information Processing Systems* **23**:1-9.
- Swofford, H. J. 2005. Fingerprint Patterns: a study on the finger and ethnicity prioritized order of occurrence. *Journal of Forensic Identification* **55**:480-488.
- Ulery, B. T., R. A. Hicklin, J. Buscaglia, and M. A. Roberts. 2012. Repeatability and reproducibility of decisions by latent fingerprint examiners. *Public Library of Science (PLoS)* **7**:1-12.
- United States vs. Byron Mitchell. Criminal Action No. 96-407, US District Court for the Eastern District of Pennsylvania 1999
- United States vs. Brian Keith Rose. 672 F. Supp. 2d 723 - Dist. Court, D. Maryland 2009
- United States Federal Bureau of Investigation and Department of Justice. 1990. The science of fingerprints: Classification and uses. U. S. Government Printing Office, Washington D. C.
- Wentworth, B. and H.H. Wilder. 1932. Personal Identification - Methods for the Identification of Individuals Living or Dead. 2nd edition. T. G. Cooke, editor. The Fingerprint Publishing Association, Chicago

Wertheim, K., G. Langenburg, and A. Moenssens. 2006. A report of latent print examiner accuracy during comparison training exercises. *Journal of Forensic Identification* **56**:55-93.

Zhu, Y., S. C. Dass, and A. K. Jain. 2007. Statistical models for assessing the individuality of fingerprints. *IEEE Transactions on Information Forensics and Security* **2**:391-401.

CHAPTER 2 – GEOGRAPHIC INFORMATION SYSTEMS, DATA ACQUISITION AND PATTERN CHARACTERIZATION

1. INTRODUCTION

A Geographic Information System (GIS) is a collection of hardware and software components that integrate digital map elements with relational database functionality. GIS data are typically captured in the form of either raster grids (e.g., pixels) or vector features (i.e., points, lines, and polygons) with points referenced in space using X, Y and sometimes Z coordinate values (Price 2012). The power of a GIS is in its ability to allow users to integrate, store, edit and analyze spatial features and relationships, as well as query and display spatial information. Such systems include traditional mapping capabilities (e.g., land surveying and aerial photography) and provide users with tools to interactively search and analyze spatial information (Figure 2-1A).

GIS technology was initially developed for cartography with one of the first computerized land-management systems in Canada in 1962 (Tomlinson 1967, 1970). Since then, GIS systems have been applied in increasingly novel ways to include land use planning, environmental management, marketing, and criminology. Most recently, GIS has been used for characterizing surgical procedures (Garb et al. 2007), conducting dental EMR imaging (Wu et al. 2006) and for in neuroanatomical and anthropological research (Ungar and M’Kirera 2003, Martone et al. 2004). While GIS is widely used for crime pattern analysis and emergency management applications, (ESRI 2000, 2001; Chainey et al. 2005; Bodbyl-Mast 2009), its analytical capabilities have not been previously applied to fingerprint characterization and pattern recognition (Stanley et al. 2012).

GIS-based spatial analysis involves analyzing the positions, patterns and relationships between objects located in a defined space, similar to graph theory in discrete mathematics (Maguire et al. 2005; Smith et al. 2007). Collections of objects in a defined coordinate space may be linked or associated with one another geometrically or by functional associations. Techniques in spatial analysis include data modeling, image processing, grid algebra, surface analysis, network analysis and visualization. The GIS-based tools available for spatial analysis have grown exponentially in recent years, all driven by the practical need to understand, predict, and model relationships between objects located in space. Given that fingerprint analyses and latent print comparisons are based on spatial associations between minutiae and ridgelines (e.g., minutia patterns, ridge counts, minutiae location), GIS-based tools are a natural extension (Figure 2-1B). Utilization of GIS in conducting dactylographic research is particularly appealing given that fingerprint minutiae and ridge patterns are very analogous to geometries reflected in Earth surface topography, a traditional focus of GIS.

This project takes a novel approach utilizing GIS and related tools to derive spatial statistics for fingerprint patterns, with the ultimate deliverable involving the development of false-match probability estimates for use on active casework in forensics laboratories. The methodologies presented herein provide a framework for cataloging, characterizing and quantifying fingerprint features using custom GIS tools. Following is a summary of methodology and results as applied to fingerprint characterization.

2. METHODS

The Python (version 2.6.5, 2010; software available from <http://www.python.org>) programming language was used in conjunction with ArcGIS software (Ver. 10.0; ESRI 2010; Price 2012) to create custom tools and automate complex project workflows (Figure 2-2). The fundamental steps in the fingerprint data conversion process included: (1) scanning ten-print cards using TWAIN-compliant software at 1000 dpi resolution, (2) image processing using Adobe Photoshop CS4 (image

rotation, fingerprint cropping, image enhancements), (3) export of unregistered images to the Universal Latent Workstation (ULW; Watson et al., 2007) software package for initial minutia detection, (4) georegistration of vector minutia point files and print images into a standardized coordinate reference system, and (5) export of vector and raster data layers to GIS-compliant data formats for use in the ESRI ArcGIS software suite.

Metadata were also generated to describe the function and output of each software script and resultant data files. The resultant data products were used to measure a wide variety of fingerprint metrics, along with spatial assessment of the density of minutiae for fingerprint pattern types, as well as within a given fingerprint region. Table 2-1 presents a list of the primary GIS-based methods developed as part of this study. The GIS-based workflow has been systematically divided into three categories, each with a range of assigned method numbers to assist the project team with communication and data organization. One hundred level techniques involve data collection and conversion of fingerprint images into vector-based data models. Two hundred level techniques focus on pattern characterization and morphometric derivatives from the 100-level data models. Three hundred level methods include statistical analyses, probability modeling and geometric morphometric analyses. A summary of key workflow elements and GIS methods utilized in this study and the types of data resulting from these techniques are presented in Table 2-1 and Figure 2-2 (after Aldrich 2010; Dutton 2010; Dutton et al. 2010a, 2010b; Dutton et al. 2011; Taylor et al. 2012).

A. Fingerprint Data Collection, Visual Assessment and Image Processing

The project sample set was obtained from a random selection of over 5000 ten-print cards supplied by the Oregon State Police (OSP), Forensic Services Division, as derived from state criminal records. As part of an inter-institutional agreement, all personal identification was removed before processing by project staff.

The first step in the data collection process was to visually assess the quality of ten-print cards to select those samples with the best image clarity. Approximately 1836 ten-print cards were qualitatively separated into four categories (1 = best, 2 = good, 3 = fair, 4 = poor) and evaluated for the clarity of ridgeline resolution, blotching, smudging, and scarring (Figure 2-3A). A quality rating 1 (best) image displays clear ridge line resolution, no-to-minimal blotching or smudging and no major scarring. Minor blemishes outside the core were acceptable. Of the 1836 ten-print cards visually assessed, 957 were fair (rating 3) to poor (rating 4) with 879 categorized as best (rating 1) and good (rating 2).

Following the initial qualitative image assessment, the 1 and 2 quality-rated images were scanned at 1000 dpi as an 8 bit grayscale image (Figure 2-3B). The ten-print was digitally separated into individual fingers; the initial phase of the project focused on the right thumb, right index, left thumb and left index (i.e., fingers 1, 2, 6, 7; Figure 2-3B). Scanned images were then processed with Adobe Photoshop using a series of enhancements (noise filter, black/white balance, contrast, brightness enhancements) and subsequently oriented with the distal interphalangeal crease aligned to horizontal. To date, greater than 600 ten-print cards have been scanned and processed providing a total of 2400 fingerprint images available for minutiae detection and friction ridge vectorization (Table 2-2).

B. Minutiae Detection

To assist project staff in establishing standards for minutiae detection, two software applications, MINDTCT and Universal Latent Workstation (ULW), were compared early on in the project for both accuracy and ease of use. Both of these applications are readily available in the public domain. MINDTCT is an older software application developed by the National Institute of Standards and Technology (NIST) in the early 1990s, while the ULW application is an upgraded version of MINDTCT developed by the FBI. After an evaluation of both of these applications, the ULW system was selected as the project standard for assisting research staff in consistently identifying and locating minutiae on fingerprints. Through empirical testing, the project team concluded that ULW provides more accurate minutiae detection, fewer falsely labeled minutiae, better image file visualization of detected minutiae, greater ease of use, and better image manipulation for quality control (e.g., delete false minutiae, label missed minutiae). Thus, ULW, which only identifies bifurcations and ridge endings, was used for minutiae detection and extraction at a 30% threshold. The 30% threshold was utilized to reduce the amount of false minutiae initially detected by the software. After minutiae acquisition, the image was imported into the GIS system. The fingerprint image was subsequently subjected to a visual inspection by the researchers to identify and correct, missed minutiae, mislabeled minutiae and falsely marked minutiae. To ensure systematic image orientation, accurate minutiae detection, core and delta placement and pattern type identification, OSP Latent Print Examiners performed an independent quality control assessment. Their review led to improvements in the data collection process with the addition of a second level of quality assurance during GIS data conversion (refer to Section 2C below). Thus, image orientation, pattern type designation, minutiae detection and core and delta placement procedures involved a combination of automated software algorithms and operator judgment.

C. GIS Data Conversion and Geo-Referencing

Custom Python-based software routine (scripts) tools were created in ArcGIS to assist with fingerprint data collection, pattern characterization, and statistical analysis (Figure 2-2 & Table 2-1). Initial minutiae detection was conducted using latent fingerprint processing software, with results exported as ANSI/NIST Type-9 records. A tool was created to parse finger and minutia information from a Type-9 text file and transpose the data into a standardized coordinate graph space. Coordinate referencing (georeferencing) places the fingerprint image and related features in quadrant I (+,+) of a Cartesian coordinate system. The Type-9 ULW summary output file was georeferenced to adjust the X-axis and Y-axis origin (0,0) to -100 mm distant from the fingerprint core (Figure 2-4). The core was defined as: Arches = highest point of recurve, Loops = ridge ending at top of 1st full loop and Whorls = ridge ending or bulls-eye at core. The resultant transformation placed all cores of each fingerprint at a standard (100,100) mm position within Cartesian coordinate space. The georeferenced fingerprint coordinate space is oriented such that geographic-based azimuth directions are applied with due north set at 0 degrees, oriented parallel to the positive Y-axis direction, with subsequent orientations relative to clockwise angular measurements of East (90°), South (180°), and West (270°) (Figure 2-4 inset). Once imported and registered in GIS, minutiae were subjected to an additional level of QC and secondary processing. Feature points were moved to more accurately mark the placement of minutiae and any minutiae incorrectly labeled or falsely marked were corrected. In addition, the delta regions were marked. The delta region was defined according to Kucken and Newell (2005) as a triradius consisting of three ridge systems converging with each other at an angle of roughly 120 degrees and marked.

The final step in the GIS-data conversion process was to attribute the minutiae vector points with identifying information attached via an indexed relational database file. Tabled information includes X-Y location, minutia direction, minutia identification, minutia type, fingerprint type and file identification (Figure 2-5). The net result of the data acquisition process described above was to create a spatially-referenced set of fingerprint data, including the georeferenced fingerprint image, the minutia vector overlay and the associated database file. This data set, georeferenced in standardized coordinate space, in turn formed the fundamental framework for subsequent geometric measurements, spatial analyses and statistical models (Table 2-1).

D. Minutiae Location Confidence Zone

The scaling of the data acquisition process described above was such that the coordinates of resulting georeferenced minutia locations were associated with a small degree of +/- positional error that was an artifact of the digitization process. The digitized minutiae coordinates were precise to nanometers while ridge widths were precise to micrometers, resulting in a minutia point location smaller than the physical feature it represents. Thus, while two minutiae may actually be in same location on a fingerprint, analysis of this coordinate position in GIS may indicate that they are not. To account for this difference in precision as an artifact of image digitization, a minutiae location confidence zone around each point was statistically estimated using ridge widths that encompass 99.7% of the observed variation. Fifty fingerprints were randomly selected from the available dataset. Within each fingerprint, 10 points were randomly placed using a script in GIS that restricted positioning on ridges and not in white space. The ridge width was then measured at the location resulting in 10 measurements each for 50 prints, with a total N of 500. The mean and variance of the ridge widths was calculated for each finger. The resulting 50 values were in turn pooled with a calculated mean = 0.4 mm, standard deviation = 0.76 mm and a margin of error = 0.32 mm. The analysis suggests that our data collection and digitization techniques were associated with a minutia positional tolerance of +/- 0.32 mm. This positional tolerance buffer was accounted for in subsequent geometric measurements, spatial analyses and statistical tests (Table 2-1).

E. Friction Ridge Vectorization

Following acquisition and georeferencing of fingerprint images, the friction ridges were vectorized into line layers for subsequent attribution and morphometric analysis (Figure 2-1B). At sub-millimeter scale, friction ridges are polygonal features associated with pore openings in the skin. Fingerprint analysis treats ridges as line patterns for use in identifications. Vectorization of ridge lines from raster print images involved a process of center-line skeletonization of binarized pixels representing two-dimensional polygon space. A custom ArcGIS/ArcScan extension was used to digitize ridge center lines from raster images and attribute them according to ridge-ending type. Ridge line segments end at one of three conditions: outer convex hull (H) boundary, ridge ending (RE) minutia, or bifurcation (B) minutia. Thus, each ridge line segment was attributed with one of six boundary conditions: RE-RE, RE-B, RE-H, B-B, B-H, or H-H (Figure 2-6). Skeletonization/vectorization allows for efficient counting of ridge lines between all minutiae on a fingerprint and for the derivation of other morphometric data products such as ridge density. Additionally, line length and line curvature were calculated for each ridge. Once the vectorized ridge lines were created and georeferenced in standardized coordinate space, a complete set of fingerprint data layers (raster-based fingerprint image, vector-based minutia point layer, vector-based ridge line layer) were available for subsequent geometric measurements, spatial analyses and statistical models (Table 2-1).

Accurate minutiae placement and ridgeline skeletonization depends upon positively identifying false ridge endings. Fingerprint artifacts such as ridge breaks introduce errors during the automated skeletonization process. For example, ridge counts between the core and delta may vary if false ridge endings have not been identified and corrected. To minimize this condition, we established a set of rules by which to assess false ridge endings. The User's Guide to NIST Biometric Image Software (Watson et al. 2007) defines an overlap as a discontinuity in a ridge or valley usually introduced via the fingerprint impression process. The NBIS selection threshold for overlaps is defined by two minutiae within an eight pixel distance and nearly opposite directions. The eight pixel distance was intended for analysis of images scanned at 500 ppi. Adjusting this process to accommodate our 1000 ppi fingerprint images required doubling of the pixel tolerance to 16 cells. The pixel tolerance approach was one method considered when skeletonizing ridges. To verify our skeletonization technique, ten Oregon State Police latent print examiners independently traced ridges from the same set of fingerprint images. Analysis of the latent examiners' ridge tracings produced a consensus for determining false ridge endings. In addition, when ridge endings were questionable, a comparison of slapped vs. rolled prints was performed. Slap prints typically do not display the same degree of distortion inherent in rolled prints, thus, the former may lack false ridge endings associated with the latter. This systematic methodology for identifying false ridge endings increased skeletonization accuracy, established a standard for comparison, and decreased errors in subsequent analyses that required ridge-line vector data.

F. Data Management and GIS Analysis

A SQL Server database was developed to manage and store the large amount of minutiae information. Our database management system is comprised of a SQL Server 2008 R2 running on a Windows Server 2008 R2 operating system at the back end, with a custom front end consisting of programs written in both Java and C++ controls that allow for a wide variety of searches to be performed. Our output data categories included gender, finger (1, 2, 6, 7), pattern type (right slant loop, left slant loop, arch, tented arch, whorl, double loop whorl), minutiae type (bifurcation or ridge ending) and ridgelines. These categories, in turn, formed the basis for grouping observations on the frequency of minutiae type per finger, frequency of minutiae type per pattern type, location of minutiae with respect to core, and the density of minutiae per finger, pattern type and quadrant. Additional query tools were constructed to further refine these searches to evaluate minutiae frequency and distribution in select areas of a finger based on either the X-Y minutia coordinate location, azimuth from the core and/or the distance from the core.

Geo-referenced fingerprint images, minutiae point layers and ridgeline coverages were systematically aggregated within a GIS geodatabase for subsequent querying and spatial analysis. Python-based GIS tools were custom built and implemented for extracting specific fingerprint metrics (Table 2-1). A ridge counting tool provides the capacity to count fingerprint ridges between all minutiae, which allows for additional levels of analysis compared to raster grids. Pattern characterization scripts were created to analyze point density and percent minutiae frequency by spatially intersecting minutiae with pre-established templates, such as a 2-mm grid overlay and a core-centered 'dart board' diagram. Distance and azimuth (0-360 degrees) from the finger core were calculated for all minutiae within the database. Using these values, minutiae were combined by fingerprint pattern type and summarized in rose diagrams, which serve as circular histograms to visually display minutia distributions relative to the core. Minutia densities were also calculated within a standardized grid composed of 2 mm x 2 mm cells in standard georeferenced coordinate space. Minutiae from the project database were aggregated according to pattern type and then tallied

within the 2 mm grid cells. The resulting grid layer contains attribute data that records the number of minutiae and ridgelines per grid cell for all fingerprint patterns.

In addition to those GIS techniques described above, other analyses focused on delineating sub-regions of fingerprint space in support of spatial distribution and pattern analysis (Figure 2-7). A convex hull bounding polygon was defined by the inked margins of a fingerprint image with area, perimeter and fingerprint ID included in the output layer. An interior detailed hull was defined as a bounding polygon that circumscribes the outer most minutiae cluster on the interior of a point-based vector model (Figure 2-7A). For purposes of geometric measurement and comparison, hull axes were defined as north-south (longitudinal) and east-west (transverse) oriented lines, drawn over the fingerprint with perpendicular lines intersecting at the core (Figure 2-7B). This axis layer was subsequently clipped using the corresponding convex hull polygon. Axial line lengths and axis ratios were calculated and attributed in the resulting polyline data layer. Voronoi diagram techniques were used to conduct nearest-neighbor analyses for point patterns and to establish weighting for positional relationships. Thiessen polygons, examples of this approach, are used in surface analysis and hydrology (Maguire et al. 2005, Smith et al. 2007). Thiessen polygons were constructed by a network of lines derived using the minutiae as the centroids rather than line nodes. The size, area, and complexity of the polygon created indicate the density of minutiae surrounding it. The resulting polygon features were attributed with area, perimeter, shape index and minutia-centroid type (ridge ending vs. bifurcation) (Figure 2-7C). Voronoi tessellation polygons were used to characterize the recurring patterns of minutia (ridge- ending, bifurcations) distributions and to created generalized likely-location maps for minutia occurrence across fingerprint pattern types (loops, arches, whorls).

G. Analysis of Variance

Basic statistical analyses of fingerprint metrics were performed to determine if there were differences between pattern types. The goal of the ANOVAs is simply to determine, for the given measurement, whether there is a significant difference between pattern type. Of interest is whether total minutiae differ between pattern type when normalized by convex and detailed hull. Because the hull area is an artifact of the rolling process, both the convex hull and the detailed hull were analyzed. Secondly, the axial dimensions were explored to determine if there were differences between pattern types. The lateral versus transverse ratio by its very nature takes into account finger size; however, the north-south ratio (ratio of the area above the core and below the core) does not. Thus, a two-way ANOVA was performed for the north-south ratio with pattern type and finger as the main effects. Finally, an ANOVA was performed to evaluate differences in the Thiessen polygon analysis per pattern type.

3. RESULTS

A variety of spatial analyses (Table 2-1) were completed for the 1200 images to evaluate fingerprint characteristics for each of six pattern types (left slant loop, right slant loop, whorls, double loop whorls, arches and tented arches). The fingerprint characteristics evaluated include:

- the number of minutiae type per pattern type,
- the ratio of minutiae type per pattern type,
- the distribution and density of minutiae per pattern type,
- the distribution and density of ridge lines per pattern type,

- the average convex hull area and hull axis dimensions per pattern type,
- the average detailed hull area per pattern type, and
- the Thiessen polygon distribution per pattern type.

These analyses characterize the general distribution and geometry of fingerprint features per pattern type and were utilized to establish the foundational framework of fingerprint probabilities that describe the discriminating value of these fingerprint features. The following is a summary of results associated with these pattern characterization studies.

A. Census of Fingerprint Pattern Types

To date, over 600 ten print cards have been scanned and digitized with 1200 images from fingers 1, 2, 6 and 7 processed through ULW, digitally converted to a GIS vector format and uploaded into the image database. Of the 1200 fingerprint images, 54.8% were loops, 35.2% whorls and 10.0% arches (Table 2-2). There were 85.6% more left slant loops on the left hand and 84.8% more right slant loops on the right hand. Double loop whorls (DLW) and whorls (W) displayed an ~60:40 handedness with DLW being 55:45 for left hand (LH) to right hand (RH) and whorls 39.4:60.4 LH to RH split. Arches and tented arches were equally distributed per hand. However, there are more double loop whorls on thumbs (75%) than on index fingers (25%) and more arches on index fingers (72.2%) than on thumbs (27.8%). To date, we have not identified any tented arches on thumbs from the available Oregon State Police source data. It should be noted that because we were lacking a statistically significant number of arches in our sample set, we preferentially weighted selecting ten-print cards containing arches so that we could conduct comparative analyses between pattern types. Thus, the census numbers presented in Table 2-2 reflect the pattern types residing in our database only and do not reflect the percentages associated with a random sample of the Oregon population.

B. Minutiae Distribution

From 1200 fingerprints in the database, over 102,000 minutiae were digitized and identified, 58% of which are ridge endings and 42% bifurcations (Tables 2-3 and 2-4, Figure 2-8). The average number of minutiae per fingerprint is 85 with all pattern types showing a greater density of minutiae in the lower half of the fingerprint, around and below the core (Figure 2-9). Double loop whorls had the greatest average number of minutiae per fingerprint (99.5) and tented arches had the least (65.2) (Table 2-3, Figure 2-8). The ratio of bifurcations to ridge endings varies between pattern type. On average, there was one bifurcation per 1.4 ridge endings for all pattern types with arches, loops and whorls having a 1:1.1, 1:1.4 and a 1:1.5 ratio, respectively (Table 2-3, Figure 2-8).

The spatial distribution of minutiae in fingerprint coordinate space is depicted in rose diagrams (10-degree azimuthal bins, Figure 2-9) and point density maps (total minutiae per mm², Figure 2-10), (bifurcations per mm², Figure 2-11; ridge endings per mm², Figure 2-12). The average minutiae density per fingerprint convex hull for all pattern types was 0.119 minutiae per mm² with whorls having the greatest density of minutiae (0.130 per mm²) and arches the least (0.101 per mm²). The minutiae density per fingerprint detailed hull was similar. As noted above, minutiae were concentrated in the lower half of the fingerprint around and south of the core distributed between 100 and 270 degrees and there were more minutiae per mm² in the southeast quadrant for left slant loops and in the southwest quadrant for right slant loops. Minutiae had a bimodal distribution for whorls, double loop whorls and arches where minutiae appeared to be clustered equally in both the

southeast and southwest quadrants (Figure 2-9). The minutiae distribution for tented arches was more concentrated directly south of the core (Figure 2-10).

The general minutiae density pattern described above for the various pattern types was similar for bifurcations and ridge endings (Figures 2-11 and 2-12); the average minutiae densities for bifurcation and ridge ending were 0.052 per mm^2 and 0.067 per mm^2 , respectively. However, bifurcations displayed the greatest density in the core region whereas ridge endings were most dense in the delta regions.

C. Friction Ridge Distribution

A total of 188 fingerprint images were skeletonized to create georeferenced vector ridgeline data layers. A sample of 179 images was used for the ridgeline density data analysis and included 30 right-slant loops, 30 left-slant loops, 38 whorls, 22 double-loop whorls, 29 arches and 30 tented arches. Ridgelines were attributed according to the technique illustrated in Figure 2-6, with over 20,300 ridgelines digitized and georegistered across the six fingerprint pattern types. Ridgeline lengths per 2-mm grid were tallied for the 179 images to evaluate the ridgeline distribution per pattern type (Figure 2-13). For all pattern types, there was more total ridgeline length per 2-mm grid below the core (24.5 mm/mm^2) than above the core (21.4 mm/mm^2) with the greatest amount of ridgeline length per mm^2 near the core region. For left slant loops, there was more ridgeline length per unit area in the northeast quadrant and for right slant loops in the northwest quadrant. The greatest amount of ridgeline length was in a concentric distribution about the core for whorls and double loop whorls, and appeared to be clustered symmetrically above the core in arches and tented arches. Whorls and double-loop whorls had more 2-mm quadrats with a greater concentration of ridgelines per mm^2 (Figure 2-13) with whorls having the greatest average of ridgeline length per mm^2 (29.8 mm/mm^2).

In consideration of the number ridgelines per 2-mm quadrats above and below the core, in contrast to ridgeline length distribution, the total number of ridgelines per 2-mm quadrat and the average number of ridgelines per pattern type above and below the core was calculated for 188 skeletonized fingerprint images (Figure 2-14). For all pattern types, there were more ridgelines, on average, below the core (91.76) than above the core (71.29) with the average number of ridgelines per 2-mm quadrat being $0.61/\text{mm}^2$ and $0.54/\text{mm}^2$ below and above the core, respectively. As with the 1200 fingerprint images, there was a greater number and density of minutiae below the core than above the core; for the 188 images utilized in this study, the average number of minutiae below and above the core was 57.81 and 29.23, respectively. To evaluate whether the increased number of minutiae below the core was simply due to the density of ridgelines below the core, we calculated a ratio of minutiae per ridgelines for all pattern types and compared the values. This ratio of minutiae to ridgelines was similar for all pattern types (Figure 2-14) with the average ratio for all pattern types being 0.63 and 0.41 for below and above the core, respectively. A paired t-test of the average minutiae to ridgeline ratios calculated for above and below the core for all pattern types was significantly different ($t_{(0.05, 187)} = -24.525$).

D. Convex Hull and Detailed Hull Analysis

The average fingerprint convex hull area for all pattern types and digits (1, 2, 6, & 7) is 719.2 mm^2 . (Table 2-4,) Double loop whorls have the largest average convex hull area (811.6 mm^2) and tented arches the smallest average convex hull area (568.8 mm^2). When evaluating the convex hull by digit, thumbs have a larger average convex hull area (860.9 mm^2) for all pattern types compared to index fingers (611.7 mm^2 ; Figure 2-15). When combining minutiae counts with convex hull

areas, bulk minutiae densities (counts per mm²) can be calculated across pattern types (Table 2-4, Figure 2-16). The average minutiae density per convex hull area was similar in range for all pattern types (0.10-0.13 per mm² with arches exhibiting the smallest total minutiae density per convex hull area ratio at 0.10 per mm² and whorls the largest (0.13 per mm²).

A one-way Analysis of Variance (ANOVA) was performed to assess significance for minutiae densities/convex hull area across pattern types and a significant difference was found with an $\alpha=0.05$ ($F_{(5,1194)}=14.8$ $p=0.0000000000000417$). Using Tukey's Honestly Significant Difference post-hoc test to examine the difference of the means of the pattern types, arches were different from all other pattern types except right slant loops (Figure 2-16). The two whorl types were different from right slant loops, but only whorls different from tented arches and left slant loops, with p-values of 0.0172 and 0.0000090 respectively. Interestingly, using this metric of normalized minutiae count, tented arches appear to more similar to the loops than the pure arch. In general it appears that pattern types with greater ridge complexity produce a greater number of minutiae.

Analysis of the detailed hull area and minutia distribution yielded similar results to those for the bounding convex hull above (Table 2-5 and Figure 2-17). Similar to the convex hull area, tented arches had the smallest average detailed hull area (328.2 mm²) and double loop whorls had the largest (486.8 mm²). The current sample set was limited in that no tented arches have been identified for thumbs in the Oregon data set. Of the detailed hull data available for thumbs, arches are associated with the largest average detailed hull areas (577.5 mm²), and directly parallel the observations described for the bounding convex hulls above. A one-way Analysis of Variance (ANOVA) was performed to assess significance for minutiae densities per detailed hull area across pattern types and significance was found with an $\alpha=0.05$ ($F_{(5,1194)}=15.04$, $p=0.0000000000000242$). As similarly described for convex hulls, arches were significantly different from all patterns except for right-slant loops. Whorls were significantly different from the two loop pattern types. However, for detailed hulls, left slant loops and double loop whorls were no longer significantly different. Thus, there seems to be a larger amount of minutia-free space on the edges of double loop whorls (Figure 2-17).

Comparisons of the axial hull dimensions are summarized in Table 2-6 and Figures 2-18, 2-19 and 2-20. The longitudinal (L) and transverse (T) axes lengths are similar for all pattern types except for tented arches which were approximately 3 mm shorter compared to the average (Table 2-6). Although arches had shorter L and T axes, the ratio of the L-to-T axes was the same for all pattern types (Table 2-6) and digits (1, 2, 6 & 7; Figure 2-18). Double loop whorls had the longest south axis (i.e., core to crease) length (15.7 mm) and tented arches the shortest (13.5 mm). Tented arches and whorls had the largest south to north axis ratio; 1.4 compared to 1.2 for loops, 1.3 for double loop whorls and 1.1 for arches (Table 2-6).

A one-way Analysis of Variance (ANOVA) was performed to assess the significance of the L-to-T axis ratios across pattern types. The resultant analysis was not significant ($F_{(5,1194)}=1.075$, $p=0.373$; Figure 2-19). A two-way ANOVA of north-south axis ratios was conducted to evaluate differences in dimensions above and below the core in fingerprint coordinate space (Figure 2-20). The attribute variables included pattern type, finger, and pattern type times finger (i.e., interaction term). Results indicate that pattern type and finger were associated with significant differences in the N-S axes ratios, $F_{(5,1189)}=4.708$; $p=0.00291$ and $F_{(1,1189)}=29.951$; $p=0.000000054$, respectively. However, the interaction term (pattern type *finger) was not significant with a $p=0.1755787$. Both parameters were significant, but finger was highly significant indicating that it has a much larger influence over the north-south ratio than pattern type. Using Tukey's Honestly Significant Difference (Tukey HSD) for a post-hoc test to analyze the differences between the means from the ANOVA, there were no differences in the ratio within finger, but quite a few differences between fingers. Left slant loops on thumbs were different from all pattern types on index fingers except for

arches at the 0.05 level. Right slant loops on thumbs were significantly different from both whorl patterns on index fingers, while arches on thumbs were significantly different from double loops whorls on index fingers. Results suggest that there is a fundamental difference in the placement of the core within certain pattern types that alters the ratio of the north and south axial dimensions.

E. Thiessen Polygon Analysis

The average Thiessen polygon area across all pattern types for bifurcations and ridge endings was 8.35 mm² and 8.79 mm², respectively (Table 2-7). Arches had the largest average Thiessen polygon areas for both bifurcations (9.94 mm²) and ridge endings (10.2 mm²) and whorls had the smallest average Thiessen polygon areas for bifurcations and ridge endings (7.27 mm² and 7.94 mm² respectively).

The total Thiessen polygon area for bifurcations and ridge endings was calculated per image and averaged across all images. A ratio of bifurcations to ridge endings per pattern type was then calculated and a one-way Analysis of Variance (ANOVA; $F_{(5,1194)}=7.359$; $p=0.000000833$) performed. The ratio (B:RE) for total Thiessen polygon area was significant for the two whorl patterns when compared to all other pattern types except whorls and right slant loops, but do not differ amongst themselves. There was no significant difference between the other pattern types. The two whorl patterns were closer to each other in minutiae distribution than the other pattern types. While there was no difference between the arches and loops, the box plots and means indicate a trend, with arches having the lowest ratios of Thiessen ridge ending-to-bifurcation areas and the whorls with the largest ratios (Figure 2-21).

4. CONCLUSIONS

An extensive set of GIS-based analytical tools were developed and have yielded valuable results that aid in the quantification of fingerprint characteristics and spatial distribution of minutiae and ridge lines in georeferenced coordinate space. The above narrative, tables and figures provide examples of the results generated thus far. The analytical tools are very robust and provide a firm foundation upon which to expand our fingerprint probabilities.

The primary results of the GIS-based spatial characterization component of the study may be summarized as follows:

- (1) Techniques in Geographic Information Systems can be successfully applied to spatially analyze fingerprint patterns;
- (2) The standardized georeference system developed for this study provides a standardized coordinate system that allows complex analysis of minutiae and ridgeline distributions across fingerprint space;
- (3) A wide variety of spatial analysis tools can be developed in the GIS software environment to characterize fingerprint features and statistically characterize distributions between pattern types;
- (4) A robust sample set of over 1200 fingerprints, 102,000 minutiae and 20,000 ridge lines were digitally captured from the Oregon population as part of this project effort;
- (5) The average number of minutiae per fingerprint is 85.1, with ridge endings outnumbering bifurcations by a factor of 1.4;

- (6) Minutiae and ridge lines are most densely packed in the region below the core, with the greatest line-length density surrounding the core;
- (7) More complex ridge patterns with higher degrees of line curvature (e.g. whorls and double loop whorls) are associated with a greater number of minutiae as compared to more streamlined patterns (e.g. arches).

Discussion

GIS methodologies and standardized georeferencing allowed for the placement of fingerprint features within a common coordinate space. Once fingers were aligned in coordinate space, the spatial analyses were conducted to characterize pattern types, minutiae distributions and ridge line configurations. Overall, there was a greater density of minutiae and ridgelines below the core than above for all pattern types with the distribution of bifurcations and ridge endings being more similar within any pattern type rather than among them. On average there were more ridge endings than bifurcations for all pattern types with whorls having the greatest number of minutiae followed by loops then arches. The overall characterization of the spatial distribution, frequency and density of minutiae and ridgelines in our study are similar to previously published work (Stoney and Thornton, 1987; Champod and Margot, 1996; Gutierrez et al., 2007; Srihari, 2009). Similar pattern types (e.g., right and left slant loops) tend to have greater similarity between them when comparing various metrics such as hull axis ratios and Thiessen polygon ratios, suggesting that these patterns arise through similar biological phenomena.

As latent examiners have observed, fingerprint minutiae distributions are not uniform nor do they appear to be random. Furthermore, when taking into account the greater number of ridges in the lower region of the fingerprint, as compared with the upper, it does not explain the differential distribution of the minutiae across the fingerprint. It appears that the more complex the ridge pattern type (e.g., double loop whorls vs. arches), the greater number of minutiae present on the finger. The spatial variation between the upper and lower regions of the finger also implies that this differential minutiae distribution is influenced by the complexity of pattern type as the lower sections are where the deltas and other disruptions in ridge flow occur more frequently. Conversely, the upper regions of the finger have a relatively uniform flow of ridgelines with simpler line geometries. Thus, the more complex pattern types (whorls and double loop whorls) tend to be similar to each other, are associated with larger pattern dimensions, and significantly differ from all other pattern types. The less complex pattern types, as exemplified by arches, tend to display fingerprint metrics at the other end of the scale.

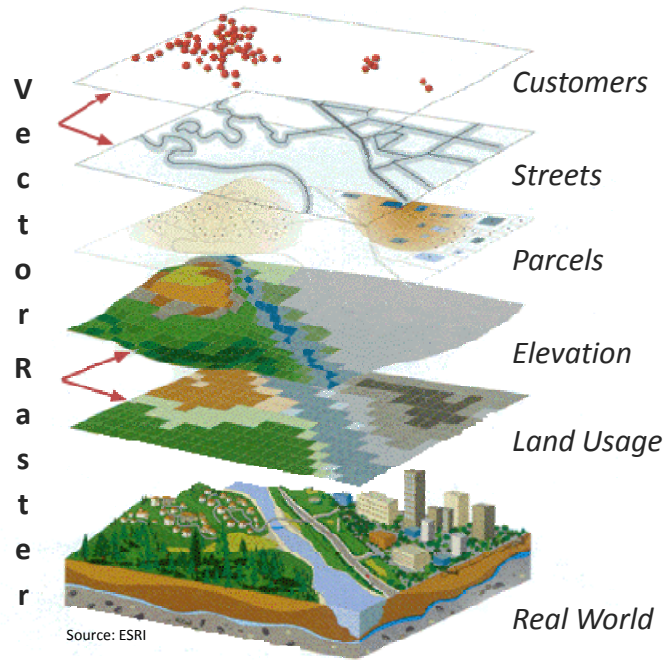
5. REFERENCES

- Aldrich, P.R. 2010. Application of spatial statistics to latent print identification: towards improved forensic science methodologies. Page 66, *in* Proceedings of International Association for Identification, 95th International Educational Conference.
- Bodbyl-Mast, A. 2009. Enhancing the law enforcement workflow: Server GIS app supports analysis, resource management and communication. *ArcUser Magazine*, Winter Edition:20-21.
- Burns, G. A. P. C., W.-C. Cheng, R. H. Thompson, and L. W. Swanson. 2006. The NeuARt II system: A viewing tool for neuroanatomical data based on published neuroanatomical atlases. *BMC Bioinformatics* 7:531-549.

- Chainey, S. and J. Ratcliffe. 2005. GIS and Crime Mapping. John Wiley & Sons Ltd, Hoboken, New Jersey.
- Champod, C. and P. A. Margot. 1996. Computer assisted analysis of minutiae occurrences on fingerprints. pp. 305-318, *in* Proceedings of the International Symposium on Fingerprint Detection and Identification. J. Almog, E. Springer, M. Yisrael, eds., Israel National Police, Neurim, Israel.
- Dutton, E. K. 2010. Application of spatial statistics to latent print identifications: Towards improved forensic science methodologies. Office of Investigative and Forensic Sciences, National Institute of Justice, U.S. Department of Justice.
- Dutton, E. K., S. B. Taylor, P.R. Aldrich, and B. E. Dutton. 2010a. NIJ Grant Project. Page 31 *in* 24th Annual AFIS Internet User's Conference, Portland, Oregon.
- Dutton, E. K., S. B. Taylor, P.R. Aldrich, and B. E. Dutton. 2010b. Application of spatial statistics to latent print identifications, *in* Proceedings of Northwest Association of Forensic Scientists, Portland, Oregon.
- Dutton, E. K., S. B. Taylor, P.R. Aldrich, and B. E. Dutton. 2011. Application of geographic information systems and spatial statistics to probability estimates in latent-print identification. Presented at the International Association for Identification 96th Annual International Educational Conference, Milwaukee, Wisconsin.
- ESRI. 2000. Risk analysis and response - GIS and public safety. ArcUser Magazine, January-March Edition.
- ESRI. 2001. GIS aids emergency response. ArcUser Magazine, July-September Edition.
- ESRI. 2010. Getting to Know ArcGIS Desktop. ESRI Press, Redlands, CA.
- Garb, J., S. Ganai, R. Skinner, C. S. Boyd, and R. B. Wait. 2007. Using GIS for spatial analysis of rectal lesions in the human body. *International Journal of Health Geographics* **6**:11-24.
- Gutierrez, E., V. Galera, J. M. Martinez, and C. Alonso. 2007. Biological variability of the minutiae in the fingerprints of a sample of the Spanish population. *Forensic Science International* **172**:98-105.
- Kucken, M. and A. C. Newell. 2005. Fingerprint formation. *Journal of Theoretical Biology* **235**:71-83.
- Maguire, D. J., M. Batty, and M. F. Goodchild. 2005. GIS, Spatial Analysis and Modeling. ESRI Press, Redlands, CA.
- Martone, M. E., A. Gupta, and M. H. Ellisman. 2004. e-Neuroscience: challenges and triumphs in integrating distributed data from molecules to brains. *Nature Neuroscience* **7**:467-472.
- Price, M. 2012. Mastering ArcGIS, Fifth Edition. McGraw Hill, Boston, Massachusetts.

- Smith, M., M. F. Goodchild, and P. A. Longley. 2007. *Geospatial Analysis - A Comprehensive Guide to Principles, Techniques and Software Tools*. Winchelsea Press, Leicester, England.
- Srihari, S. N. 2009. Quantitative assessment of the individuality of friction ridge patterns. Research report, University at Buffalo, State University of New York, Buffalo, New York.
- Stanley, R. J., E. K. Dutton, S. B. Taylor, P. Aldrich, and B. E. Dutton. 2012. Geographic information systems and spatial analysis - Part 1: Quantifying fingerprint patterns and minutiae distributions. Presented at the AAFS 64th Annual Scientific Meeting, Atlanta, Georgia.
- Stoney, D. A. and J. I. Thornton. 1987. A systematic study of epidermal ridge minutiae. *Journal of Forensic Sciences* **32**:1182-1203.
- Taylor, S. B., R. J. Stanley, E. K. Dutton, P. R. Aldrich, B. E. Dutton, and S. C. Hidalgo. 2012. Novel Use of GIS for Spatial Analysis of Fingerprint Patterns. Presented at the 2012 Annual Meeting of the Urban and Regional Information Systems Association (URISA) GIS Pro Conference, Portland, Oregon.
- Tomlinson, R. F. 1967. An introduction to the Geo-information system of the Canada Land Inventory. ARDA, Canada Land Inventory, Dept. of Forestry and Rural Development, Ottawa, Canada.
- Tomlinson, R. F. 1970. Computer-based Geographical Data Handling Methods, *in* New Possibilities and Techniques for Land Use and Related Surveys. I. H. Cox, editor., Geographical Publications Ltd., Berkhamsted, England.
- Ungar, P. S. and F. M'Kirera. 2003. A solution to the worn tooth conundrum in primate functional anatomy. *Proceedings of the National Academy of Sciences* **100**:3874-3877.
- Watson, C. I., M. D. Garris, E. Tabassi, C. L. Wilson, R. M. McCabe, S. Janet, and K. Ko. 2007. *User's Guide to NIST Biometric Image Software (NBIS)*. National Institute of Standards and Technology.
- Wu, M., L. Koenig, J. Lynch, and T. Wirtz. 2006. Spatially-oriented EMR for Dental Surgery. *in* AMIA 2006 Symposium, Washington D.C., pg. 1147.

A. Example GIS Application



B. GIS Applied to Fingerprints

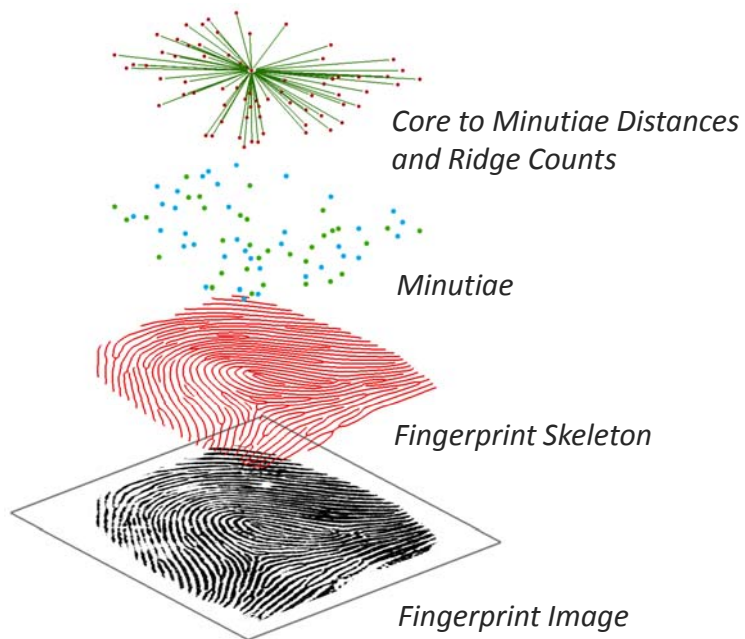


Figure 2-1. Diagram showing components of geographic information systems and related applications to fingerprint analysis.

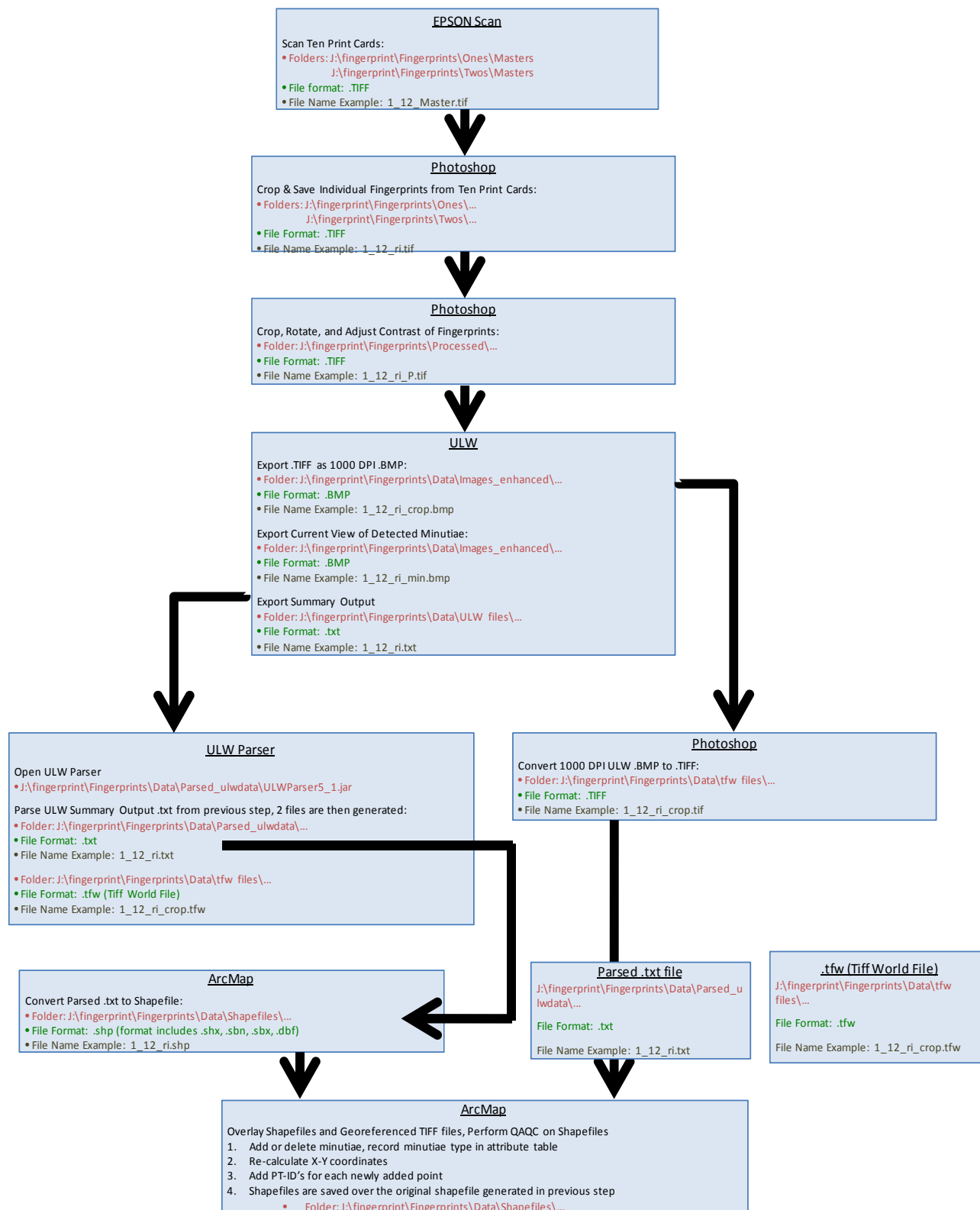


Figure 2-2. Workflow processes developed for data acquisition.

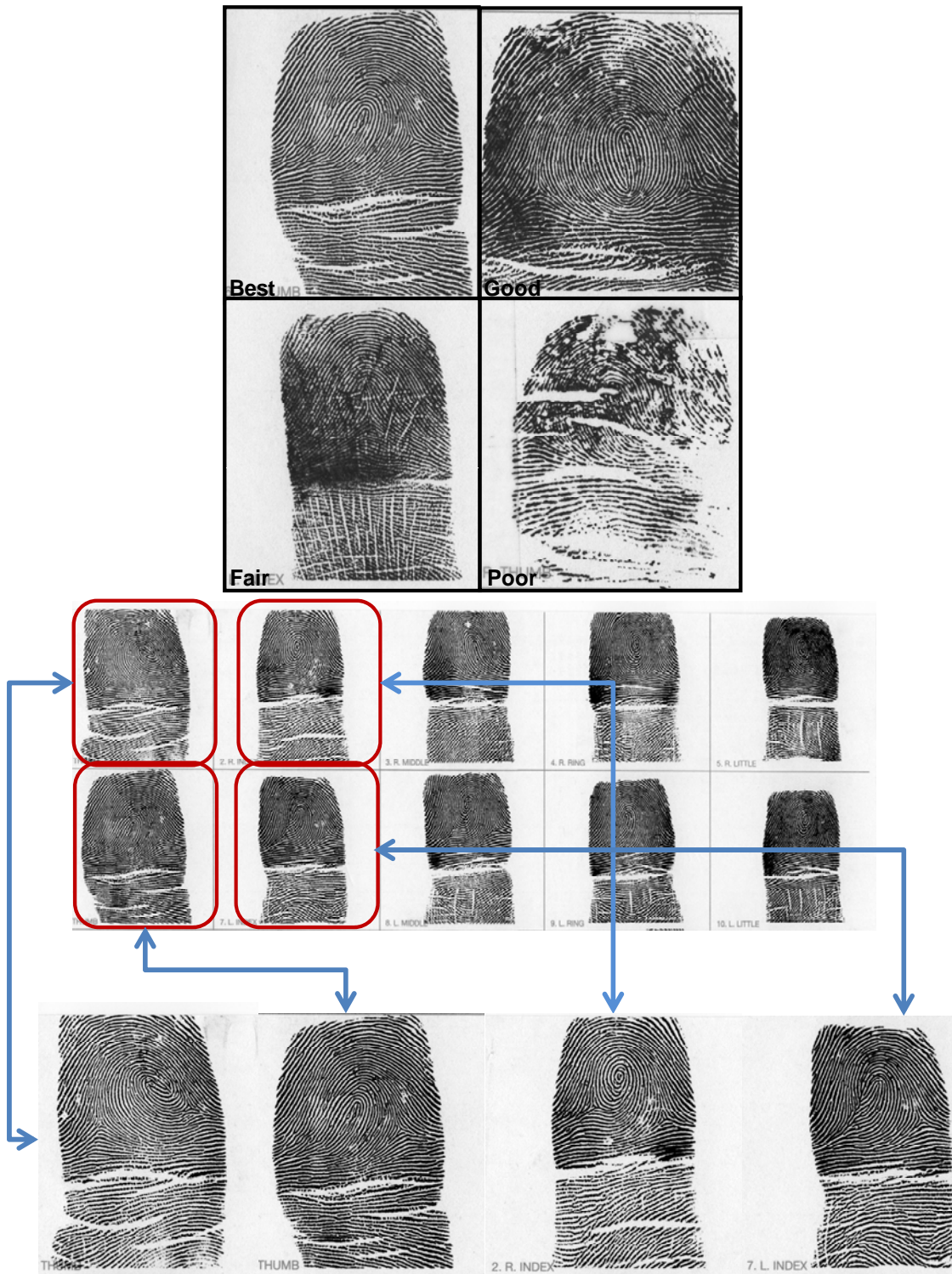


Figure 2-3. Illustration of methods used to assess fingerprint quality and process images as part of the data acquisition techniques .

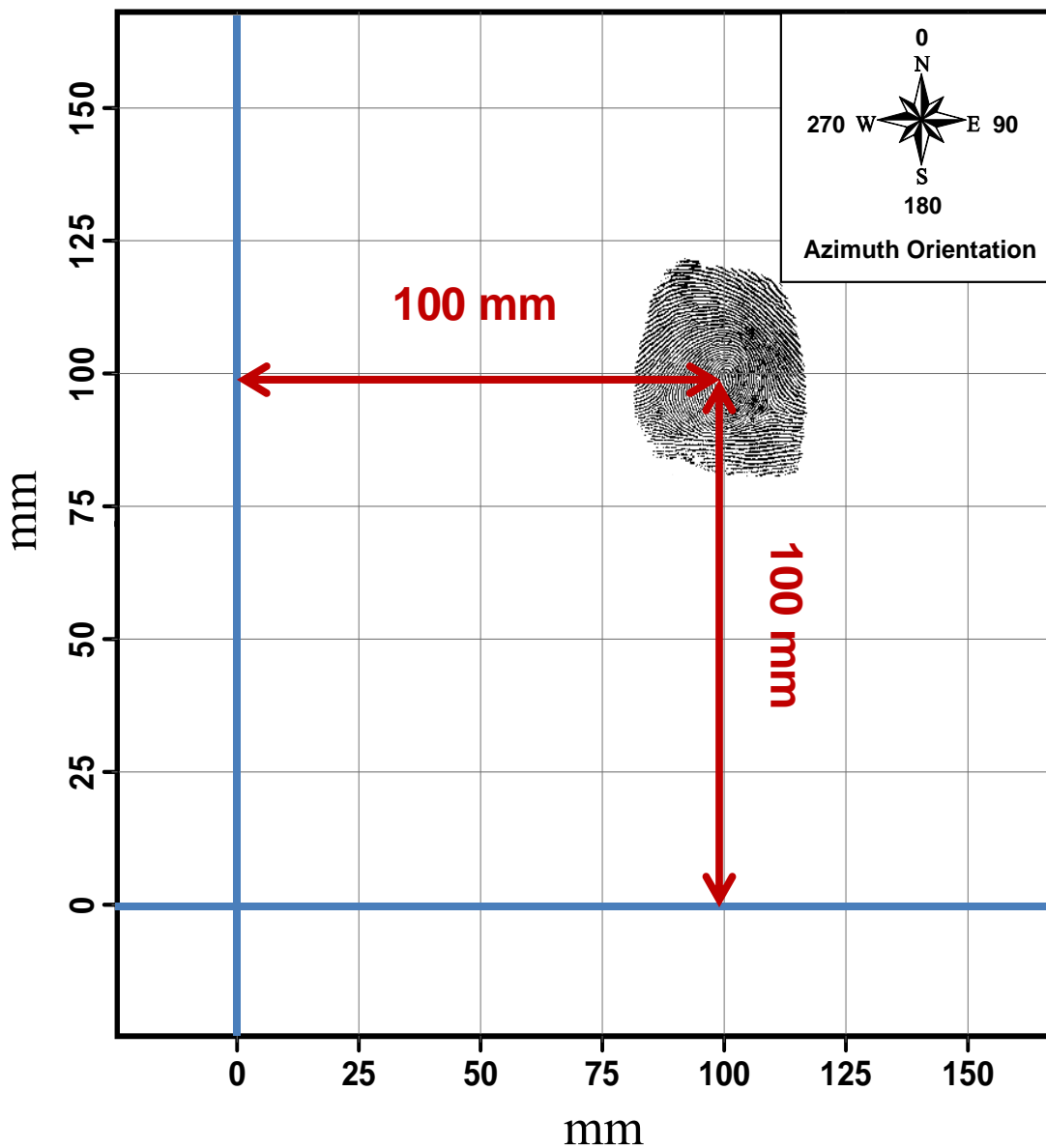


Figure 2-4. Standardized coordinate system to georeference fingerprint images, minutiae and friction ridge lines. The fingerprint core is placed at the (100,100) mm coordinate location placing all fingerprint features in ++ graph space.

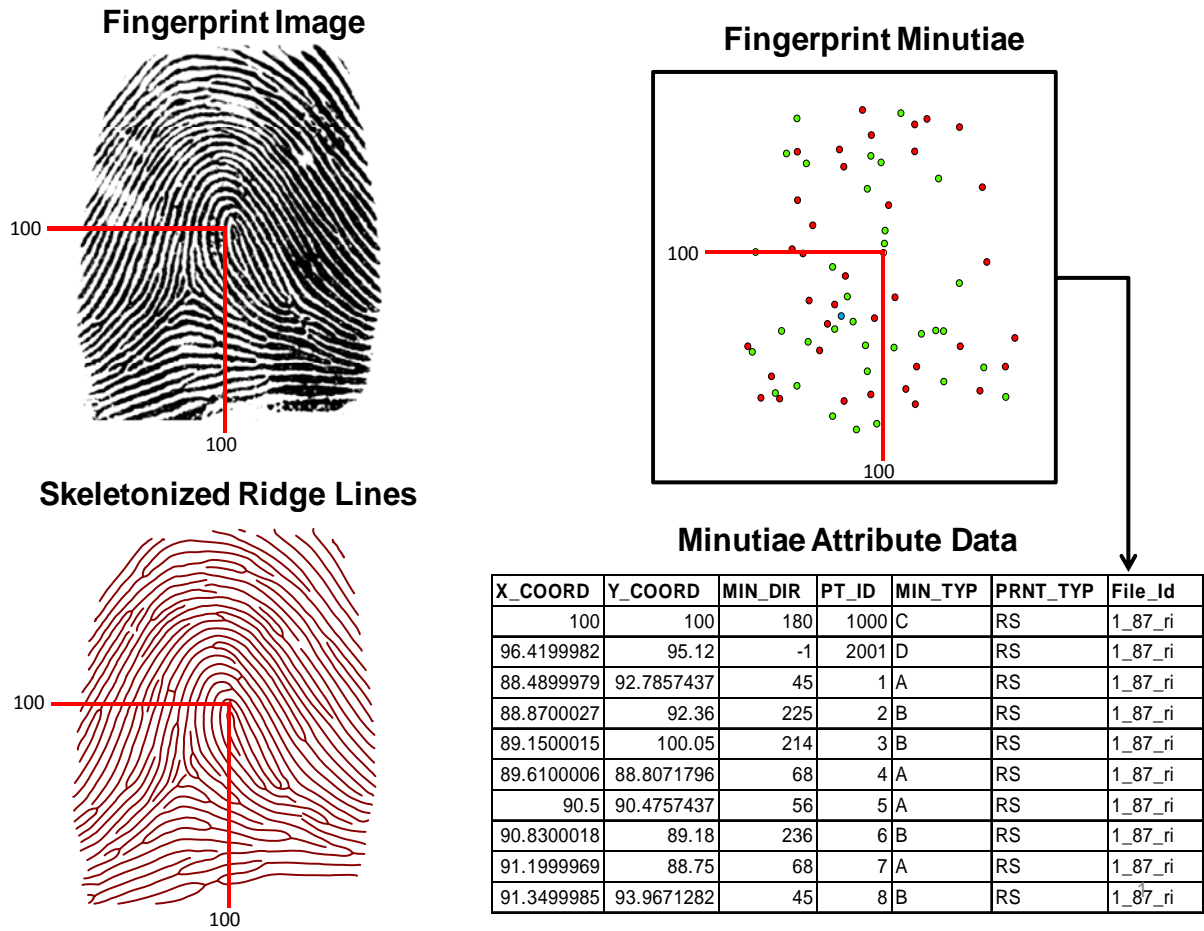
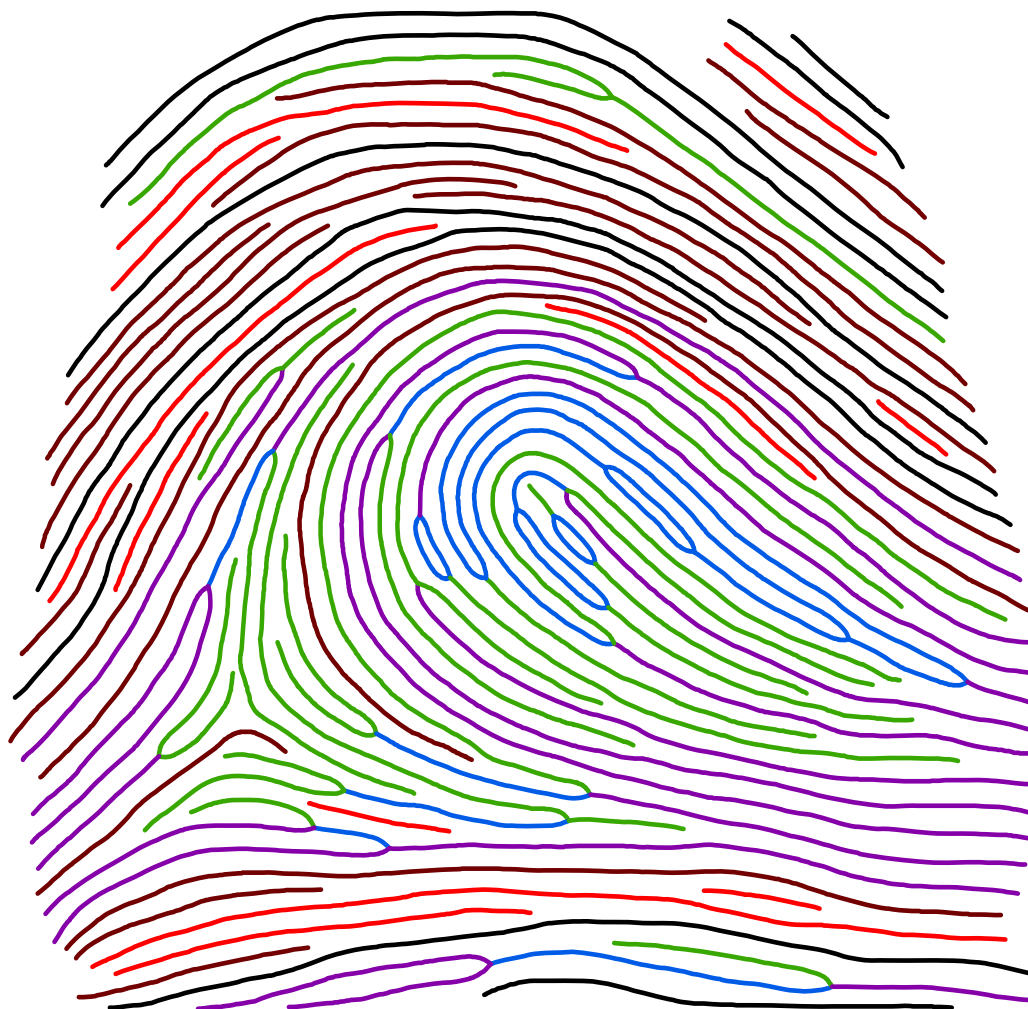


Figure 2-5. Process employed to convert scanned fingerprint images into attributed raster and vector GIS data layers.



Ridgeline Codes

- | | |
|-------------------------------|-----------------------------|
| — Ridge Ending - Ridge Ending | — Bifurcation - Bifurcation |
| — Ridge Ending - Bifurcation | — Bifurcation - Hull |
| — Ridge Ending - Hull | — Hull - Hull |

Figure 2-6. Attribute coding applied to friction ridgelines.

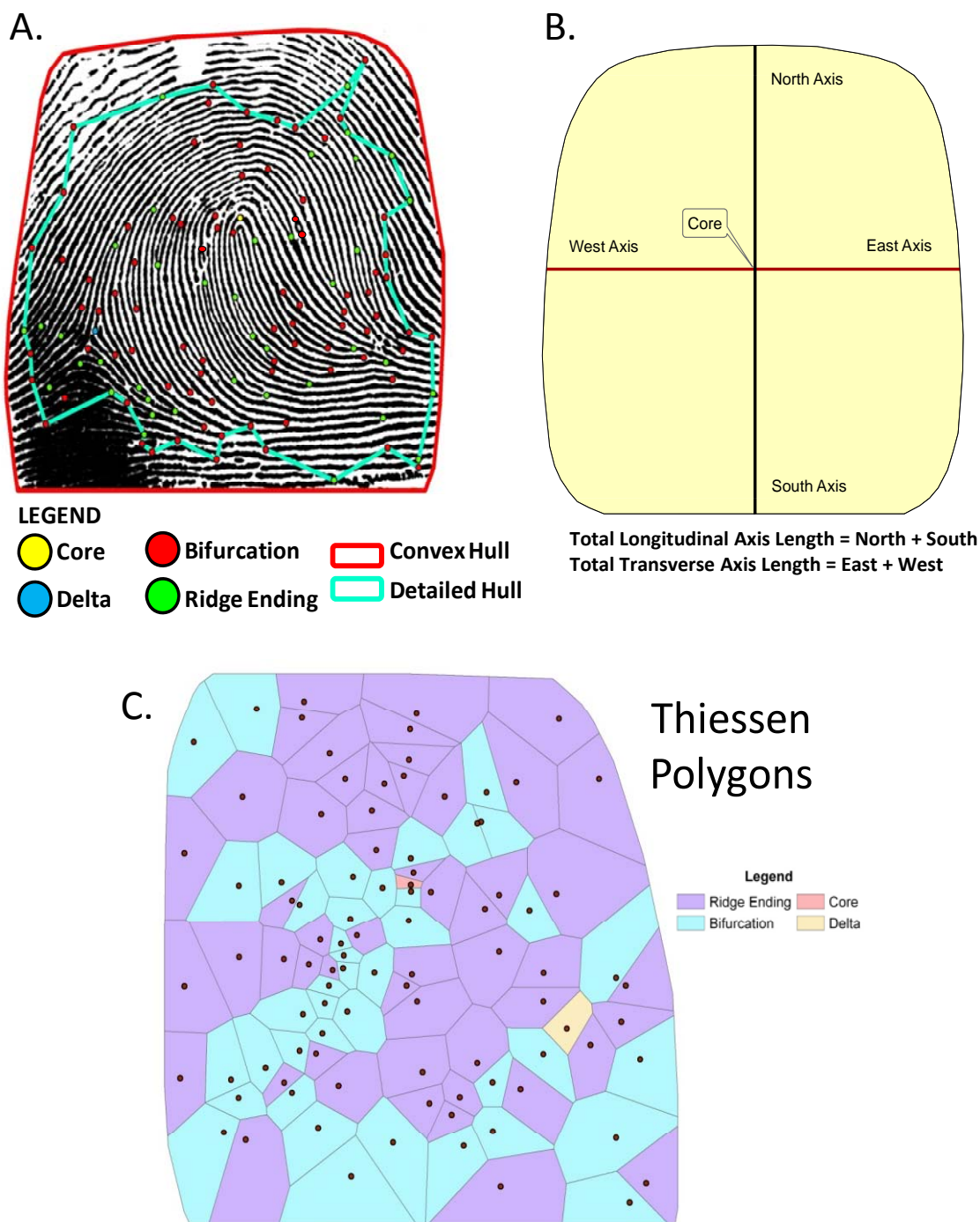


Figure 2-7. Geometric elements used to analyze fingerprint space. A. Outline of convex hull circumscribing the outer fingerprint image; detail hull is defined by polygon circumscribing the inner minutiae point field. B. Axial geometries used to derive convex hull dimensional metrics. C. Thiessen polygon technique in which minutiae are used to define the centroids of a mutually intersecting set of polygons covering fingerprint space. The polygons are attributed by the minutiae type and defined by perimeter and area.

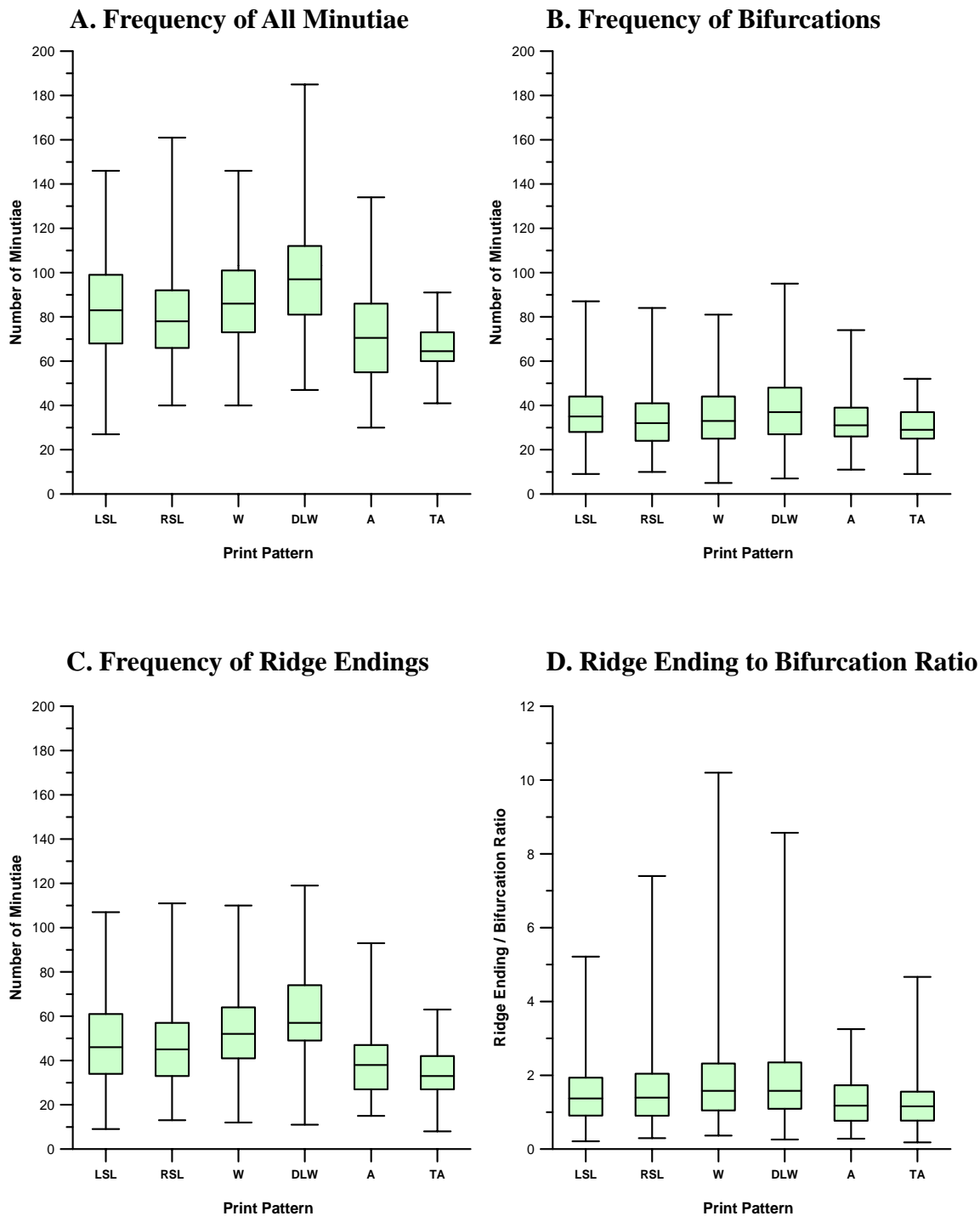
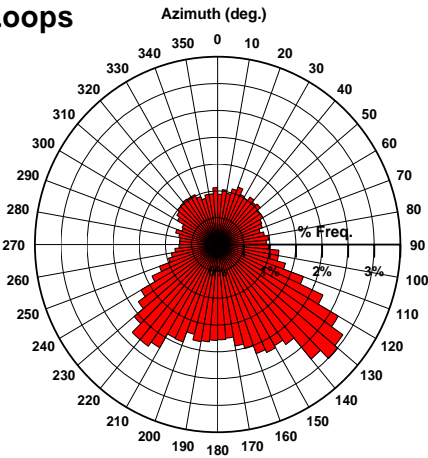
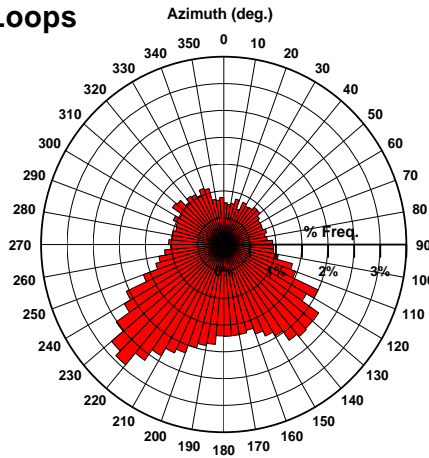


Figure 2-8. Box plots showing frequency distribution of minutiae types distributed across pattern types. Refer to Table 2-3 for related data summary.

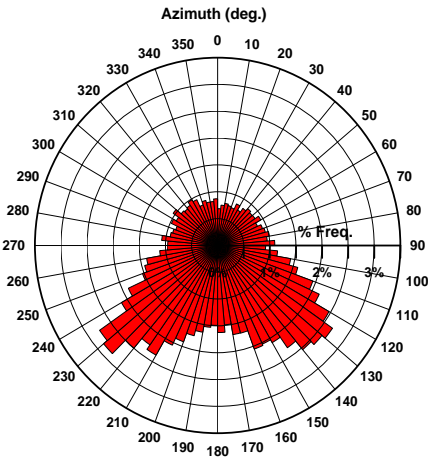
A. Left Slant Loops



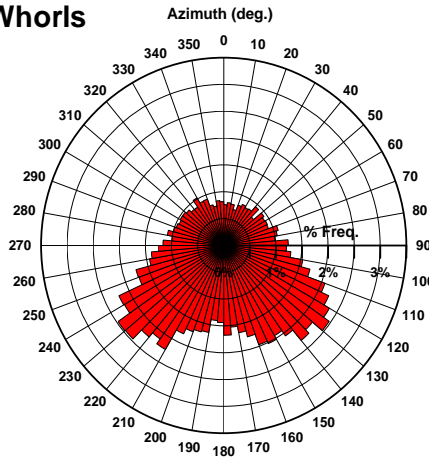
B. Right Slant Loops



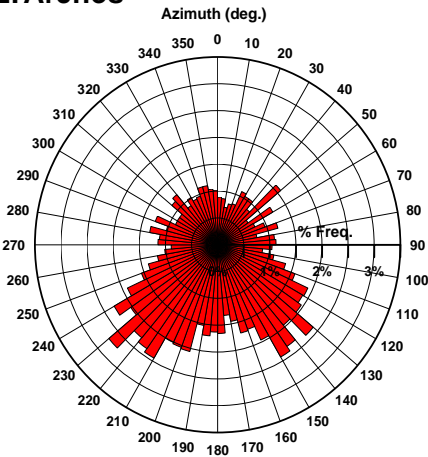
C. Whorls



D. Double Loop Whorls



E. Arches



F. Tented Arches

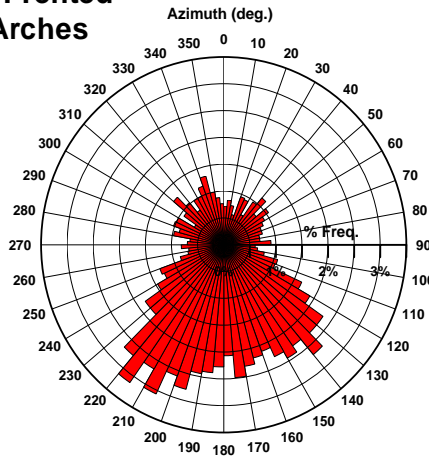


Figure 2-9. Rose plots showing frequency distribution of minutiae locations by pattern type, organized by azimuth direction from core in 10-degree bins.

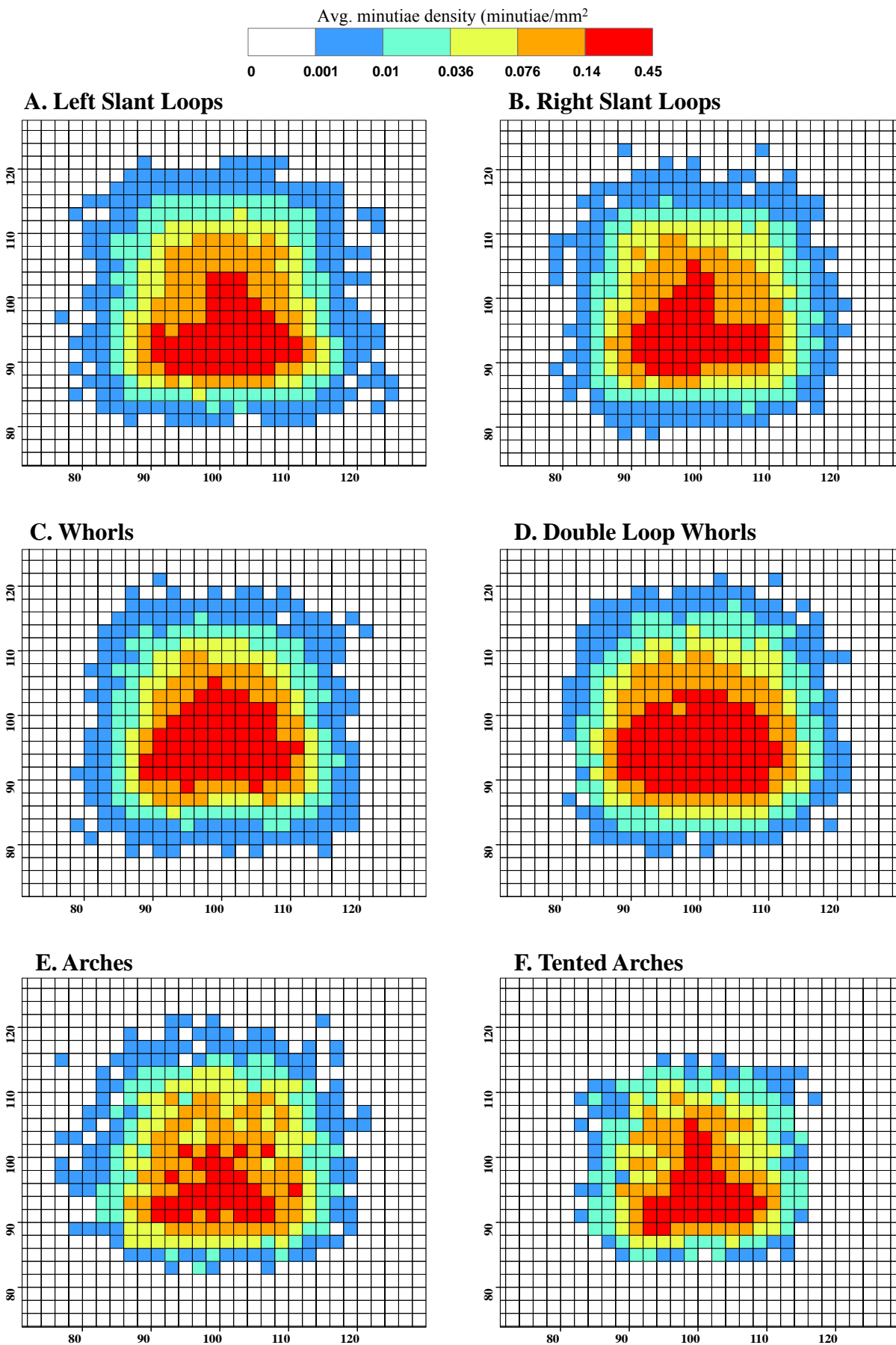


Figure 2-10. Maps showing total minutiae density (count per mm²) as distributed across a standardized 2-mm grid in georeferenced fingerprint space.

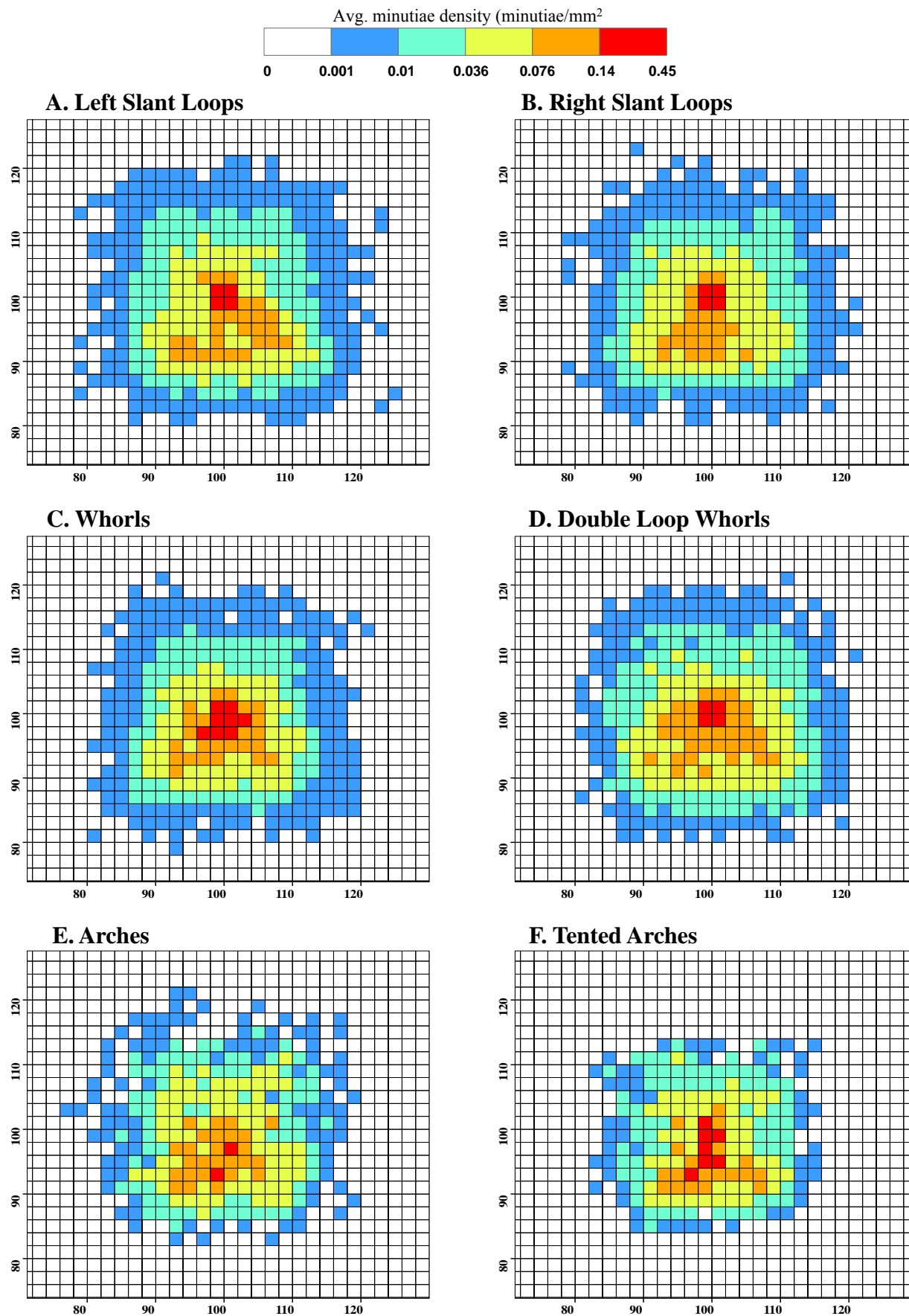


Figure 2-11. Maps showing bifurcation density (count per mm²) as distributed across a standardized 2-mm grid in georeferenced fingerprint space.

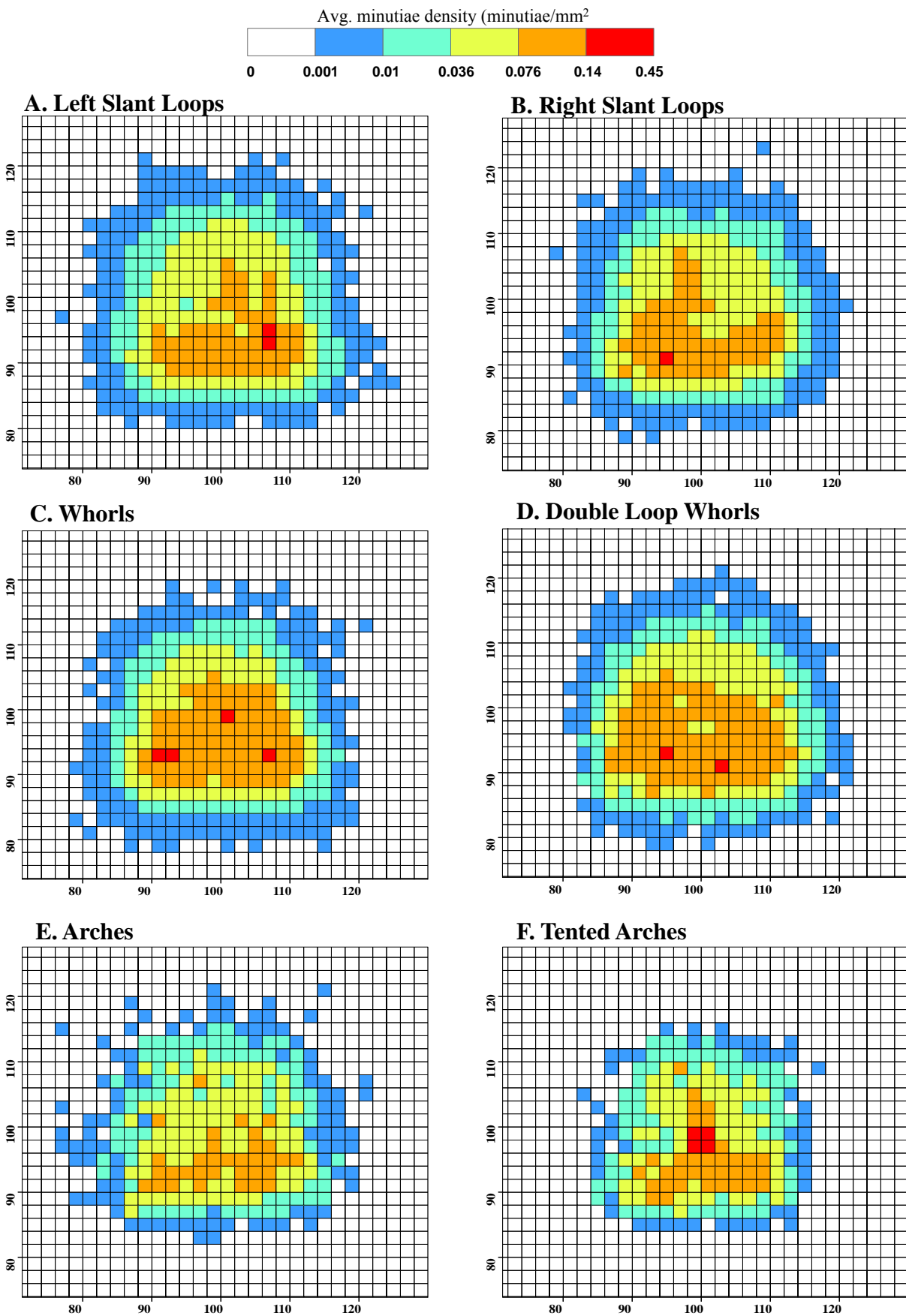


Figure 2-12. Maps showing ridge-ending density (count per mm²) as distributed across a standardized 2-mm grid in georeferenced fingerprint space.

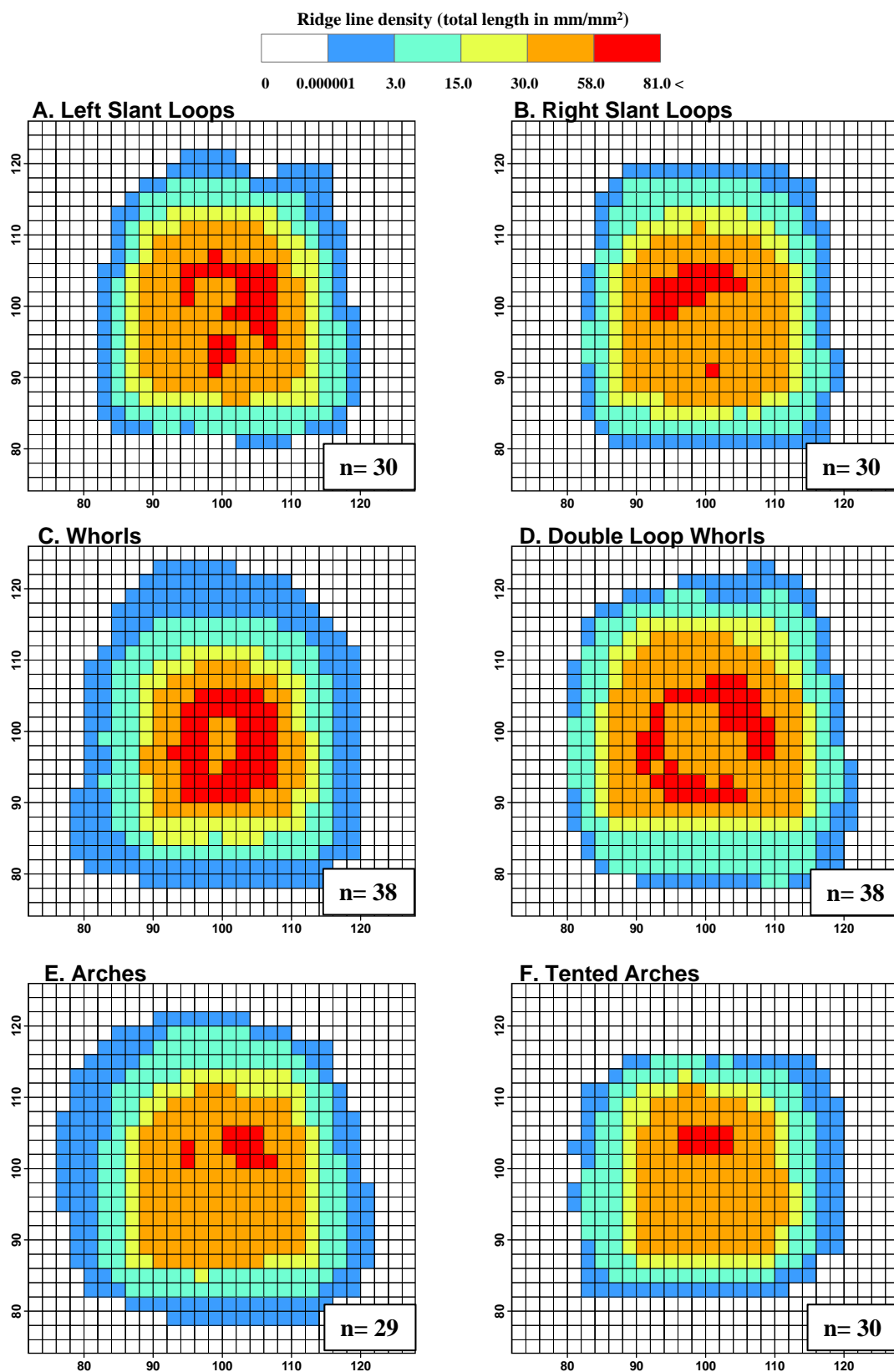
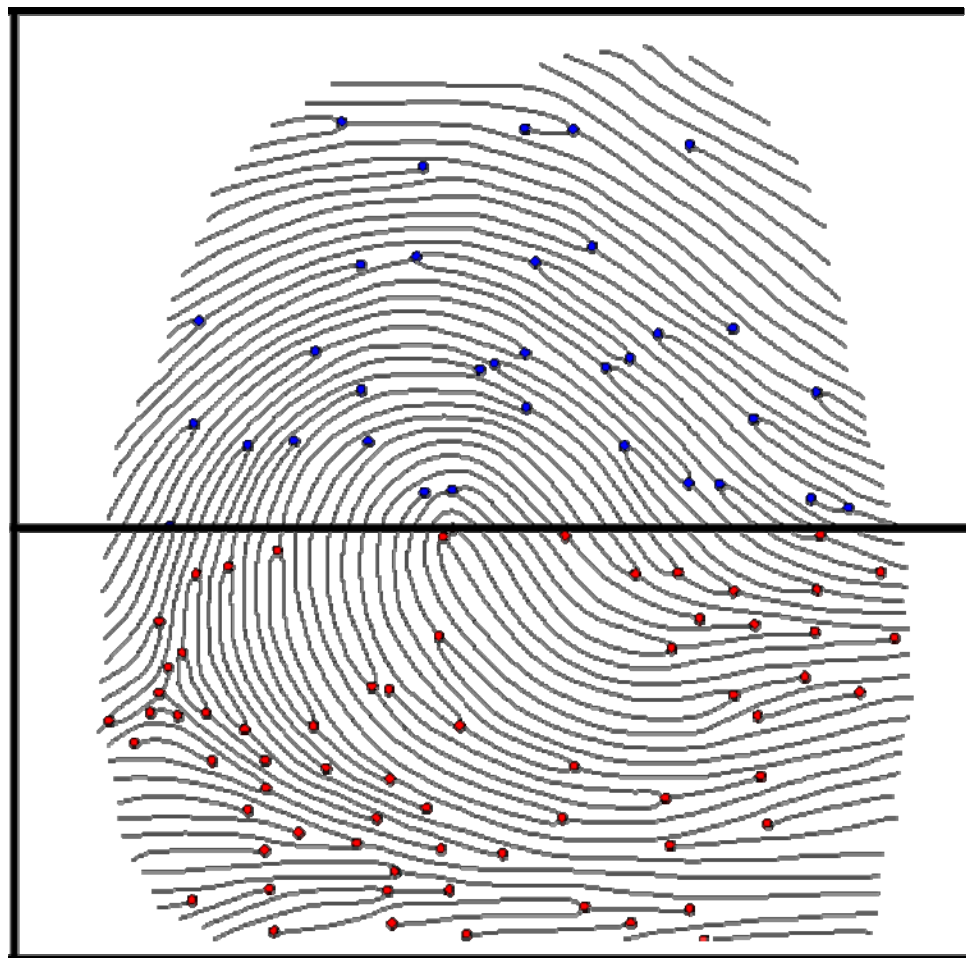


Figure 2-13. Maps showing ridge-line density (total length in mm per mm²) as distributed across a standardized 2-mm grid in georeferenced fingerprint space.



Pattern Type	Minutiae/Ridgeline Ratio Above Core	Minutiae/Ridgeline Ratio Below Core
All Images (n=188)	0.41	0.63
LSL (n=31)	0.47	0.64
RSL (n=33)	0.45	0.63
W (n=41)	0.49	0.71
DLW (n=23)	0.51	0.68
A (n=30)	0.46	0.64
TA (n=30)	0.44	0.66

Figure 2-14. Analysis of minutiae and ridgelines distributions across all fingerprint pattern types, separated by position above and below the core, in the northern and southern hemispheres of fingerprint space, respectively.

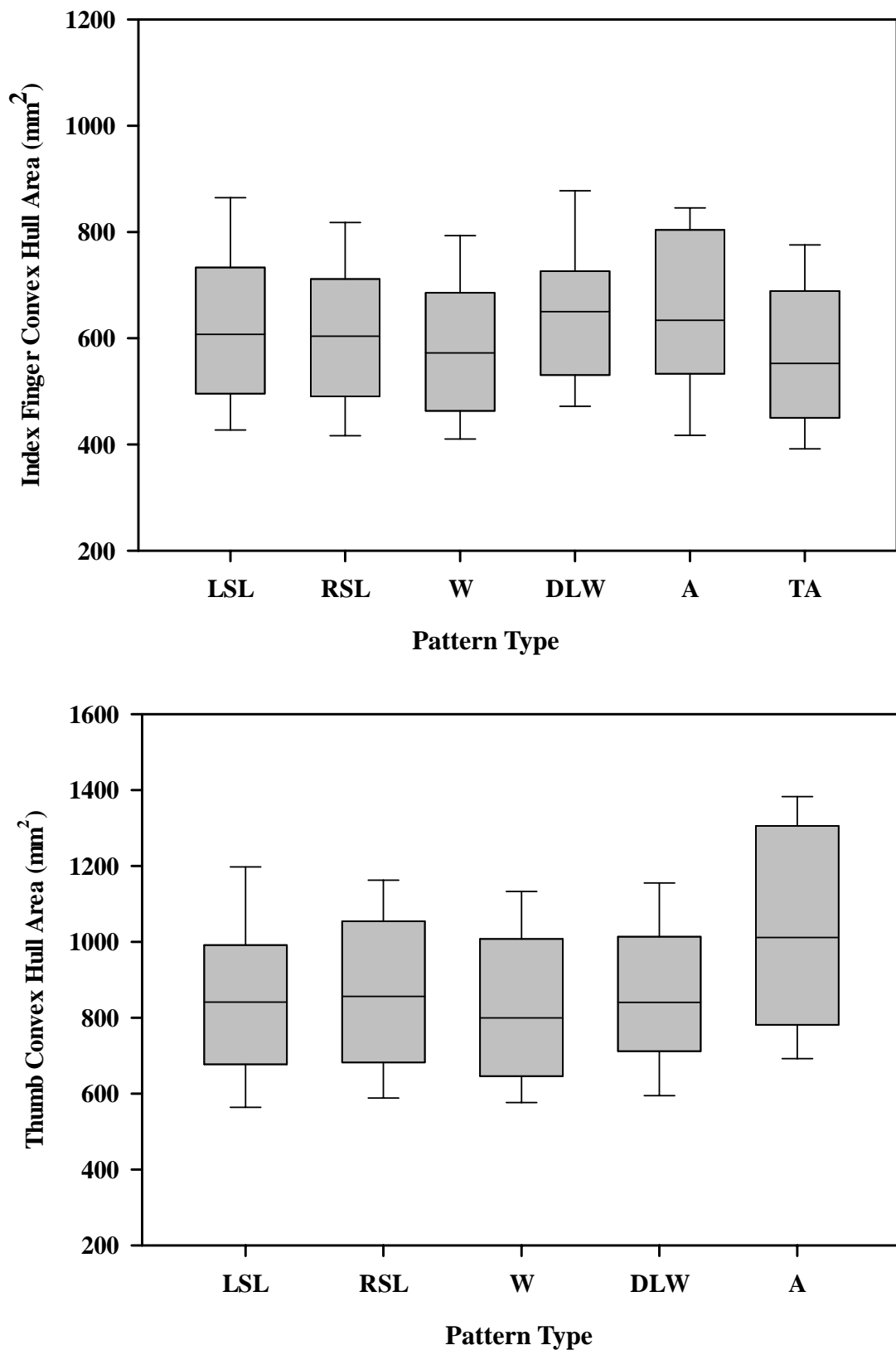
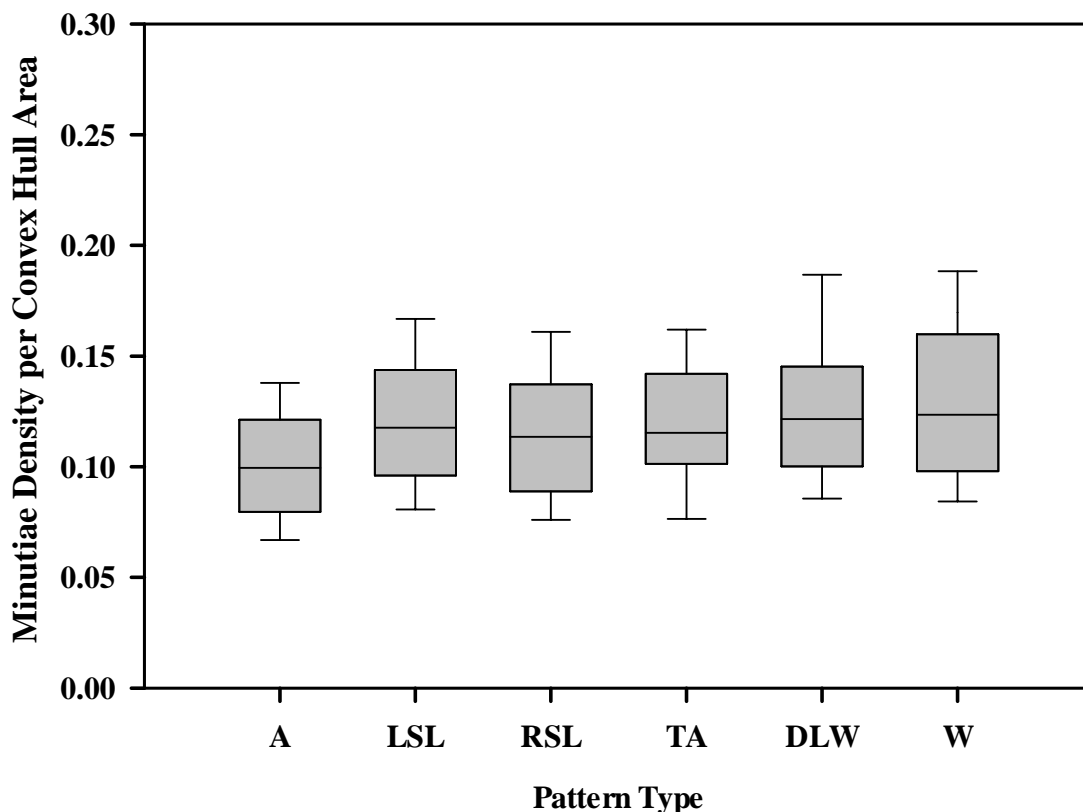


Figure 2-15. Box plots showing distribution of convex hull area (mm²) across all pattern types. Refer to Table 2-4 for related data summary (note: tented arches did not occur on thumbs in dataset).

Total Minutiae Density Over Convex Hull Area



ANOVA: Total minutiae density (no./mm²) over convex hull area separated by pattern type

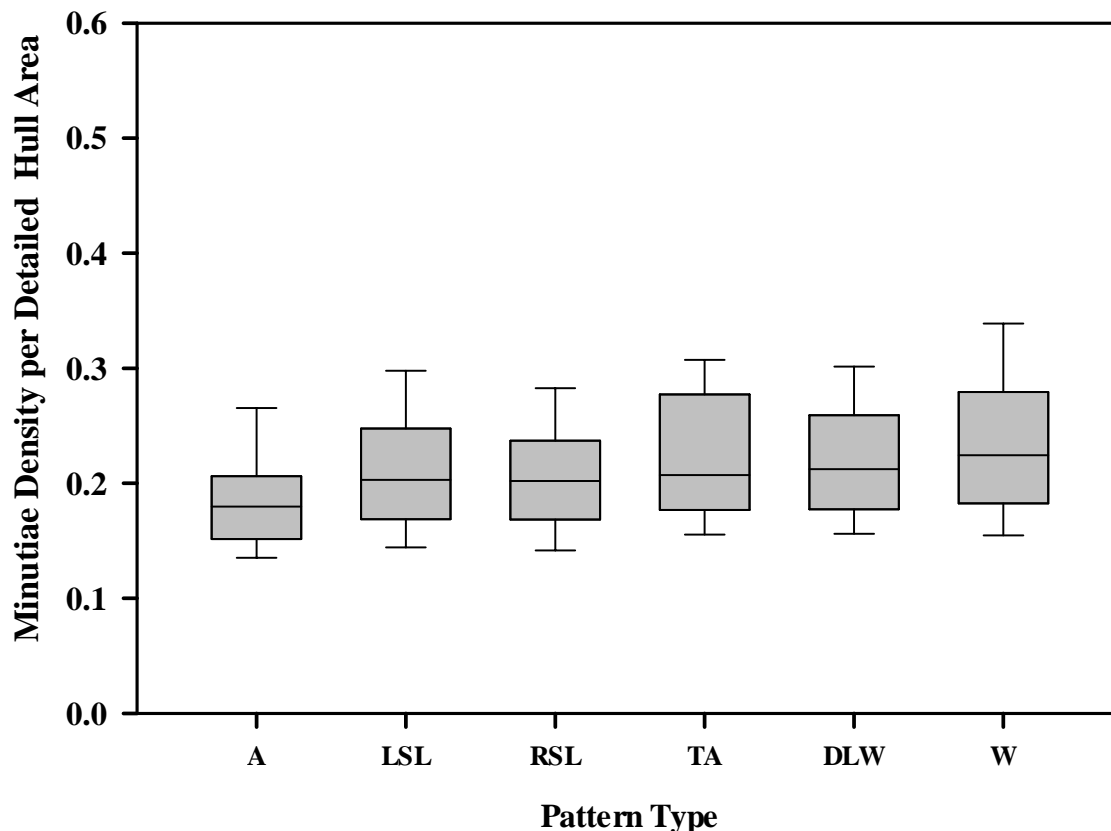
	df	SSE	MSE	F value	p-value
Pattern Type	5	0.0921	0.018425	14.8	0.0000000000000417
Residuals	1194	1.4867	0.001245		

P-values: $\alpha=0.05$

	Arch	LSL	RSL	T.arch	Dbl loop	Whorl
Arch	NA	0.0015032	0.0669361	0.0391189	0.0000092	0.0000000
LSL	0.0015032	NA	0.2955132	0.9999392	0.1971476	0.0000090
RSL	0.0669361	0.2955132	NA	0.9212220	0.0011341	0.0000000
T.arch	0.0391189	0.9999392	0.9212220	NA	0.5482928	0.0172091
Dbl loop	0.0000092	0.1971476	0.0011341	0.5482928	NA	0.3276075
Whorl	0.0000000	0.0000090	0.0000000	0.0172091	0.3276075	N/A

Figure 2-16. Box plots showing distribution of total minutiae density per convex hull area (no. per mm²). Analysis of variance (ANOVA) across pattern types are summarized below. Refer to Table 2-4 for related data summary.

Total Minutiae Density Over Detailed Hull Area



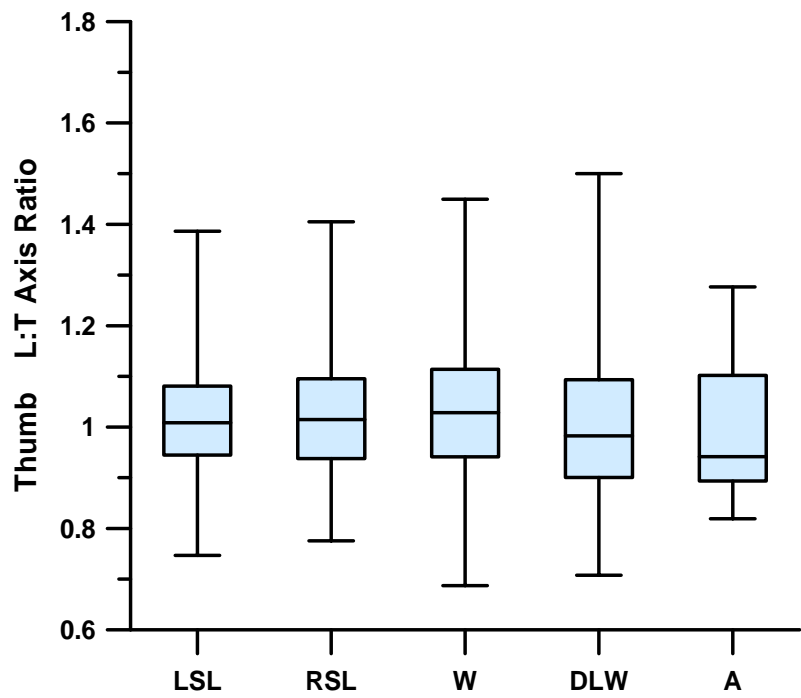
ANOVA: Total minutiae density (no./mm²) over detailed hull area separated by pattern type

	df	SSE	MSE	F value	p-value
Pattern Type	5	0.290	0.05807	15.04	0.0000000000000242
Residuals	1194	4.611	0.00386		

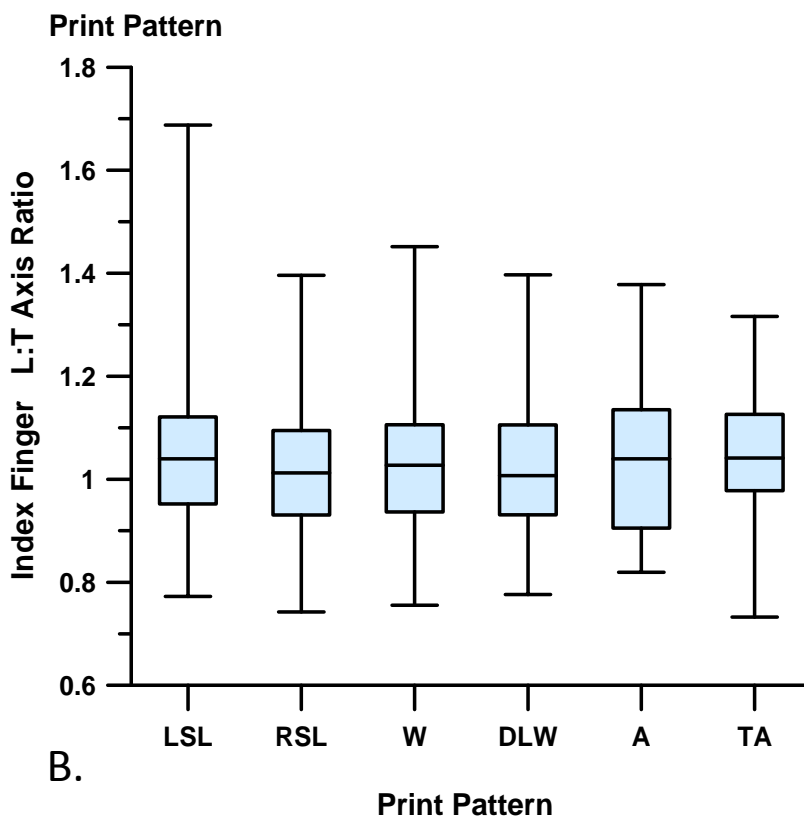
P-values: $\alpha=0.05$

	Arch	LSL	RSL	T.Arch	Dbl loop	Whorl
Arch	NA	0.0144153	0.0855195	0.0041448	0.0003037	0.0000000
LSL	0.0144153	NA	0.8829769	0.7303483	0.3259980	0.0000000
RSL	0.0855195	0.8829769	NA	0.3359697	0.0456987	0.0000000
T.arch	0.0041448	0.7303483	0.3359697	NA	1.0000000	0.1954212
Dbl loop	0.0003037	0.3259980	0.0456987	1.0000000	NA	0.0186161
Whorl	0.0000000	0.0000000	0.0000000	0.1954212	0.0186161	NA

Figure 2-17. Box plots showing distribution of minutiae density per detailed hull area (no. per mm²). Analysis of variance (ANOVA) across pattern types are summarized below. Refer to Table 2-5 for related data summary.



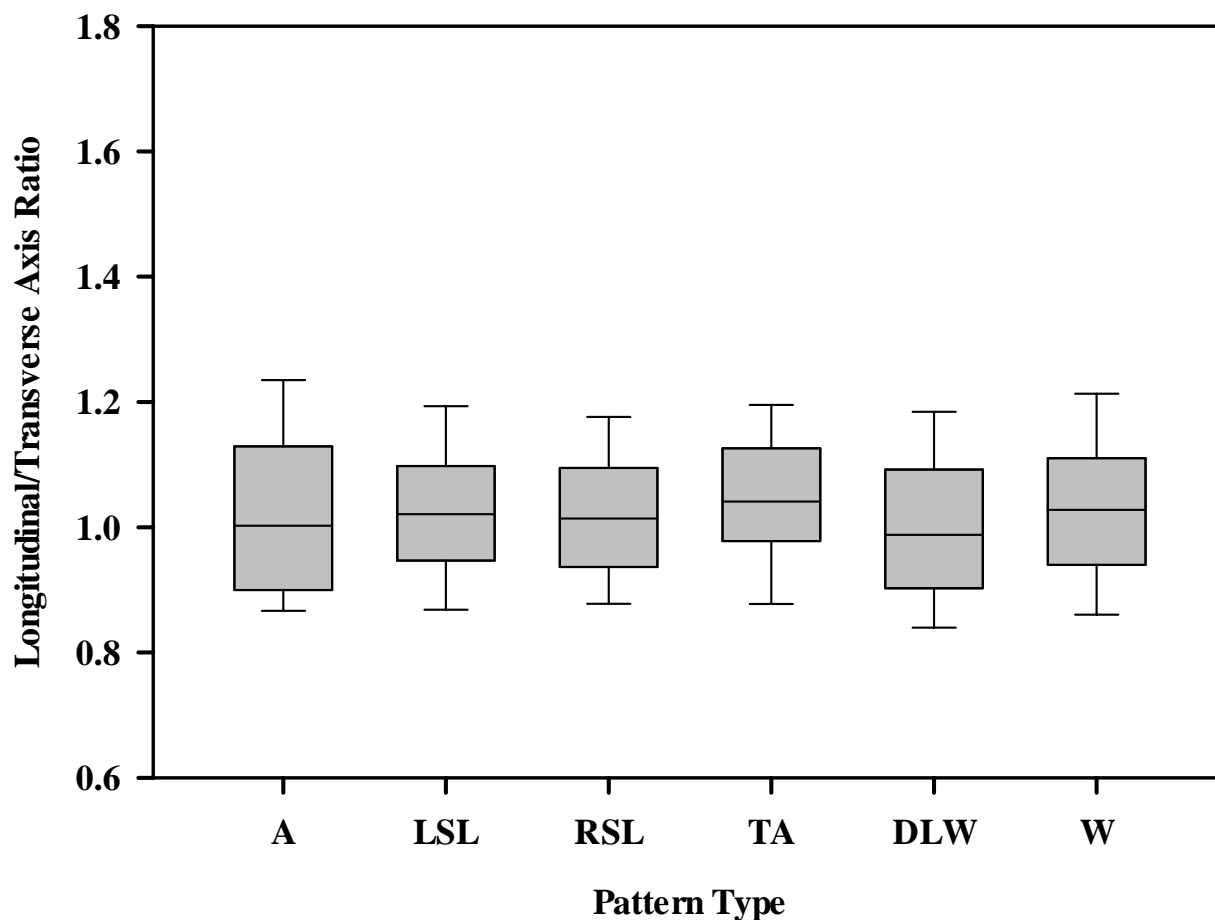
A.



B.

Figure 2-18. Box plots showing distribution of convex hull axial ratios across all pattern types examined in this study. Refer to Table 2-6 for related data summary and to Figure 2-7B for diagrammatic illustration of axial dimensions used to measure hull geometry (L = longitudinal axis length in mm; T = transverse axis length in mm) (note: tented arches did not occur on thumbs in dataset).

Longitudinal-Transverse Ratio by Pattern Type

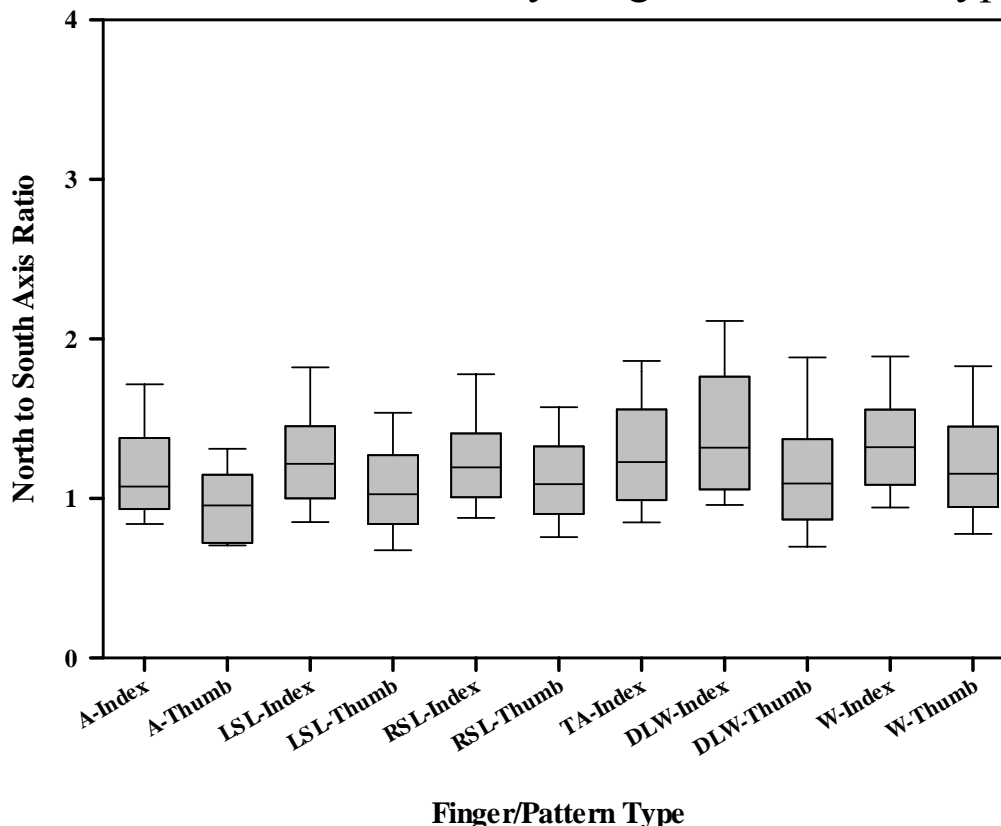


ANOVA: Longitudinal/Transverse axis ratio by pattern type

	df	SSE	MSE	F value	p-value
Pattern Type	5	0.096	0.01923	1.075	0.373
Residuals	1194	21.360	0.01789		

Figure 2-19. Box plots showing distribution of convex hull axial ratios. Analysis of variance (ANOVA) across pattern types are summarized below. Refer to Table 2-6 for related data summary and to Figure 2-7B for diagrammatic illustration of axial dimensions used to measure hull geometry.

North-South Axis Ratio by Finger and Pattern Type



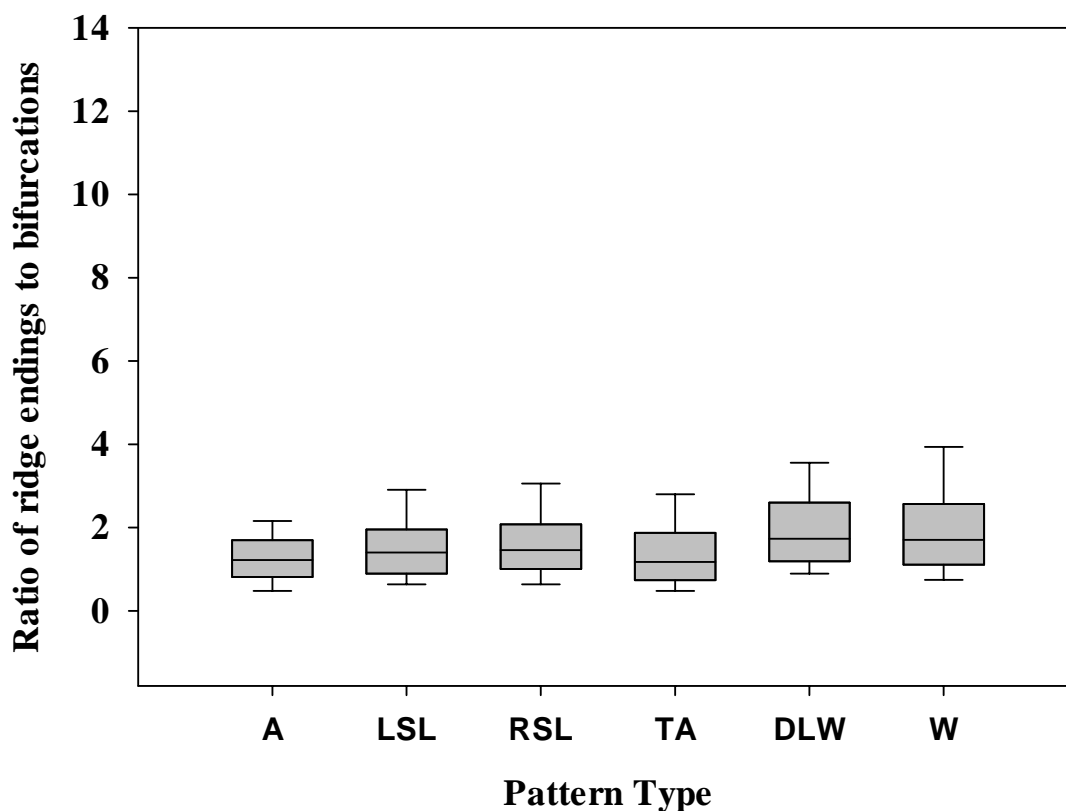
ANOVA: North/South axis ratio by pattern type

	df	SSE	MSE	F value	p-value
Pattern Type	5	6.08	1.217	4.708	0.000291
Finger	1	7.74	7.739	29.951	0.000000054
Pattern Type*Finger	4	1.64	0.410	1.586	0.175578
Residuals	1189	307.23	0.258		

	Arch:I	LSL:I	RSL:I	T.Arch:I	DbI loop:I	Whorl:I	Arch:T	LSL:T	RSL:T	T.Arch:T	DbI loop:T	Whorl:T
Arch:I	NA	0.8835113	0.9973559	0.8192346	0.1758699	0.4679175	0.9499467	0.9967518	1	NA	0.9999969	0.9459585
LSL:I	0.8835113	NA	0.9971687	0.9999987	0.7483235	0.9951065	0.2038209	0.0005255	0.098428	NA	0.8545904	1
RSL:I	0.9973559	0.9971687	NA	0.9863364	0.3084518	0.6751565	0.4644285	0.0435598	0.7182466	NA	0.999867	0.9998494
T.Arch:I	0.8192346	0.9999987	0.9863364	NA	0.9764705	1	0.1710767	0.0087225	0.2034831	NA	0.8296569	0.9999895
DbI loop:I	0.1758699	0.7483235	0.3084518	0.9764705	NA	0.9920498	0.0199723	0.0001542	0.0070114	NA	0.1104891	0.7302978
Whorl:I	0.4679175	0.9951065	0.6751565	1	0.9920498	NA	0.0666095	9.70E-06	0.0051905	NA	0.2525371	0.9921769
Arch:T	0.9499467	0.2038209	0.4644285	0.1710767	0.0199723	0.0666095	NA	0.9982791	0.9426147	NA	0.7121668	0.2700999
LSL:T	0.9967518	0.0005255	0.0435598	0.0087225	0.0001542	9.70E-06	0.9982791	NA	0.9795118	NA	0.4150379	0.0078023
RSL:T	1	0.098428	0.7182466	0.2034831	0.0070114	0.0051905	0.9426147	0.9795118	NA	NA	0.9934509	0.3030109
T.Arch:T	NA	NA	NA	NA	NA	NA	NA	NA	NA	NA	NA	NA
DbI loop:T	0.9999969	0.8545904	0.999867	0.8296569	0.1104891	0.2525371	0.7121668	0.4150379	0.9934509	NA	NA	0.9624923
Whorl:T	0.9459585	1	0.9998494	0.9999895	0.7302978	0.9921769	0.2700999	0.0078023	0.3030109	NA	0.9624923	NA

Figure 2-20. Box plots showing distribution of convex hull, north/south axial ratios. Two-way analysis of variance (ANOVA) by finger and across print types are summarized below. Refer to Table 2-6 for related data summary and to Figure 2-7B for diagrammatic illustration of axial dimensions used to measure hull geometry.

Ratio of Thiessen Polygon Areas by Pattern Type



ANOVA: Thiessen polygon ratio by pattern type

	df	SSE	MSE	F value	p-value
Pattern Type	5	48.6	9.717	7.359	0.000000833
Residuals	1194	1576.6	1.320		

P-values: Thiessen Polygon ratio: $\alpha=0.05$

	Arch	LSL	RSL	T.arch	Dbl loop	Whorl
Arch	NA	0.5252503	0.1539685	0.990632	0.0005655	0.0046764
LSL	0.5252503	NA	0.7588360	0.906176	0.0003792	0.0068614
RSL	0.1539685	0.7588360	NA	0.466062	0.0301573	0.2614357
T.arch	0.990632	0.906176	0.466062	NA	0.003369	0.0252534
Dbl loop	0.0005655	0.0003792	0.0301573	0.003369	NA	0.8945737
Whorl	0.0046764	0.0068614	0.2614357	0.025254	0.8945737	NA

Figure 2-21. Box plots showing distribution of Thiessen polygon area ratios of ridge endings to bifurcations. Analysis of variance (ANOVA) across pattern types are summarized below. Refer to Table 2-7 for related data summary and Figure 2-7C for diagrammatic illustration of Thiessen polygon geometry.

TABLES

Table 2-1. Summary of analytical methods developed for GIS-based fingerprint analysis		
100 - Data Collection Methods	200 - Pattern Characterization Methods	300 – Statistical/Probability Methods
Image Database Entry	Dart Board Min-Point Frequency-Density Quadrat	Minutiae Azimuth Frequency Histograms
Core-to-Minutia Point-to-Point Digitization		
Delta-to-Minutia Point-to-Point Digitization	Thiessen Polygons I (Clipped to Hull)	Minutiae Azimuth Frequency Rose Diagrams
Minutia-to-Minutia Point-to-Point Digitization I (w/o Core + Delta)	Thiessen Polygons II (Dissolved by Min-Type)	
Minutia-to-Minutia Point-to-Point Digitization II (with Core + Delta)	TIN Polygons	Radar Plot Minutiae Positions (azimuth vs. dist. from core)
Ridge Counts	Min-Point Frequency Density Quadrat (2 mm Grid)	Nearest Neighbor Analysis
Ridgeline Skeletonization		
Core-Only Point Layer	Ridge Line Frequency Density Quadrat (2 mm Grid)	Principle Components Analysis (PCA)
Delta-Only Point Layer		
Convex & Detailed Hull Bounding Polygons		Generalized Procrustes Analysis (GPA)
Axis Layer (Longitudinal/Transverse)	Ridge Line Frequency Density TIN-Based & Thiessen Polygon-Based	Thin-Plate Spline (TPS) Deformation Modeling
Minutiae Buffers		
Coded Ridgelines	Superimposition	
Landmark/Semilandmark Designation		

Table 2-2. Census summary of fingers and pattern types analyzed							
Frequency of Pattern Type by Finger and Hand							
FINGER	Left Slant Loops	Right Slant Loops	Double Loop Whorls	Whorls	Arches	Tented Arches	TOTAL
Left Index	125	45	28	58	18	30	304
Right Index	48	110	15	78	21	36	308
Left Thumb	173	2	66	41	9	0	291
Right Thumb	2	152	63	74	6	0	297
TOTAL	349	309	171	251	54	66	1200
HAND	Left Slant Loops	Right Slant Loops	Double Loop Whorls	Whorls	Arches	Tented Arches	TOTAL
Left Hand	298	47	94	99	27	30	595
Right Hand	50	262	78	152	27	36	605

Table 2-3. Summary of minutiae types identified and processed					
Pattern Types: Left Slant Loops (LSL), Right Slant Loops (RSL), Whorls (W), Double Loop Whorls (DLW), Arches (A), and Tented Arches (TA)					
Pattern type	No. of Images	No. Bifurcations (B)	No. Ridge Endings (RE)	Ratio of B:RE	Total No. Minutiae
LSL	348	12701	16936	1:1.3	29637
RSL	309	10390	14420	1:1.4	24810
W	251	9085	13166	1:1.5	22251
DLW	172	6812	10306	1:1.5	17118
A	54	1843	2092	1:1.1	3935
TA	66	2044	2259	1:1.1	4303
Total	1200	42875	59179	1:1.4	102054

Table 2-4. Summary of Minutiae Type and Convex Hull Area for Left Slant Loops (LSL), Right Slant Loops (RSL), Whorls (W), Double Loop Whorls (DLW), Arches (A) and Tented Arches (TA)										
Pattern type	No. of Images	No. Bifurcations (B)	No. Ridge Endings (RE)	Ratio of B:RE	Total No. Minutiae	Convex Hull Area (mm²)		Avg. Minutiae Density/Convex Hull (no./mm² hull area)		
						Avg.	Stdev.	B	RE	Total Minutiae
LSL	348	12701	16936	1:1.3	29637	742.62	236.93	0.05	0.07	0.11
RSL	309	10390	14420	1:1.4	24810	739.69	232.85	0.05	0.06	0.11
W	251	9085	13166	1:1.5	22251	698.70	230.11	0.05	0.08	0.13
DLW	172	6812	10306	1:1.5	17118	811.64	225.85	0.05	0.07	0.12
A	54	1843	2092	1:1.1	3935	753.63	260.93	0.05	0.05	0.10
TA	66	2044	2259	1:1.1	4303	568.77	152.88	0.05	0.06	0.11
Total	1200	42875	59179	1:1.4	102054	719.17	223.26	0.05	0.06	0.11

Table 2-5. Summary of detailed hull area, minutiae density and hull shape factor across all pattern types.							
Pattern type	Detailed Hull Area (mm²)		Avg. Minutiae Density (no./mm²hull area)			Avg. Shape Factor	
	Avg.	Stdev.	B	RE	Total Minutiae	Avg.	Stdev.
LSL	447.81	153.67	0.09	0.11	0.20	1.27	0.08
RSL	424.78	133.90	0.09	0.11	0.20	1.27	0.08
W	409.34	140.26	0.10	0.13	0.23	1.29	0.09
DLW	486.82	148.03	0.08	0.13	0.21	1.28	0.09
A	434.39	157.74	0.08	0.09	0.17	1.28	0.09
TA	328.16	92.28	0.10	0.11	0.21	1.28	0.08

Shape Factor = perimeter/(2 x $\sqrt{(\pi \times \text{area})}$)

Table 2-6. Summary of convex hull dimensions across all pattern types. Refer to Figure 2-7B for diagrammatic illustration of axial dimension used to measure hull geometry.												
Pattern Type	Longitudinal Axis Length (mm)		Transverse Axis Length (mm)		South Axis Length (mm)		L:T Axis Ratio		W:E Axis Ratio		S:N Axis Ratio	
	Avg.	Stdev	Avg.	Stdev	Avg.	Stdev	Avg.	Stdev	Avg.	Stdev	Avg.	Stdev
LSL	28.06	4.58	27.47	4.97	14.69	2.62	1.03	0.14	0.98	0.24	1.20	0.49
RSL	27.94	4.71	27.50	4.77	14.83	2.61	1.02	0.12	1.02	0.26	1.21	0.44
W	27.19	4.76	26.54	4.87	15.18	2.87	1.04	0.14	1.04	0.26	1.36	0.46
DLW	29.18	4.64	29.17	4.37	15.74	2.96	1.01	0.14	1.00	0.24	1.31	0.62
A	28.10	4.52	28.01	5.56	14.51	2.29	1.02	0.14	1.16	0.41	1.14	0.34
TA	24.63	3.54	23.72	3.64	13.54	1.80	1.05	0.12	1.04	0.35	1.37	0.76
Avg. Total	27.52		27.07		14.75		1.03		1.04		1.27	

Table 2-7. Summary of Thiessen polygon area by pattern types and by minutiae type. Refer to Figure 2-7C for diagrammatic illustration of Thiessen polygon geometry

Pattern type	Thiessen Polygons Bifurcation Area (mm ²)		Thiessen Polygons Ridge Ending Area (mm ²)		Thiessen Polygons Core Area (mm ²)		Thiessen Polygons Delta Area (mm ²)	
	Avg.	Stdev.	Avg.	Stdev.	Avg.	Stdev.	Avg.	Stdev.
LSL	8.39	7.08	8.63	7.15	3.41	3.08	2.80	4.28
RSL	8.64	7.87	9.14	7.80	4.18	3.84	3.50	4.28
W	7.27	6.70	7.94	6.78	3.38	2.67	3.40	4.64
DLW	7.53	6.93	8.20	7.28	3.35	2.52	3.98	5.63
A	9.94	8.50	10.15	8.06	6.64	4.42	N/A	N/A
TA	8.31	7.10	8.68	7.18	3.46	3.43	N/A	N/A
Average	8.35	7.36	8.79	7.38	4.07	3.33	3.42	4.71

CHAPTER 3 – GEOMETRIC MORPHOMETRIC ANALYSES

1. INTRODUCTION

Research on the spatial relationship of fingerprint features, (e.g., minutiae and ridge lines) and the application of this information to automatic fingerprint identification systems have historically employed biometric techniques. These methods generally involve analyzing linear geometrical properties of the fingerprint physical characteristics (e.g., the distances between minutiae and the geometric pattern formed). While biometric techniques are an invaluable tool for exploring covariance among sets of geometric comparators, these techniques ignore the biomathematical aspects of the original measurements (Bookstein 1996). These biomathematical aspects include inherent biological properties (e.g., homology and embryology) of biological features (i.e., minutiae) that can be represented by their spatial arrangements. Furthermore, failure to consider these aspects when analyzing minutiae may exclude important spatial patterns that are dictated by underlying embryological and evolutionary cues. As a biomathematical modeling method, geometric morphometrics utilizes biologically-based features (i.e., homologies) that are useful for quantitatively studying shape variation and is what distinguishes it from biometric approaches. Geometric morphometrics includes techniques from statistics, non-Euclidean geometry, multivariate biometrics and computer graphics that do not sacrifice biomathematical aspects (Bookstein 1996).

Within the forensic science community, forensic anthropology has led the way in exploring the applicability of geometric morphometric techniques. Examples include analyzing mandibular morphology (Franklin et al. 2007, Franklin et al. 2008) and craniofacial landmarks (Kimmerle et al. 2008), studying frontal sinus radiography methods for making identifications (Christensen 2005), creating a virtual 3-D reconstruction of a fragmented cranium (Benazzi et al. 2009), and estimating pediatric skeletal age (Braga and Treil 2007). However, to date, there has been very little exploration of the use of geometric morphometric techniques for the study of fingerprint shape variation.

For this project, geometric morphometric analyses were employed to study shape variation of four fingerprint pattern types in an effort to ascertain the extent and degree of variation within and among fingerprint patterns. These analyses were conducted utilizing GIS spatial analysis tools described in Chapter 2 as it minimized data manipulation and increased the overall efficiency of spatial analyses. Tasks completed include: (1) establishing a methodology for conducting geometric morphometric analyses on fingerprints in a GIS environment in combination with Python programming language and R statistical software (version 2.15.0; software available from <http://www.r-project.org/>), and (2) completing an initial analysis of shape variation on four fingerprint patterns [(A) left slant loops (LSL), (B) right slant loops (RSL), (C) whorls (W) and (D) double loop whorls (DLW)] using generalized Procrustes analysis, thin plate spline and principle components analysis. The resulting data were used to characterize the shape of four fingerprint pattern types and describe the foundational shape variation within and among these pattern types.

2. METHODS

The methods developed and employed include the following steps:

- A. Landmark/Semilandmark Designation and Acquisition
- B. Generalized Procrustes Analysis (GPA)
- C. Thin-Plate Spline (TPS)
- D. Principle Components Analysis (PCA)

See (Slice 2007) for definitions and further discussion.

A. Landmark and Semilandmark Designation and Acquisition:

As described in Chapter 2, fingerprint images were obtained from ten-print cards provided by the Oregon State Police Forensic Services Division. All images were georeferenced in ArcGIS to position the core at (100, 100 mm) within Cartesian coordinate space. Each image was vectorized (i.e., skeletonized) prior to analysis to clearly demarcate the ridge lines.

Determination of landmarks (putative biological homologues) and selection of semilandmarks (points along a ridge line, see Figure 3-1) followed the definitions used by Zelditch et al. (2004) in conjunction with fingerprint features described by Wertheim (2011). Landmarks and semilandmarks were designated and acquired for 30 images from each of the four pattern types (LSL, RSL, W and DLW). Due to similarities between LSLs and RSLs, and Ws and DLWs, landmark and semilandmark designation and acquisition for each of these fingerprint pattern type pairs was conducted in a comparable fashion as described below.

Features associated with the core and the delta regions were designated as landmarks/semilandmarks. For loops, the core was defined as a point along the innermost ridgeline that forms the first full loop where the tangential angle most closely approximates 0 degrees (i.e., highest point of recurve). For whorls, the core was defined as the ridge ending or “bulls-eye” at the center of the whorls. All cores were georeferenced at 100, 100 mm in Cartesian coordinate space. The delta region was defined according to Kücken and Newell (2005) as a triradius consisting of three ridge systems converging with each other at an angle of roughly 120 degrees. A scalable equilateral triangle was utilized for placement of the delta. One operator placed all the delta-defining triangles in a manner that best reflected the flow of each of the ridge systems while keeping each defining triangle as small as possible. Quality control measures included visual inspection of the placement of each delta-defining triangle and 100% consensus among project staff. Three landmarks were then derived from the vertices of the equilateral triangle that approximated the delta region (Figure 3-2).

Four landmarks and nineteen semilandmarks were chosen for LSL and RSL pattern types. The four landmarks included the core and the three landmarks derived from vertices of the equilateral triangle that approximated the delta region (Figure 3-1). Following designation of the core landmark, a radial line template composed of seven lines separated by 18 degree increments was drawn such that all segments radiated distally from the core. Seven semilandmarks were calculated at points of intersection between the radial line template and the first continuous ridgeline distal to the core (Figure 3-2A; Points 1-7). Two reference lines were drawn; a vertical reference line from the core X-coordinate to the distal interphalangeal crease and a horizontal reference line from the Y-coordinate of the lowermost delta vertex to the vertical reference line (Figure 3-2A). Ten equidistant horizontal lines were then drawn perpendicular to the vertical reference line extending from the core landmark to where it intersected with the delta reference vertex (six lines are shown). The points of intersection between the uppermost six horizontal lines and the innermost loop ridgeline (i.e., the core ridgeline) yielded 11 semilandmarks; six semilandmarks were designated along the core ridgeline distal to the delta (semilandmarks 9-14), and five were designated along the ridgeline proximal to the delta (semilandmarks 15-19). The final semilandmark (23) was designated at the point of intersection between the X-coordinate of the core landmark and the distal interphalangeal crease of the finger. The crease line geometry was derived from the convex hull fingerprint polygon (Figure 3-2A).

Six landmarks and fourteen semilandmarks were chosen for whorl and double loop whorl pattern types. The six landmarks were derived from the three vertices of the two equilateral triangles that approximated each delta region (Figure 3-2B, landmarks 14-19). Following the establishment of the core reference point, a radial line template composed of thirteen lines separated by nine degree increments was drawn such that all segments radiated distally from the core. Thirteen semilandmarks were calculated at points of intersection between the radial line template and the first continuous ridgeline distal to the core (Figure 3-2B, semilandmarks 1-13). The final semilandmark was calculated at the point of intersection between the X coordinate value of the core reference point and the distal interphalangeal crease of the finger (Figure 2-3B, semilandmark 20). The crease line geometry was derived from the convex hull fingerprint polygon (Figure 3-2B).

After defining landmarks and semilandmarks, a GIS automated extraction procedure was developed and employed for recording semilandmark data for all 120 fingerprint images. All landmarks and semilandmarks were captured as vector point files that corresponded to a single fingerprint image. The extraction procedure resulted in four vector files for loop patterns and three vector files for whorl patterns that were derived from individual fingerprint features. For loop pattern types, the four vector files included the single, uninterrupted, edge-to-edge ridgeline proximal to the core, the innermost recurving ridge from the fingerprint core, an equilateral triangle that best approximated the delta region triradii ridgeline convergence formations, and a convex hull polygon that bounded the margins of a cropped fingerprint image (Figure 3-2A). For whorl pattern types, the three vector files included the single, uninterrupted, edge-to-edge ridgeline proximal to the core, two equilateral triangles that best approximated the delta regions' triradii ridgeline convergence formations, and a convex hull polygon that bounded the margins of a cropped fingerprint image (Figure 3-2B).

B. Generalized Procrustes Analysis (GPA):

Using a custom ArcGIS tool, landmark and semilandmark coordinates were superimposed into a common coordinate system that preserved shape variables in order to conduct statistical analyses. This involved formatting X-Y coordinate values from landmark and semilandmark point files as numeric arrays, calculating Procrustes mean shape values and registering landmark and semilandmark coordinates using geometric transformations (i.e., translation, rotation, and scaling). Procrustes mean shape values were generated using the "procGPA" function in the 'shapes' package (Dryden and Mardia 1998; Dryden 2012) for R (version 2.15.0). This analysis included the superimposition of all landmarks and semilandmarks for LSLs and RSLs and all Ws and DLWs, respectively, in order to show inter-class variance between each pair of fingerprint pattern types that are most similar one another. This analysis was based on a total of 60 fingerprint images per each pattern type pair.

C. Thin-Plate Spline (TPS):

The Procrustes mean shape values were analyzed using the "tpsgrid" function of the 'shapes' package (Dryden and Mardia 1998; Dryden 2012) for R (version 2.15.0) to produce thin-plate spline (TPS) deformation grids. TPS deformation grids were used to provide a maximally smooth (i.e., minimally bent) interpolation of the inter-landmark space and to provide an exact mapping of the group landmark and semilandmark means of one fingerprint pattern type superimposed onto another. TPS analysis included comparison of LSL to RSL fingerprint mean shape values and W to DLW fingerprint mean shape values.

D. Principle Component Analysis (PCA):

Principle component analysis (PCA) computations were made to provide a reduced set of values that summarize the significantly larger original data set for each fingerprint pattern type. Each component “captured” a percentage of the total variation based on the distribution of these data in coordinate space. The direction of relative displacement, if any, for each of these landmarks was also determined. The X-Y coordinates of the landmarks and semilandmarks for 30 LSL, RSL, W, and DLW pattern types were formatted into numeric arrays and input into R (version 2.15.0) using the “shapepca” function of the ‘shapes’ package (Dryden and Mardia 1998; Dryden 2012). The “shapepca” function calculates principle components based on the data from the arrays. Each component “captured” a percentage of the total variation based on the distribution of these data in coordinate space. The first three PC scores explained approximately 80% of the variability in the sample. In addition, thin-plate splines were generated for each PC value used in the analysis to show deformation of shape associated with each PC.

3. RESULTS AND CONCLUSIONS

Generalized Procrustes Analysis (GPA):

A generalized Procrustes analysis was performed to evaluate overall pattern type shape and the variation of shape within each pattern type. A Procrustes analysis normalizes size and rotational effects to produce a graph that projects only shape. The landmarks and semilandmarks for 30 LSLs and 30 Ws were plotted and the mean shape calculated. Figure 3-3 demonstrates the variability in distribution for the landmarks and semilandmarks for all 30 prints with the dark triangles representing the mean of each feature’s location.

For left slant loops, each of the semilandmarks demarking the innermost core ridge line were tightly clustered around their respective mean shape indicating little shape variation along this entire ridge line. In other words, the innermost core ridgeline is similarly shaped for all 30 LSL. Likewise, the semilandmarks representing the continuous ridge line were also closely clustered around their respective means. However, there was greater dispersion of the delta landmarks and the interphalangeal crease semilandmark indicating greater shape variation for these regions.

Results were similar for whorls. The continuous ridge line semilandmarks were clustered around their calculated means indicating minimal shape variation for this entire ridge line. However, delta landmarks and interphalangeal crease semilandmarks showed more dispersion indicating greater shape variation in these regions.

To visualize the native distribution and location of all landmarks and semilandmarks for loop and whorl pattern types, the landmarks and semilandmarks for 30 LSLs and RSLs, and 30 Ws and DLWs, respectively, were superimposed in Cartesian coordinate space with all cores positioned at 100, 100 mm (Figure 3-4). This figure shows the variation in distribution of landmarks and semilandmarks within each of the paired fingerprint pattern types (i.e., LSLs-RSLs and Ws-DLWs). Landmark and semilandmark positions along the continuous ridge line were more dispersed than they were in the GPA. This difference is due to variation in the size and possible rotational effects of each of the original fingerprint images in coordinate space. These data will be useful for establishing the shape variance within pattern type as well as among pattern types and could be utilized to investigate both native finger deformation and depositional fingerprint distortion.

Thin-Plate Spline (TPS)

GPA calculated mean shape values for LSLs (Figure 3-5A) and RSLs (Figure 3-5C) were superimposed on each other (Figure 3-5 B and D). The deformation in the TPS grid (Figure 3-3B and D) shows the positional differences between the distribution of those landmark and semilandmark means as projected in 3-dimensional space. The greater the deformation in any given area of the grid, the more shape variation there is between the two pattern types in those particular regions. These results indicate a very high degree of shape consistency between left and right slant loops with the greatest degree of shape variation in the delta region. The same TPS analytical procedure was performed on Ws superimposed on DLWs to evaluate shape variation between those two pattern types (Figure 3-6). The greatest degree of shape variation was likewise found in the two delta regions (Figure 3-6 B and D).

Principle Components Analysis (PCA)

A principle components analysis (PCA) was performed on all landmarks and semilandmarks as distributed in the original fingerprints. Calculations were then executed to reduce the total of each of these landmarks and semilandmarks across all fingerprints to a single set and to summarize the degree of shape variation for each landmark/semilandmark in each pattern type. The first three principle components (PC) scores for LSL, RSL, W, and DLW fingerprint pattern types were graphed (Figures 3-7, 3-8, 3-9, 3-10 respectively). These graphs represent a reduction of the total number of landmarks and semilandmarks from 690 points to 23 for LSL and RSL patterns and 600 points to 20 for W and DLW patterns. The direction of relative displacement, if any, for each of these landmarks and semilandmarks was indicated by a vector line (Figures 3-7 through 3-10 graphs A-C). In addition, the degree of variation for each PC was indicated by the amount of deformation in the corresponding deformation grid (Figures 3-7 through 3-10 grids D-F). The direction of variation is consistent between loop patterns in the first PC with approximately 43% and 37% of the shape variation being accounted for left and right slant loops, respectively. While variation is consistent in the following two PCs, the direction of the variation is different for left and right slant loops (Figures 3-7 and 3-8). The greatest amount of shape variation occurs in the delta regions. This can be seen for all three PCs (Figures 3-7 and 3-8). The extent and pattern of variation is also similar for Ws and DLWs (Figures 3-9 and 3-10) with the greatest degree of shape variation occurring in the delta regions.

4. SUMMARY

Utilizing geometric morphometrics, in conjunction with a GIS, represents a novel approach for evaluating and quantifying spatial relationships among friction ridgeline features (i.e., minutiae). The impacts of this work include an increase in forensic science knowledge and understanding of the spatial patterns of friction skin minutiae. Additionally, there will be direct implications for quantifying another element of potential variance associated with estimating probabilities for describing the discriminating value of fingerprint features, especially when the probabilities are based on ten-print standards. This is the first empirical study that quantifies fingerprint shape variation utilizing geometric morphometric methods for latent print comparison purposes, which in turn, could have implications for the latent print comparison process and practice.

5. REFERENCES

- Benazzi, S., E. Stansfield, C. Milani, and G. Gruppioni. 2009. Geometric morphometric methods for three-dimensional virtual reconstruction of a fragmented cranium: the case of Angelo Poliziano. *International Journal of Legal Medicine* **123**:333-344.
- Bookstein, F. L. 1996. Biometrics, biomathematics and the morphometric synthesis. *Bulletin of Mathematical Biology* **58**:313-365.
- Braga, J. and J. Treil. 2007. Estimation of pediatric skeletal age using geometric morphometrics and three-dimensional cranial size changes. *International Journal of Legal Medicine* **121**:439-443.
- Christensen, A. M. 2005. Testing the reliability of frontal sinuses in positive identification. *Journal of Forensic Sciences* **50**:18-22.
- Dryden, I. L. 2012. *Shapes: Statistical shape analysis*.
- Dryden, I. L. and K. V. Mardia. 1998. *Statistical shape analysis*. John Wiley & Sons Ltd, Chichester, West Sussex, England.
- Franklin, D., P. O'Higgins, and C. E. Oxnard. 2008. Sexual dimorphism in the mandible of indigenous South Africans: A geometric morphometric approach. *South African Journal of Science* **104**:101-106.
- Franklin, D., C. E. Oxnard, P. O'Higgins, and I. Dadour. 2007. Sexual dimorphism in the subadult mandible: quantification using geometric morphometrics. *Journal of Forensic Sciences* **52**:6-10.
- Kimmerle, E. H., A. Ross, and D. E. Slice. 2008. Sexual dimorphism in America: geometric morphometric analysis of the craniofacial region. *Journal of Forensic Sciences* **53**:54-57.
- Kucken, M. and A. C. Newell. 2005. Fingerprint formation. *Journal of Theoretical Biology* **235**:71-83.
- Slice, D. E. 2007. Geometric morphometrics. *Annual Review of Anthropology* **36**:261-281.
- Wertheim, K. 2011. Embryology and morphology of friction ridge skin. Pages 3-1 - 3-26 in D. o. Justice, editor. *The Fingerprint Sourcebook*. National Institute of Justice, Washington D.C.
- Zelditch, M. L., D. L. Swiderski, H. D. Sheets, and W. L. Fink. 2004. *Geometric Morphometrics for Biologists: A Primer*. First edition. Elsevier Academic Press, New York and London.

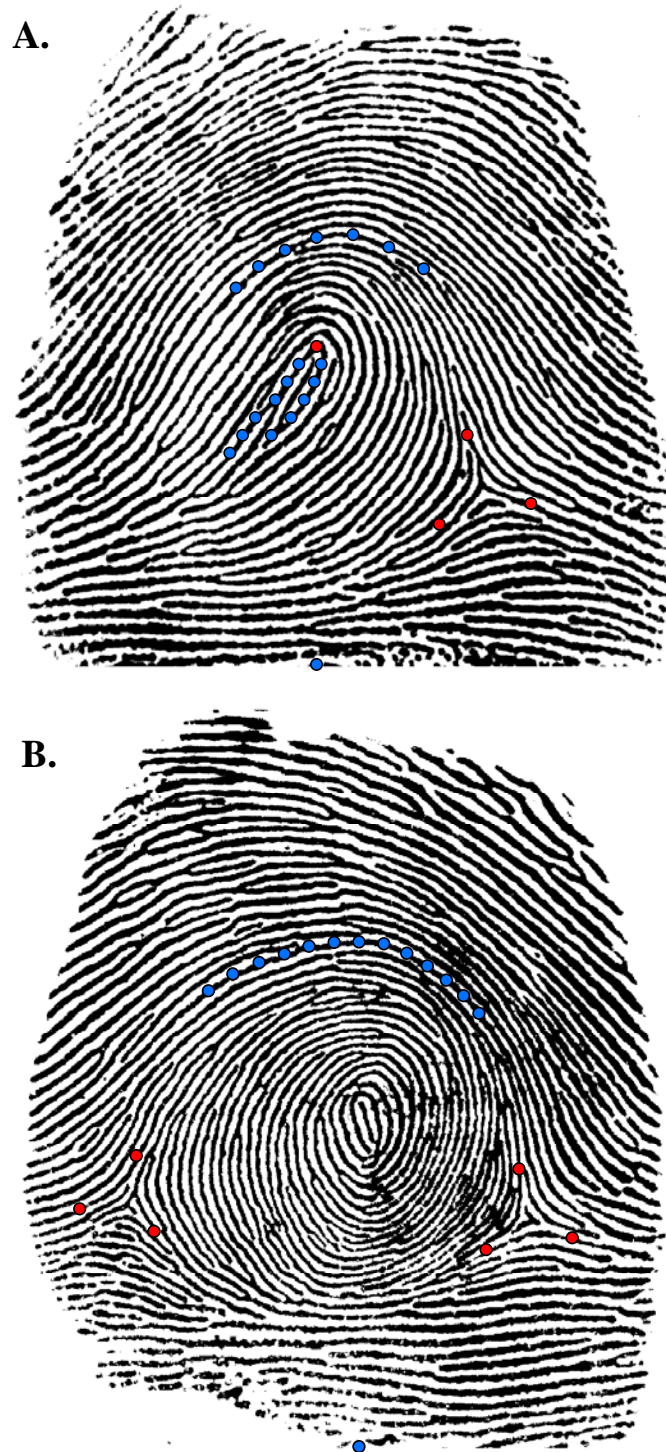


Figure 3-1. Landmark (●) Determination and Semilandmark (●) Selection for Loop (A) and Whorl (B) Pattern Types

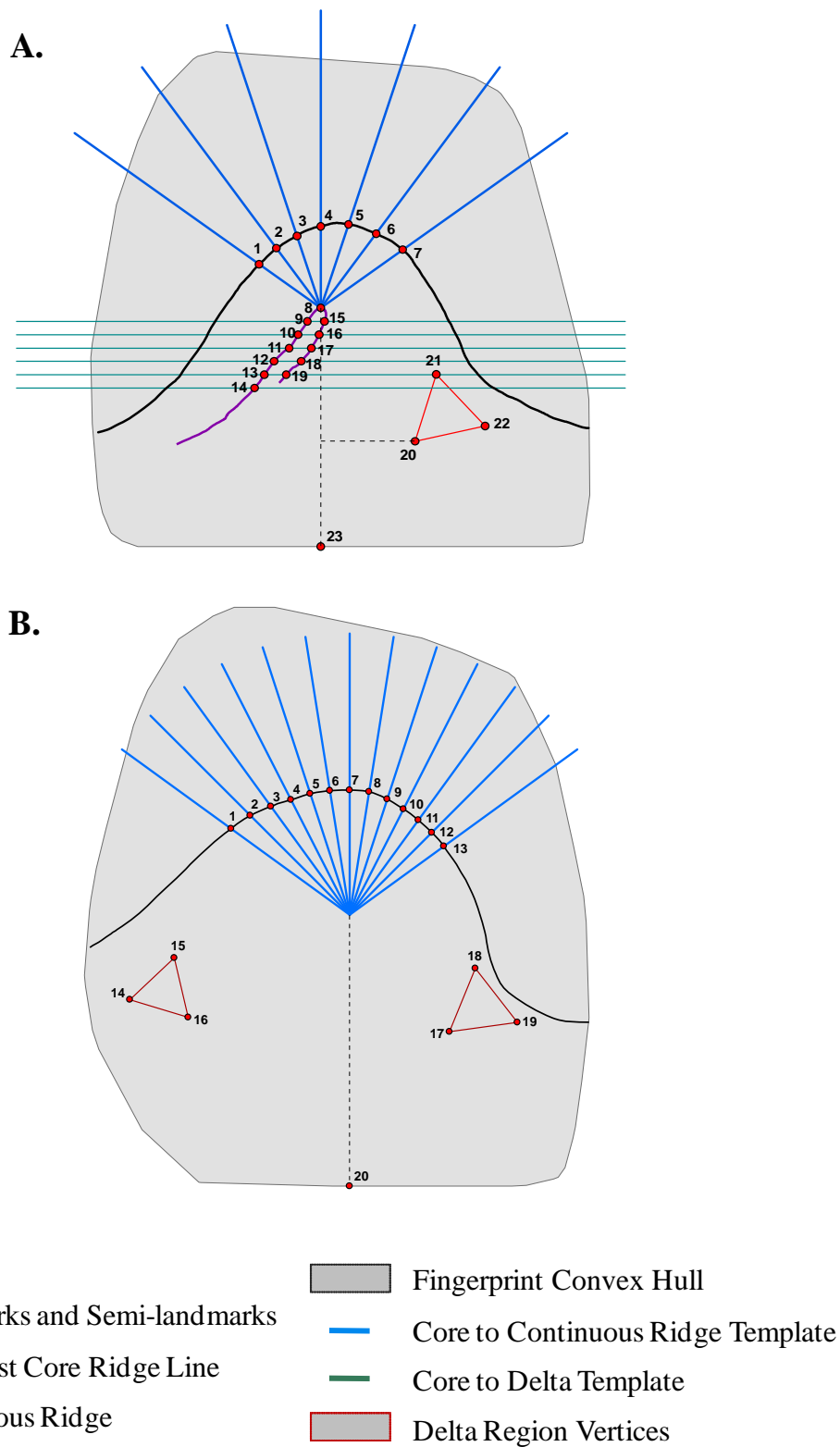


Figure 3-2. Landmark Determination and Semilandmark Selection for Loop (A) and Whorl (B) Pattern Types

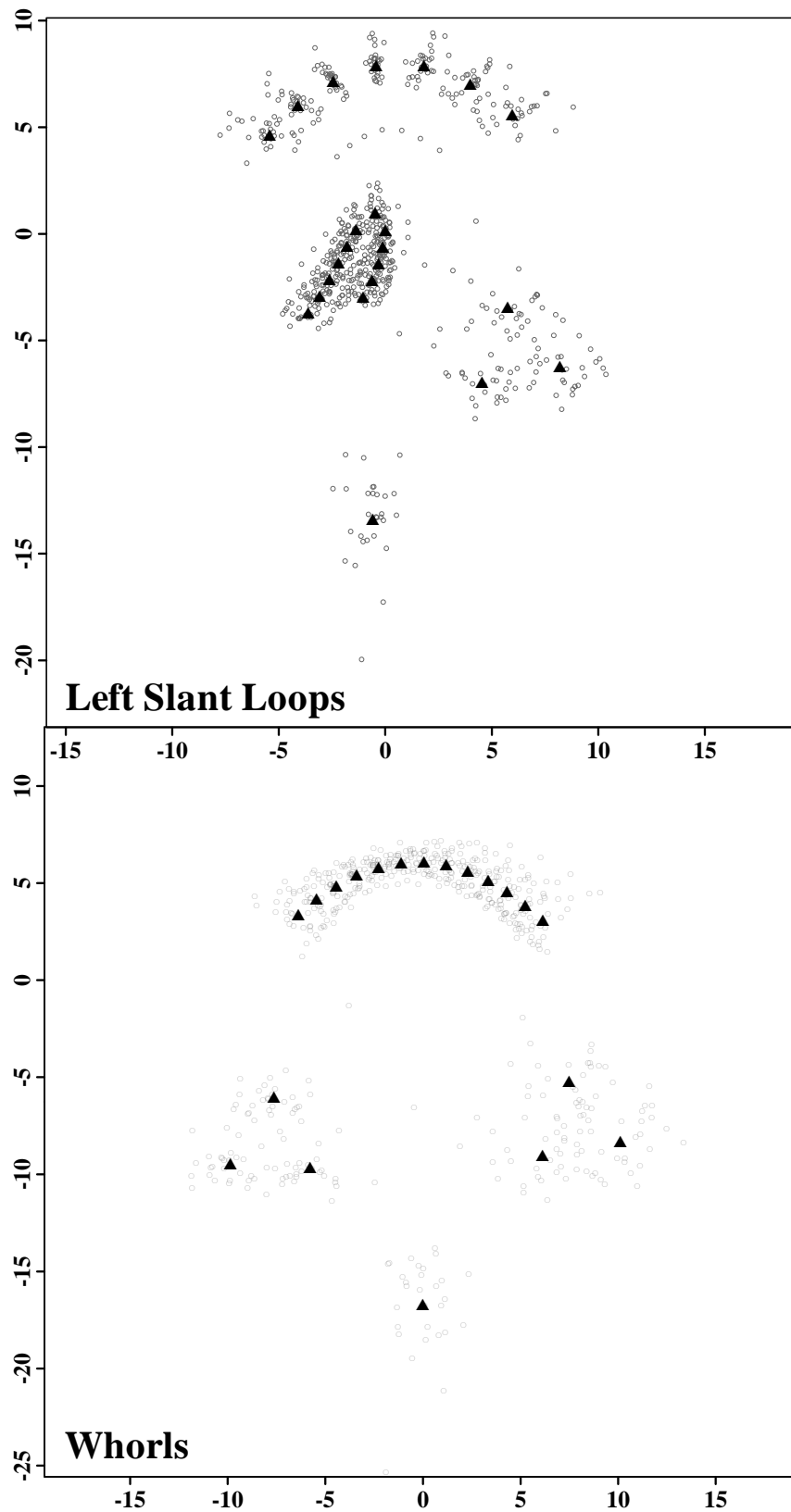


Figure 3-3. Procrustes mean shape (▲) analysis of Landmarks and Semilandmarks (○)

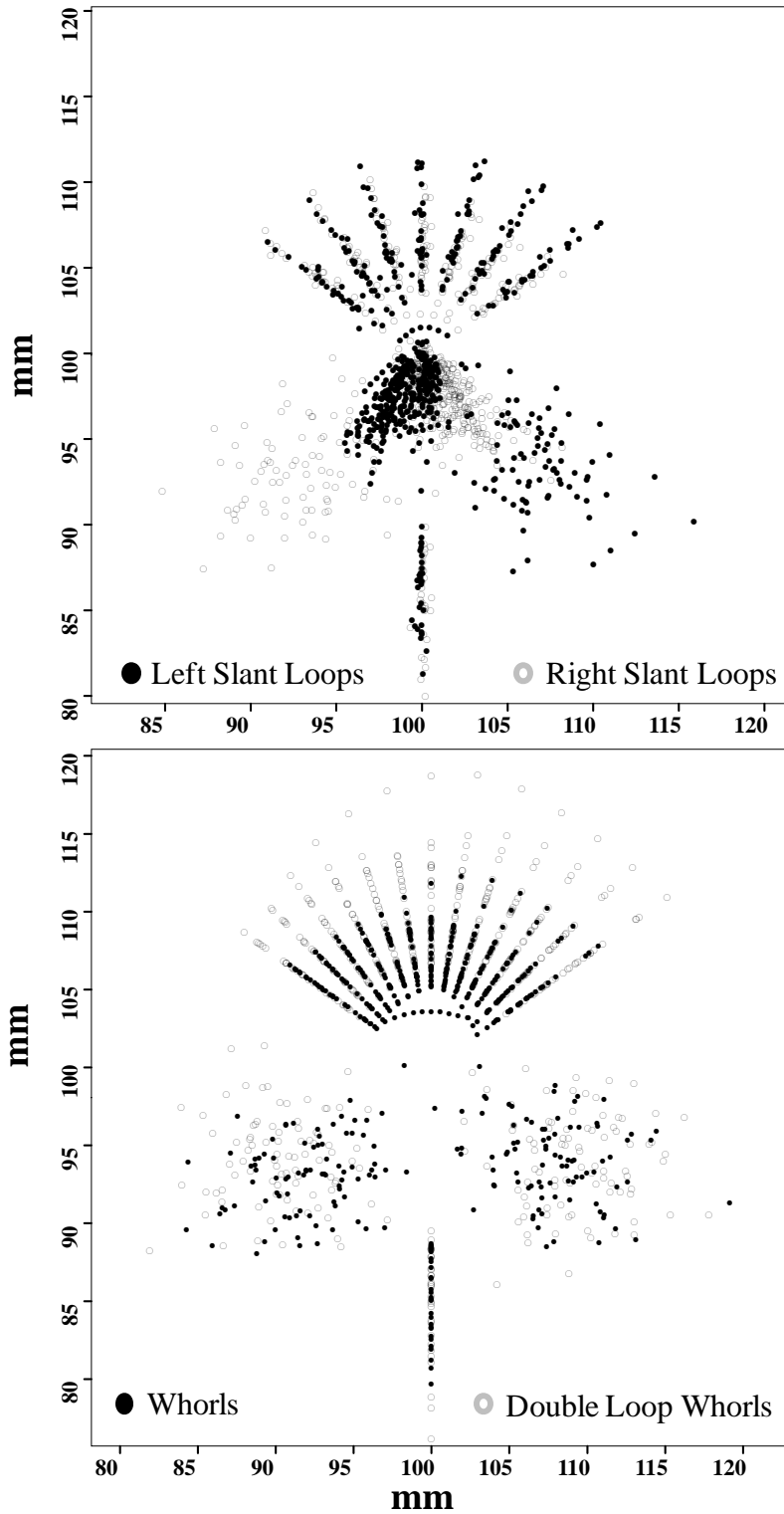
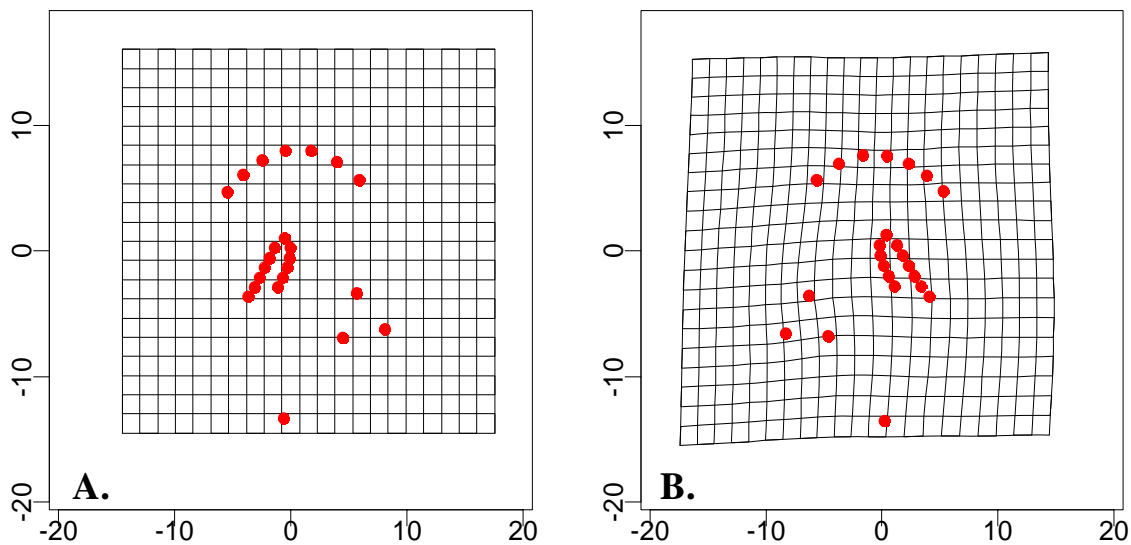


Figure 3-4. Landmarks and semilandmarks mapped in Cartesian coordinate space

Right Slant Loop mean shape (B) superimposed on Left Slant Loop mean shape (A)



Left Slant Loop mean shape (D) superimposed on Right Slant Loop mean shape (C)

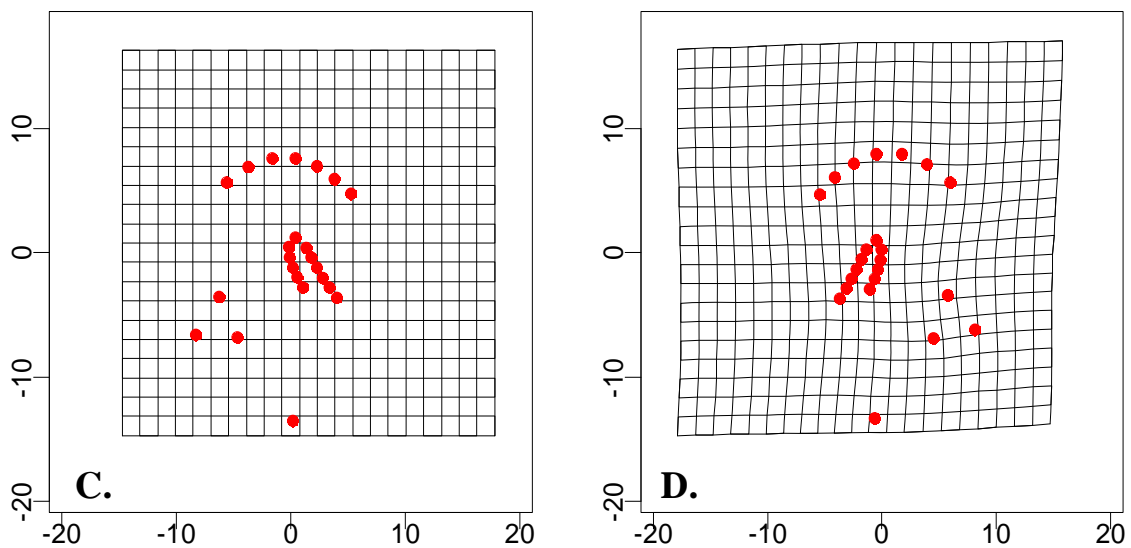
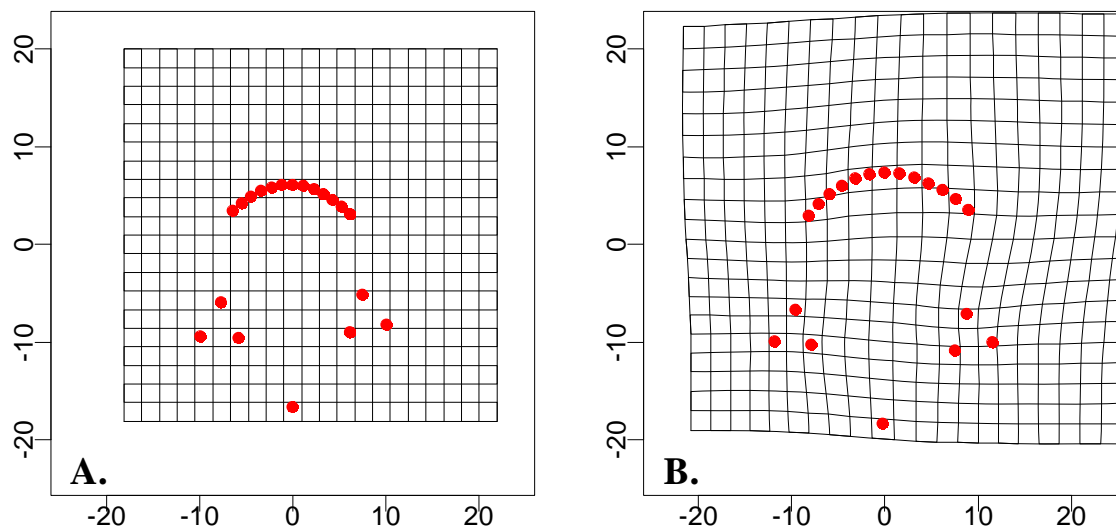


Figure 3-5. Thin plate spline deformation modeling of left slant loops and right slant loops

Double Loop Whorl mean shape (B) superimposed on Whorl mean shape (A)



Whorl mean shape (D) superimposed on Double Loop Whorl mean shape (C)

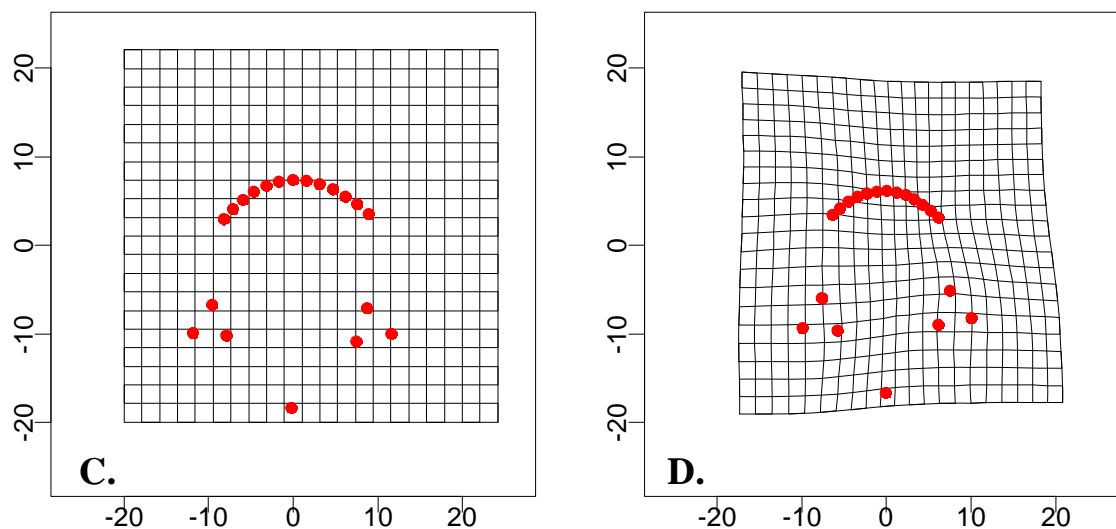


Figure 3-6. Thin plate spline deformation modeling of whorls and double loop whorls

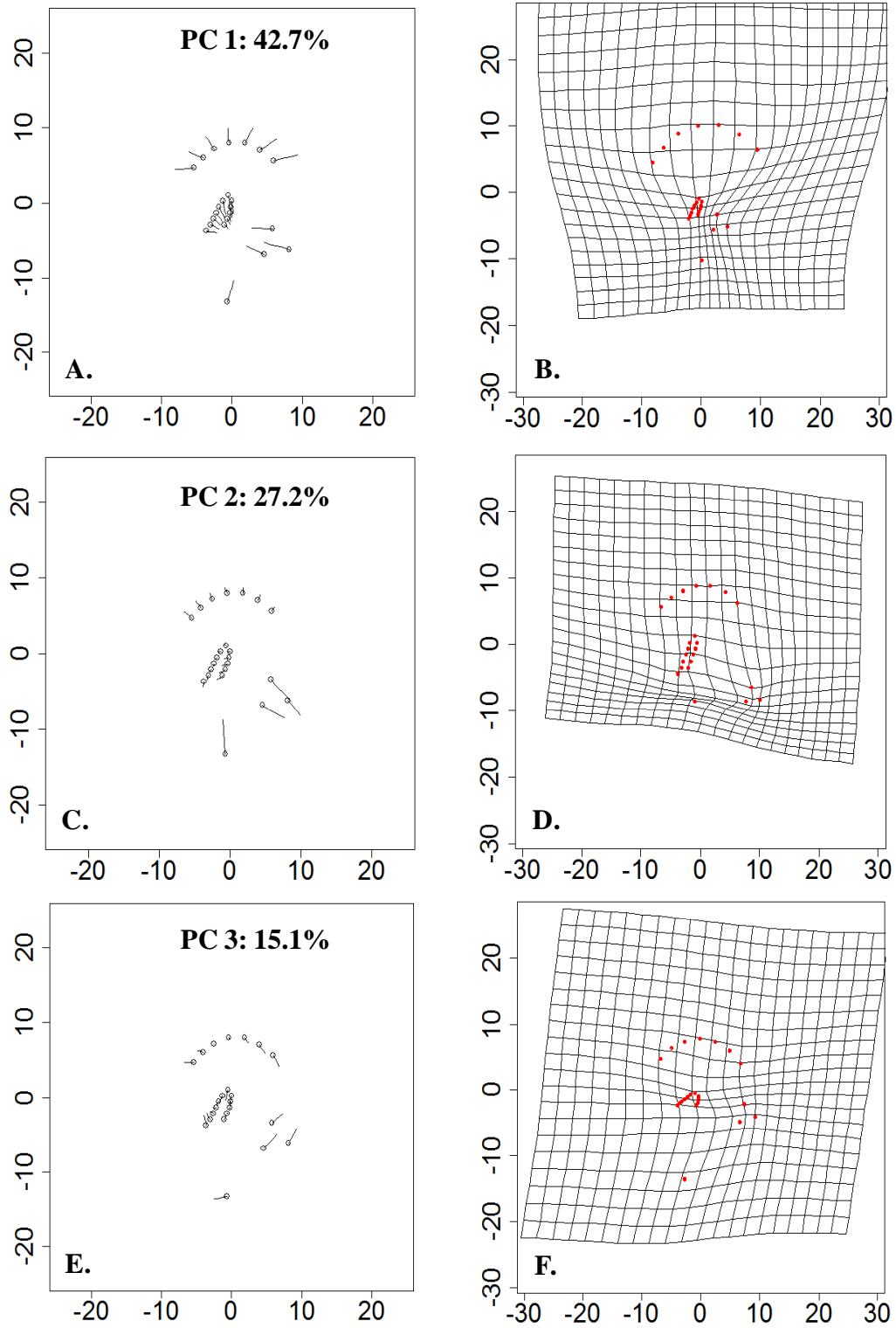


Figure 3-7. Principal component analysis and deformation modeling for left slant loops

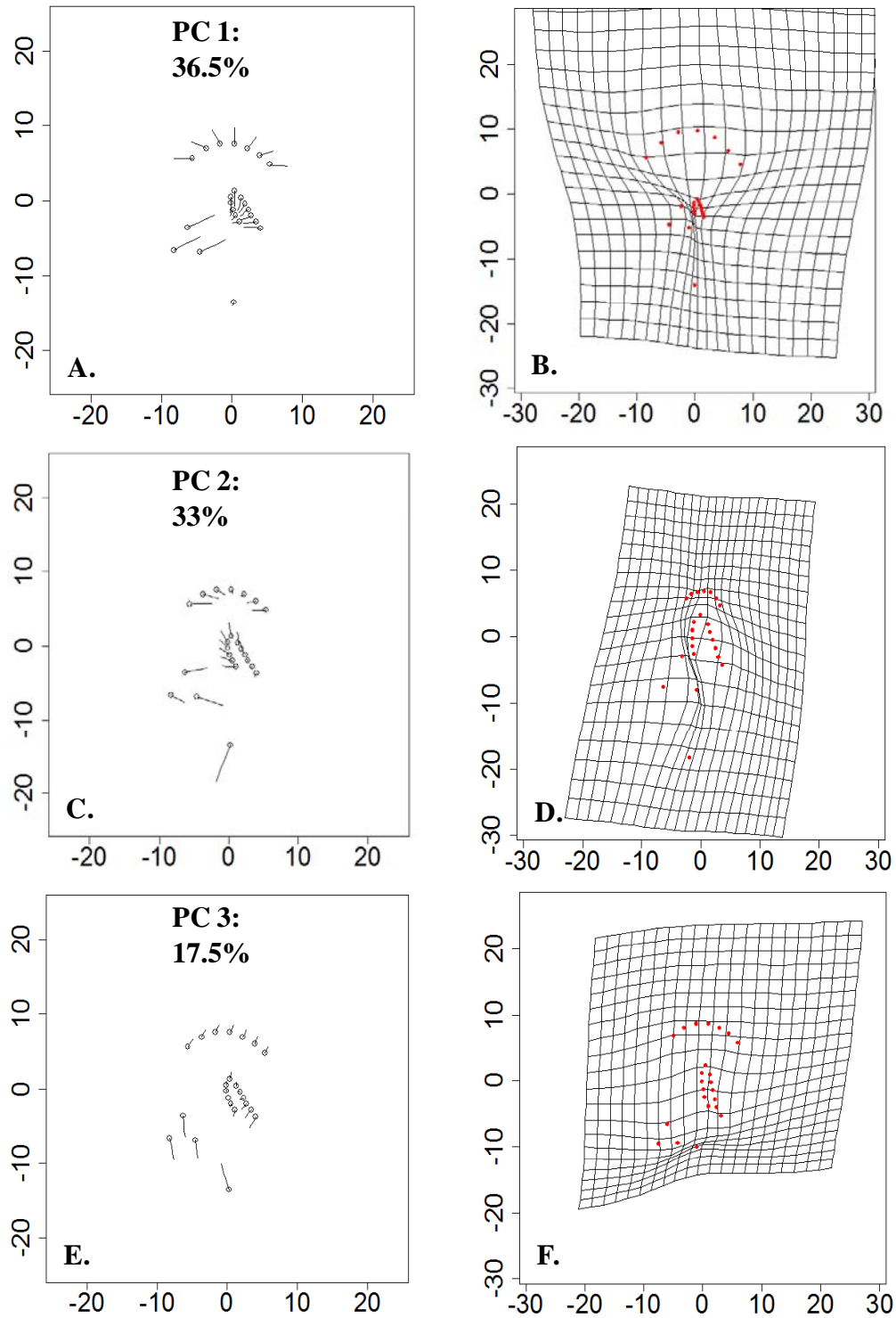


Figure 3-8. Principal component analysis and deformation modeling for Right Slant Loops

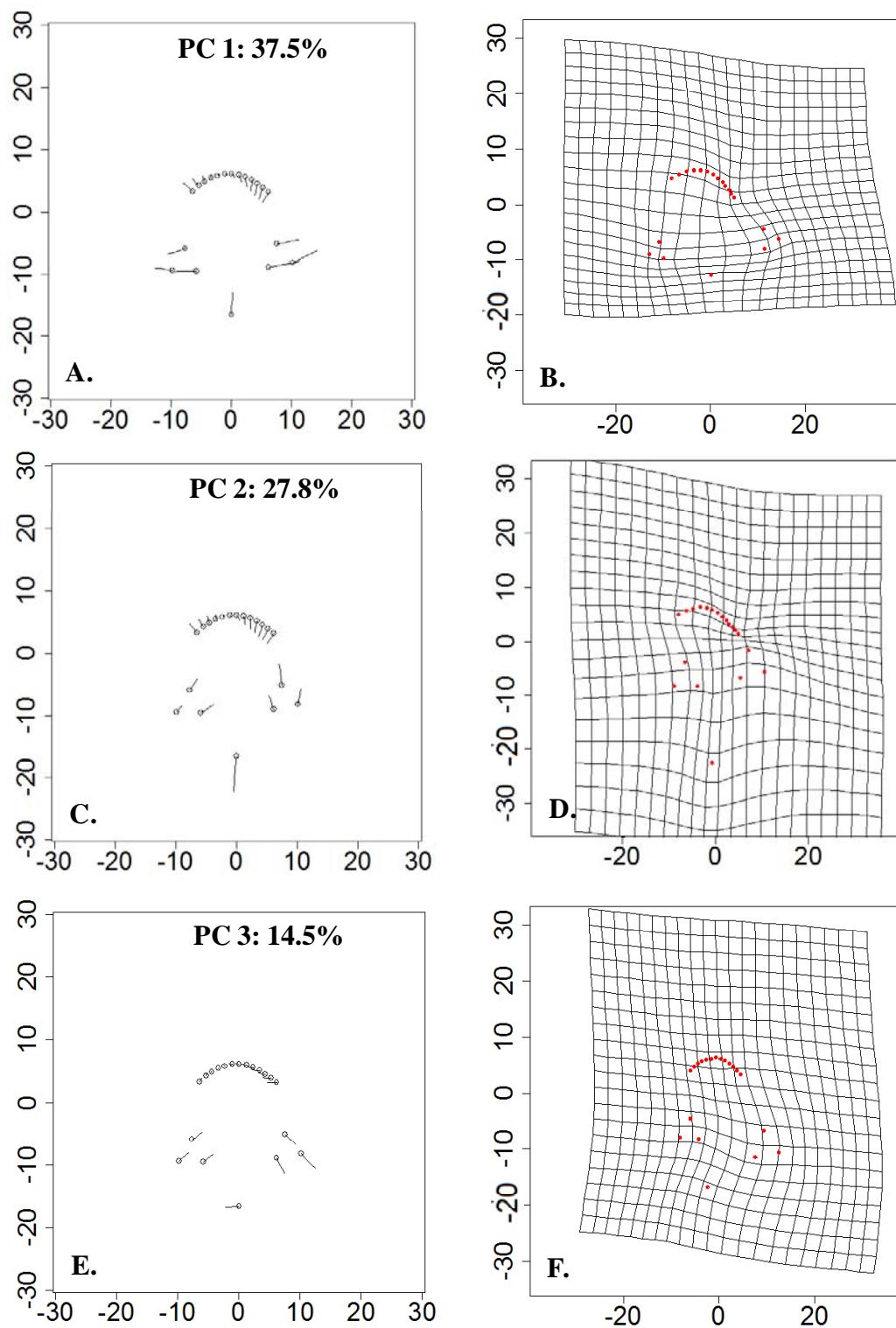


Figure 3-9. Principal component analysis and deformation modeling for whorls

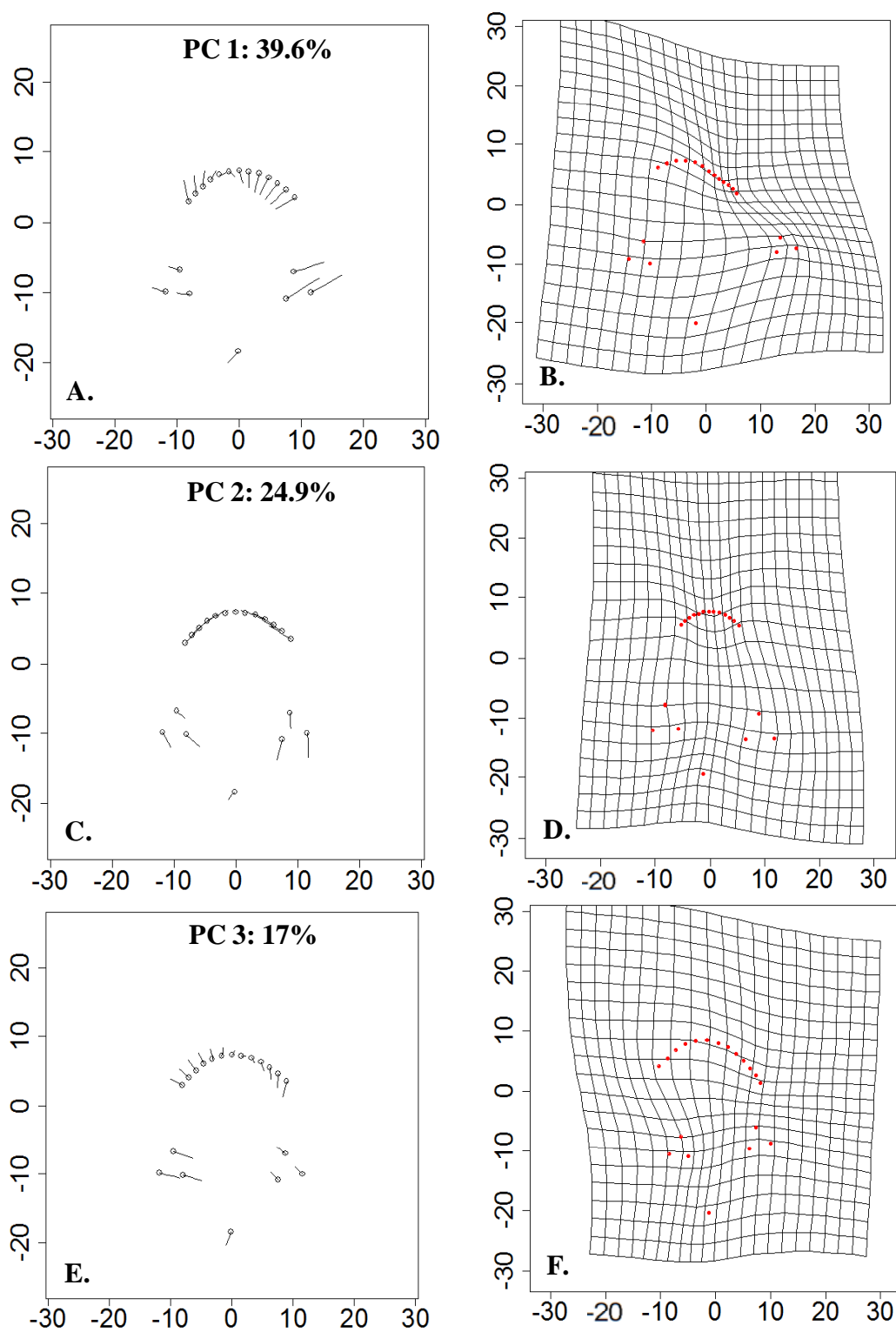


Figure 3-10. Principal component analysis and deformation modeling for double loop whorls

CHAPTER 4 – FALSE-MATCH PROBABILITIES AND MONTE CARLO ANALYSES

1. INTRODUCTION

The Monte Carlo (MC) method is a computer algorithm used to repeatedly resample data from a given population to make inferences about stochastic processes. The Monte Carlo method is one of the optimal ways to quantify rare events, events that occur with a very low probability. Because of the rare nature of these events, it is extremely difficult to evaluate them using typical analytical means. The goal of a MC simulation is to produce an expected result, $E(X)$, where X is a random variable. The Monte Carlo simulation creates n independent samples of X , and as n increases towards infinity, the average of the n independent samples ($1/n \sum_{i=1}^n x_i$) asymptotes towards μ (Rubinstein and Kroese 2007), thus producing a very large number of independent samples which allows for the detection and quantification of rare events and for the estimation of the probability of occurrence.

The MC method has been used in a variety of fields to analyze rare events. Lin and Wen (2010) used MC simulations, specifically Markov Chain Monte Carlo simulations, in the analysis of natural disasters. They studied the occurrence of large debris flows such as landslides and floods, to help determine the placement of villages to reduce the destruction caused by these phenomena. The MC simulations were used to determine where disastrous debris flows would most likely occur, and help plan where villages would be built in areas of China. In community ecology, MC methods have been employed to study the robustness of species diversity indices (Ricklefs and Lau 1980; Manly 2006). In addition, it is commonly used in the estimation of phylogenies when studying evolution (Bouchard-Côté et al. 2012). The MC method has also been used to study the frequency in which airplanes pass within close proximity to each other (Paielli and Erzberger 1996). The authors used the probabilities created by the MC method to make inferences and suggestions on how to reduce the possibility of close proximity flights. While this is not an exhaustive review, it demonstrates that this statistical method has been used in a wide variety of disciplines to make inferences about phenomena that are either rare or difficult to analytically quantify.

With the publication of the National Academy of Science report (2009) and court cases such as *Daubert vs. Merrell Dow Pharmaceuticals* (1993), there has been an increased awareness of the need to evaluate forensic methods through scientific means. A fundamental area related to fingerprint identification is the probabilities associated with random correspondence between regions of a fingerprint. For the last century, Latent Print Examiners have emphatically affirmed or provided testimony that fingerprints are unique with no two fingers, on the same individual or on different individuals, including identical twins, possessing the same fingerprint features. This has been affirmed qualitatively as no two fingerprints have been identified as being indistinguishable. Moreover, numerous arguments have been presented in the literature that fingerprints are unique (Ashbaugh 1994, 1999; Wertheim 2011; Langenburg 2011). While there is a strong biological basis for stating fingerprints are unique due to genetic and epigenetic factors that play a role in fingerprint development, statistically there is always a minute chance that an exact replica of any given fingerprint could exist somewhere in the world.

For forensic science, the premise that an entire fingerprint is unique is not in question. However, when a latent print examiner receives a latent print for comparison to a standard, the entire fingerprint is rarely available. Most latent prints are typically only a portion of the entire fingerprint. Consequently, the question is not whether an entire fingerprint is identical to another fingerprint, but rather, what is the likelihood or probability that a similar set of minutiae from a specific region of any given fingerprint exists in the world? That is, do regions differ in their similarity?

Several authors have calculated probabilities of random correspondence, or random match probabilities, in an attempt to quantify the discriminating features of a fingerprint (Champod and Margot 1996, Pankanti et al. 2002, Dass et al. 2005, Chen and Jain 2009, Dass and Li 2009). Many of these studies have been conducted employing a theoretical statistical approach in which the authors use underlying probability distributions, such as a Poisson distribution, Gaussian distribution, or von Mises distribution, to perform their analysis (Champod and Margot 1996, Pankanti et al. 2002; Dass et al. 2005; Dass and Li 2009; Su and Srihari 2009). Furthermore, many of these studies were performed in relation to matching algorithms for biometric systems (Sujan and Mulqueen 2002; Parziale and Niel 2004; Tan and Bhanu 2006), but were not employed to understand the foundational probabilities of fingerprint features having similar patterns. There have been a few studies focused exclusively on random match probability generation for use in the forensic lab such as Neumann et al. (2006, 2007), who produced likelihood ratios for a random match of both 3 minutiae and any number of minutiae. For a review of proposed fingerprint individuality statistical models from 1892 to 2001, see Langenburg (2011).

Statistical techniques that have not been explored in relation to evaluating the spatial distribution of fingerprint features are re-sampling techniques such as Monte Carlo simulations or Bootstrapping. Bootstrapping is considered to be a type of the Monte Carlo method and is a computer algorithm used to repeatedly re-sample data from a given population to make inferences about stochastic processes (Gotelli and Ellison 2004; Manly 2006; Rubinstein and Kroese 2007). Re-sampling techniques, or randomization tests, provide a relatively straight forward empirical approach for producing random correspondence probabilities of minutiae from non-progenitor fingerprints. These methods allow for the random sampling of a set of minutiae in any spatial distribution from a given pool of minutiae. The resultant minutiae sets are then used as sampling units to compare across a large sample of fingerprints. In addition, the technique makes no assumptions about underlying distributions associated with the data. Because this procedure is performed thousands of times, a sampling distribution of non-progenitor matches can be obtained (i.e., probability of a false match).

Any minutiae, m_i , can be defined as

$$m_i = (x_i, y_i, \theta_i, T_i) \quad (\text{eq 1})$$

Where x is its location on the x axis, y is its location on the y axis, θ is the angular direction in degrees, and T is a categorical variable representing the minutiae type. Any fingerprint F_j is then a sample space of all minutiae present:

$$F_j = \{m_1, m_2, m_3 \dots m_n\} \quad (\text{eq 2})$$

Where n is the total number of minutiae on a fingerprint with each minutia defined by the equation above. Each fingerprint is then defined by its sample set of minutiae with each minutia defined by equation 1. In latent print comparisons, a subset of the entire sample set is usually available for the comparison. This is typically because only a subset of the entire sample space is available or identifiable, and in the case of latent print comparisons, a “target” group of well-defined minutiae is often used. The sample used for comparison can be defined as:

$$s = \{m_1, m_2, m_3 \dots m_o\} \quad (\text{eq 3})$$

Where o is the total number of observable minutiae within the subsample. These observable minutiae create a specific spatial configuration within a given region of the finger. Employing a randomization technique allows for the exploration of the occurrence of minutiae spatial patterns across fingerprints through purely empirical means without having to invoke assumptions related to the underlying probability distributions. The large number of sampling iterations allows for creation of an empirical probability distribution that is an estimate of the true probability distribution. The greater the number of iterations, the closer the empirical distribution is to the true distribution (Rubinstein and Kroese 2007). Following Rubinstein and Kroese (2007), the expected value, $E(X)$, can be obtained, where

$$E(X) = \frac{1}{B} \sum_{i=1}^B X(s_i^*) \quad (\text{eq 4})$$

Where $s_1^*, s_2^*, \dots, s_B^*$, are a series of independent samples drawn from the sample space, and B is the total number of samples taken and $X(s_i^*)$ is a function to which the sample is applied. Minutiae within a fingerprint are not assumed to be independent. However, the sampling unit used in a randomization technique is not the single minutia but the set of minutiae that are randomly selected. Because the minutiae used in the first sample are returned to the pool prior to the next iteration, every possible minutiae set has an equal chance of being drawn for every iteration. Thus, the sampling unit for any given iteration is independent of the previous sampling unit or any subsequent iteration.

The purpose of this study was to apply boot strapping techniques to create probabilities of random correspondence, and to explore how these probabilities change across the landscape of the fingerprint. The probabilities were produced using a sample set from the Oregon population and the statistical method employed a naïve Monte Carlo, meaning no assumptions are built into the simulations. Thus, this is an empirical, “brute force” approach to estimate probabilities which describe fingerprint similarities. The MC method produces probabilities associated with the spatial patterns of fingerprint minutiae attributes. These foundational probabilities quantify the discriminating power of fingerprint ridgeline features and as such, can be employed during the comparison process to qualify the comparison conclusions.

2. METHODS

Fingerprints used in this study were acquired from ten-print cards obtained from the Oregon State Police using the techniques described in Chapter 2. Fingerprint attributes were stored in a geo-database from which the Monte Carlo data were queried. The Monte Carlo simulations were built using a combination of Python, R, and SQL languages implemented through a GIS interface that allowed for the execution of customized scripts written in these languages. The use of a Geographic Information System (GIS) allows for the placement of all fingerprints and attribute data into a common coordinate space. GIS readily allows for the subdivision of a finger into regions within which the exploration of similar minutiae sets may be explored. In addition, all data associated with a minutia are available within the GIS geo-database which allows for an examination of how different attributes such as direction and minutiae type affect the chance of a random match.

The function $X(s_i^*)$ is an algorithm that uses the sample s_i^* in order to produce fingerprints with similar patterns. For the current study, the algorithm is a series of queries to a database, and thus is not a mathematical function. The samples themselves are not of interest, per se, but the number of times the sample occurs on fingerprints that are not the progenitor is. Therefore, for each sample;

$X(s_i)$ = number of non – progenitor fingerprints found through a query

Because $X(s_i)$ is an integer, a simplification of the equation above is:

$$x_i = X(s_i) \quad (\text{eq 5})$$

Because the algorithm is searching a database with a finite population, there must be a limiting factor applied to the expected value $E(X)$ to limit the scope of the probability produced. The database size may be altered based on the type of query performed, and whether the value of interest changes when the analysis is performed on the entire fingerprint suite or if it is limited to within pattern type. Since the database size will change based on which run is performed, the database size is added to the denominator to normalize the outcome. Equation 4 becomes,

$$E(X) = \frac{1}{dB} \sum_{i=1}^B x_i \quad (\text{eq 6})$$

where d is the population size within the database to which the comparisons are made. The probability of a non-progenitor fingerprint having a similar pattern to any given minutia set is quite small, and it can be assumed that any finger chosen at random will most likely not produce any minutiae sets that will match another finger even when a large number of samples are drawn from the finger. Therefore, k fingerprints need to be used as independent replicates in order to produce an $E(X) > 0$, where $k > 1$. Equation 7 becomes,

$$E(X) = \frac{1}{k} \sum_{j=1}^k \frac{1}{dB} \sum_{i=1}^B x_{ij} \quad (\text{eq 7})$$

where k is the total number of fingerprints used, and j is an index of the fingerprint from which the minutia sets are drawn, and x_{ij} is the number of fingerprints with the same minutiae configuration for a given iteration

Eight Monte Carlo simulations were performed with variable attribute criteria added systematically to the simulation run (Table 4-1). This allows for the assessment of how each attribute (i.e., the database information used to describe the minutiae characteristics) affects the probability of a false match. The simulations were designed to test the random match probability expected value of specific regions of a fingerprint. A moving filter was designed by constructing a sampling grid comprised of nine mutually overlapping cells in a 3 x 3 matrix (Figure 4-1). Within each grid cell, the total minutiae were counted and from this set of minutiae, sets of three, five, seven or nine minutiae were selected.

Minutia sets were randomly drawn from each grid cell, without replacement, that included either three, five, seven or nine minutiae per run, using a combination of the minutia X-Y coordinate location, pattern type (left slant loops, right slant loops, whorls, double loop whorls, arches, tented arches), minutiae type (i.e., bifurcations or ridge endings) and minutiae direction. For four of the pattern types (i.e., left slant loops, right slant loops, whorls and double loop whorls), 50 randomly selected fingerprints were used for the minutiae draw. Due to the limited sample size and occurrence, only 20 fingerprints were selected to draw from for arches and 25 for tented arches. These simulations were iterated 1000 times with the results output into a database environment for subsequent analyses. Comparisons were performed across all pattern types or within pattern type depending on the Monte Carlo simulation parameters selected. Four simulation runs, each consisting of a different number of minutiae selected (i.e., 3, 5, 7, or 9), were conducted within each of the nine sampling grid cells of the filter matrix. This procedure was performed for all 50 prints (20 prints for

arches, 25 prints for tented arches) selected for a total of 50,000 iterations/grid for loops and whorls, 20,000 for arches and 25,000 for tented arches respectively. For loops and whorls, 1,800,000 iterations were performed for each pattern type and for each Monte Carlo simulation. For arches and tented arches 720,000 and 900,000 total iterations per Monte Carlo were performed, respectively. The entire set of simulations was run three times per pattern type and for each set a different group of fingerprints was randomly chosen, and the probabilities averaged. Because every simulation was performed 1000 times, 1000 can be substituted for B in equation 7. Thus, probabilities of a false match were calculated using the following equation:

$$E(X) = \frac{1}{k} \sum_{j=1}^k \frac{1}{1000d} \sum_{i=1}^{1000d} x_{ij} \quad (\text{eq 8})$$

- d =number of fingerprints the minutiae set are compared to
- j =index of print from which minutiae are drawn
- i =index of iteration
- x =number of matches per iteration
- k =number of prints actually used in the simulation

The variable x_{ij} is number of fingerprints with the same minutiae configuration for a given iteration. While ideally, k should equal the total number of prints used in the analysis, sometimes the area sampled did not have a sufficient number of minutiae to actually make a draw. For example, if there were only six minutiae in a grid cell, sample runs with seven or nine minutiae would not be possible. The variable d changes according to the number of pattern types used in the sample run.

Minutiae are not single pixel entities. Thus, they have an area associated with each of them that is in part reflected by the width of the ridge. In addition, there is operator-introduced variability when a point is placed at the center of a minutia which involves the spread of pixel dimensions across the ridge width. Thus, an operator could place two points on the same minutia and be off by nanometers, and these points would not be selected as the same entity. In order to account for these sources of variability, a confidence zone or tolerance around each minutia point was estimated. To account for this difference in precision, a 99.7% minutia location confidence zone was calculated. This measurement was based on a random sampling of 500 ridge widths from a subsample of 50 images without regard for pattern type. For each of the 50 images, ten points were randomly placed using a GIS script that restricted the placement to ridges. The ridge width was then measured at these locations resulting in 10 measurements for each of the 50 images ($N = 500$). Because independence of ridge widths within a fingerprint cannot be assumed, the mean ridge widths were calculated for each image ($n = 10$) and the resulting 50 values were in turn pooled to calculate a mean 0.4 mm and standard deviation 0.76 mm. The standard error of the mean was 0.107 mm. Thus, each minutia has a confidence zone of ± 0.32 mm. For the Monte Carlo simulations, two minutiae with overlapping confidence zones cannot be differentiated and were considered as occupying the same space.

As stated in Chapter 2, Universal Latent Workstation (ULW) was used to identify minutiae by X-Y coordinates and provided minutia direction, θ . These data were imported into ArcGIS and minutiae moved to more accurately mark their placement on the ridge line. In addition, any minutiae incorrectly labeled, not labeled or falsely marked were corrected. For those minutiae incorrectly labeled or falsely marked, minutia direction (i.e., theta) was entered manually. A margin of error was determined for both bifurcations and ridge endings to control for operator variability in this manual designation of direction. Ridge ending directions were measured along the ridge line while bifurcations were measured through the valley created by the bifurcation. Fifty bifurcations and

ridge endings were randomly chosen from images in the database. Theta (θ) was then measured by four project staff for a total of four independent measurements per minutia and a mean and standard deviation calculated. The variance for each of the four measurements from the mean was calculated and then a mean variance calculated. For ridge endings, the variance range was 1.5 to 38.5 degrees with a mean variance of 10.33 degrees and a median of 10 degrees. For bifurcations, the variance range was 0 to 46 degrees with a mean and median variance of 13.51 and 11 degrees, respectively. For the Monte Carlo simulations that included direction, a tolerance buffer of ± 5 degrees was used for both ridge endings and bifurcations directions during the searches of the database. The same tolerance buffer was used for both minutiae types to allow for consistency across the Monte Carlo simulations especially when minutiae type was not specified. Using the smaller of the two median buffers allows for a more conservative estimate of false matches.

3. RESULTS

All eight MC simulations generated similar probability results for all pattern types (Figure 4-2). All simulations accurately detected the progenitor print from which the minutiae were chosen, and in some instances, detected a non-matching fingerprint (i.e., false match) which contained minutiae in the same X-Y coordinate space as the progenitor print (Figures 4-3 and 4-4). Figure 4-2 shows an estimation of the mean probability for encountering a random correspondence for each pattern type. The magnitude difference in the probabilities between the three minutiae and other minutiae (i.e., 5, 7, and 9) renders the other bars miniscule in comparison.

The probabilities of a false match (i.e., random match probability) for all MC simulations performed are presented in Tables 4-2 through 4-13. The variation between pattern types was negligible, with each pattern type performing similarly in each Monte Carlo simulation. The probability of a false match decreases as fingerprint attributes (e.g., minutiae number, minutiae type) were added to the simulation, dependent of the type of information utilized in the sample run. For simulations based on X-Y coordinates of three minutiae and using all attribute criteria (minutiae coordinates, type, direction, and pattern type), the probability of generating a false minutiae match is about 1 in 5 million. In the case of the simplest simulation, using X-Y minutiae coordinate information only, the use of three minutiae has a chance of generating a false match of 1 in 1600. However, by increasing the number of selected minutiae to five in simulation runs, the chance of a false match drops drastically to 1 in 125000.

Monte Carlo simulations show that the probability of a false match varies across the fingerprint with a higher occurrence in the regions below the core and in the delta regions (grids 1-6). Conversely, the regions above the core (grids 7-9) are associated with less densely packed minutiae and unique arrangements. This aligns with this projects earlier fingerprint characterization (see Chapter 2) with the lower region of the fingerprint having more minutiae than the upper region. Thus, there was a greater chance of similar patterns occurring. Figures 4-3 and 4-4 are examples of matching fingerprints found using the Monte Carlo method. As can be seen, these are not fingerprints that would be mistaken for the same individual by a Latent Print Examiner. However, they do demonstrate that similar patterns can exist on fingers of different individuals. The probabilities associated with these similar patterns of minutiae form the baseline possibility of these patterns existing, and are what should be used to build a probability associated with the identification of an individual during a criminal investigation. Finally, zero probability of a false match does not reflect the true probability for those simulations. The zeroes indicate that the probabilities of a match are so small that the dataset (1200 fingerprints) is insufficient for the generation of probabilities in these regions.

4. CONCLUSIONS

The random match probabilities generated by the Monte Carlo simulations demonstrate that even with little information, if the number of known minutiae positions is sufficiently large, the probability of finding a similar pattern is quite rare. For example, in the MC1, where the only information considered is the minutiae X-Y position, the probability of a false match decreases 100 fold when the number of minutiae is increased by two, such as five selected versus three selected. This demonstrates that the number of minutiae selected drastically impacts the probability of finding a similar pattern. In addition, the location on the finger where the minutiae are selected also changes the probability of false match, with the upper regions of a finger having lower probabilities of a false match than regions below or near the core. This follows the observations noted in Chapter 2 that show a greater number of minutiae below the core than above. As one would expect, the greater number of minutiae below the core allows for a greater chance of having similar patterns exist in the region. Adding attribute parameters to the simulation made it more stringent and thus, more difficult to find false matches in our database. However, the probability of a false match was not drastically different either among pattern types or when the searches were performed within pattern type. The Monte Carlo simulations performed had difficulty finding any false matches using seven or nine minutiae. In fact, there was only a single nine false match in the entire set, and that was for the simplest Monte Carlo (MC1) based on minutiae position alone. This indicates that the probability of a false match is extremely low when large numbers of minutiae configurations are used in an identification. It must be stressed that zeroes do not mean that there is no probability of matching at these higher levels. Because the denominators of the probabilities are inherently associated with the number of fingerprints in the database, these results suggest that our database of 1200 images was of insufficient size for finding matches using the seven and nine minutiae sets.

The results of this study are similar to results from previous work that used different statistical techniques and different populations of fingerprints. For example, the probabilities for MC6 for three minutiae are very similar to what Neumann et al. (2006) obtained. They found that for the core area of right slant loops from dataset 1, the likelihood of the three minutiae configuration resulting in a false match is 1.13×10^{-7} . This is comparable to our findings in MC6 for the same pattern type with a probability of 1.54×10^{-7} . A limitation to the present study is that replicates were not used as part of a validation process during simulations. Other studies such as (Pankanti et al. 2002) were able to create a database that had two copies of the same finger as a way to verify the results from the initial test. Because the 10 print cards used were archival cards from OSP, there was no way to obtain independently rolled prints for the same fingers. Replication of the same fingerprint would be desirable in further studies because skin elasticity and distortion could be directly quantified and would allow for validation and refinement of the obtained probabilities through the use of an independent dataset.

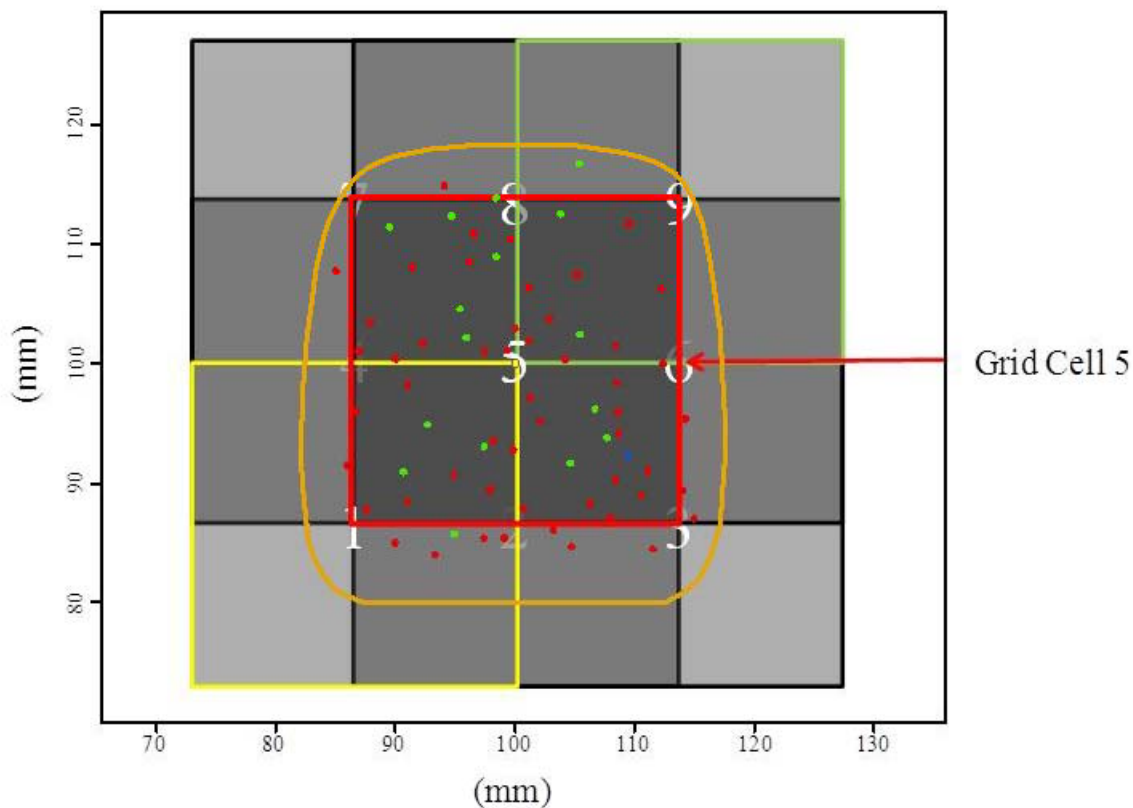
As was stated earlier, these analyses demonstrated that a population sample of 1200 fingerprint images is too small to produce false-match probabilities using sets of seven and nine minutiae. Thus, drastically increasing the fingerprint sample size would most likely allow for the identification of fingerprints with similar ridgeline feature configurations for nine minutiae and higher. In addition, incorporating ridgeline counts into the Monte Carlo simulations would include an additional primary feature used by Latent Print Examiners when performing comparisons. The drawback to including these parameters is that both the vectorization of ridge lines (to allow for ridge counting) and the preparation of fingerprint images is very time consuming. Increasing the fingerprint sample database to approximately 100,000 fingerprints would require alterations to the Monte Carlo simulation because the naïve Monte Carlo method employed here is computationally time consuming. The employment of parallel Markov Chain Monte Carlo methods, or conditional

Monte Carlo methods would need to be implemented to allow for the production of data in a relatively timely fashion. If applied to a larger dataset, the MC simulations, as performed in this study, would take approximately six to seven weeks of computer runtime for the simulations to produce data for analyses. Also, simulations that perform a modified Markov Chain Monte Carlo associated with a nearest neighbor approach would allow the simulations to be more similar to the way Latent Print Examiners search target groups of minutiae on fingerprints. These additional procedures could produce probabilities that are more closely associated with all the fingerprint features used by examiners when performing latent print comparisons.

5. REFERENCES

- Ashbaugh, D. R. 1994. The premises of friction ridge identification, clarity, and the identification process. *Journal of Forensic Identification* **44**:499-516.
- Bouchard-Côté, A., S. Sankararaman, and M. I. Jordan. 2012. Phylogenetic Inference via Sequential Monte Carlo. *Systematic Biology*.
- Champod, C. and P. A. Margot. 1996. Computer assisted analysis of minutiae occurrences on fingerprints. Pages 305-318 in J. Almog, E. Springer, M. Yisrael, and editors, editors. *Proceedings of the International Symposium on Fingerprint Detection and Identification*. Israel National Police, Neurim, Israel.
- Chen, Y. and A. K. Jain. 2009. Beyond minutiae: a fingerprint individuality model with pattern, ridge, and pore features. Pages 523-533 in *Third International Conference on Biometrics*. Springer, Alghero, Italy.
- Dass, S. C. and M. Li. 2009. Hierarchical mixture models for assessing fingerprint individuality. *The Annals of Applied Statistics* **3**:1448-1466.
- Dass, S. C., Y. Zhu, and A. K. Jain. 2005. Statistical models for assessing the individuality of fingerprints. Pages 3-9 in *Fourth IEEE Workshop on Automatic Identification Advanced Technologies*. IEEE Computer Society, Buffalo, New York.
- Daubert vs. Merrell Dow Pharmaceuticals. 509 US 579. 1993
- Gotelli, N. J. and A. M. Ellison. 2004. *A Primer of Ecological Statistics*. Sinauer Associates, Inc., Sunderland, Massachusetts.
- Langenburg, G. 2011. Scientific research supporting the foundations of friction ridge examinations, in *The Fingerprint Sourcebook*. A. McRoberts, editor. National Institute of Justice, Washington D.C. Ch. 14, pp.1-31.
- Lin, Y.-C. and K.-C. Wen. 2010. A simulation assessment by using Monte Carlo method on the risk of debris flow disaster in urban areas. *Asia GIS 2010 International Conference*, Kaohsiung, Taiwan.
- Manly, B. F. J. 2006. *Randomization, Bootstrap and Monte Carlo Methods in Biology*. 3rd. edition. Chapman & Hall/CRC, United States.

- National Research Council Committee on Identifying the Needs of the Forensic Sciences Community. 2009. Strengthening forensic science in the United States: A path forward. The National Academies Press, Washington D.C.
- Neumann, C., C. Champod, R. Puch-Solis, N. M. Egli, A. Anthonioz, and A. Bromage-Griffiths. 2007. Computation of likelihood ratios in fingerprint identification for configurations of any number of minutiae. *Journal of Forensic Sciences* **52**:54-64.
- Neumann, C., C. Champod, R. Puch-Solis, N. M. Egli, A. Anthonioz, D. Meuwly, and A. Bromage-Griffiths. 2006. Computation of likelihood ratios in fingerprint identification for configurations of three minutiae. *Journal of Forensic Sciences* **51**:1255-1266.
- Paielli, R. A. and H. Erzberger. 1996. Conflict probability estimation for free flight. Ames Research Center, Moffett Field, CA.
- Pankanti, S., S. Prabhakar, and A. K. Jain. 2002. On the individuality of fingerprints. *IEEE Transactions on Pattern Analysis and Machine Intelligence* **24**:1010-1025.
- Parziale, G. and A. Niel. 2004. A fingerprint matching using minutiae triangulation. Pages 241-248 *in* First International Conference of Biometric Authentication. Springer, Hong Kong, China.
- Ricklefs, R. E. and M. Lau. 1980. Bias and Dispersion of Overlap Indices: Results of Some Monte Carlo Simulations. *Ecology* **61**:1019-1024.
- Rubinstein, R. and D. P. Kroese. 2007. *Simulation and the Monte Carlo Method*. Second edition. John Wiley and Sons, Inc., Hoboken, New Jersey.
- Su, C. and S. N. Srihari. 2009. Probability of Random Correspondence for Fingerprints. Pages 55-66 *in* Computational Forensics, Third International Workshop, IWCF 2009. Springer-Verlag, The Hague, The Netherlands.
- Sujan, V. A. and M. P. Mulqueen. 2002. Fingerprint identification using space invariant transforms. *Pattern Recognition Letters* **23**:609-619.
- Tan, X. and B. Bhanu. 2006. Fingerprint matching by genetic algorithms. *Pattern Recognition* **39**:465-477.
- Wertheim, K. 2011. Embryology and morphology of friction ridge skin. *in* SWGFAST, editor. The Fingerprint Sourcebook. National Institute of Justice, Washington DC.



Legend

-  Fingerprint Convex Hull
-  Ridge Ending
-  Bifurcation
-  Core
-  Delta

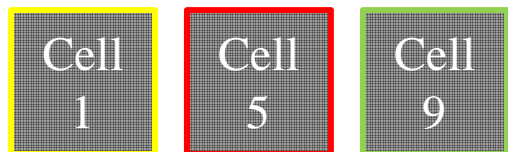


Figure 4-1. Nine grid cell filter used for Monte Carlo simulations.

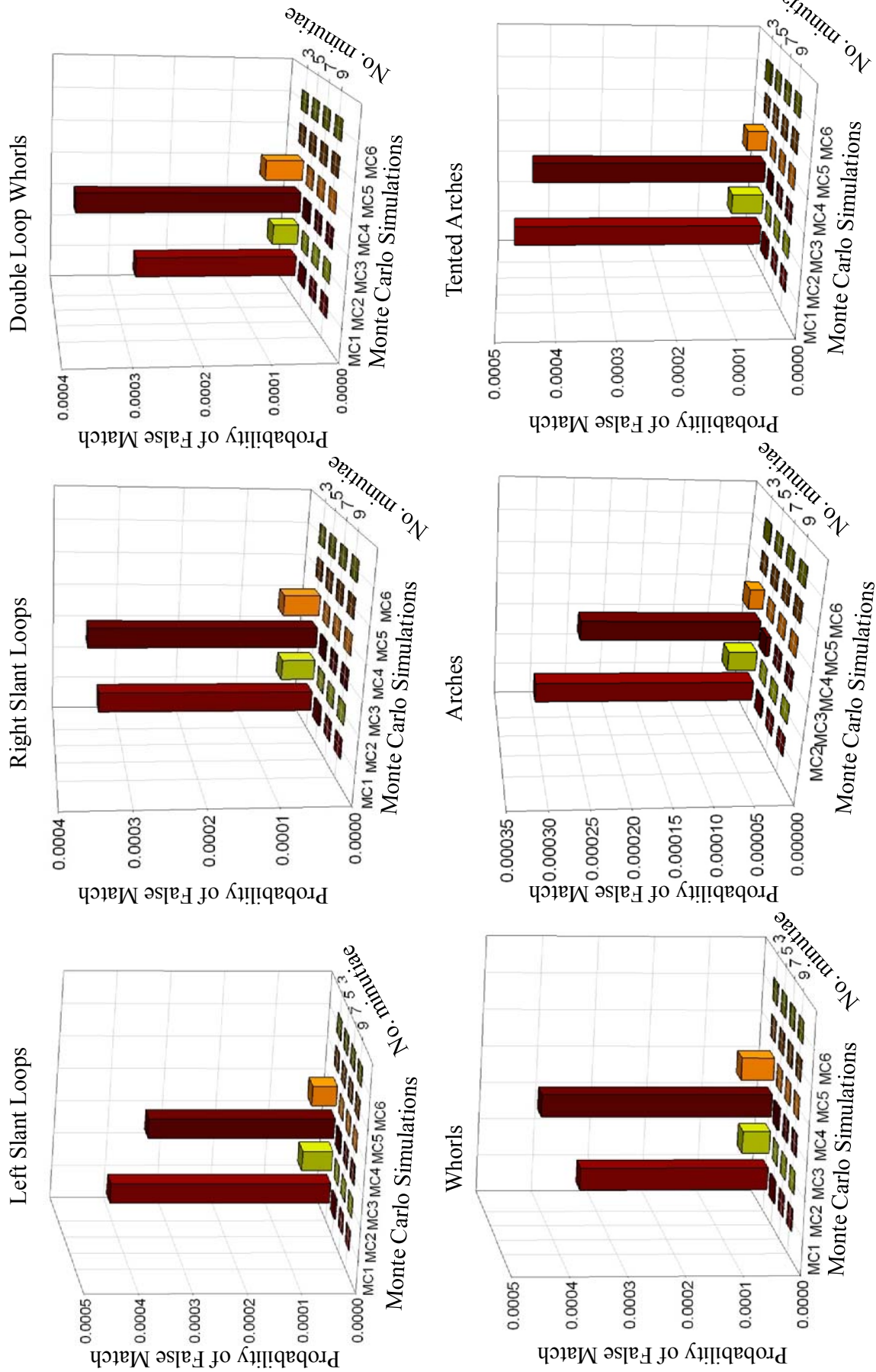
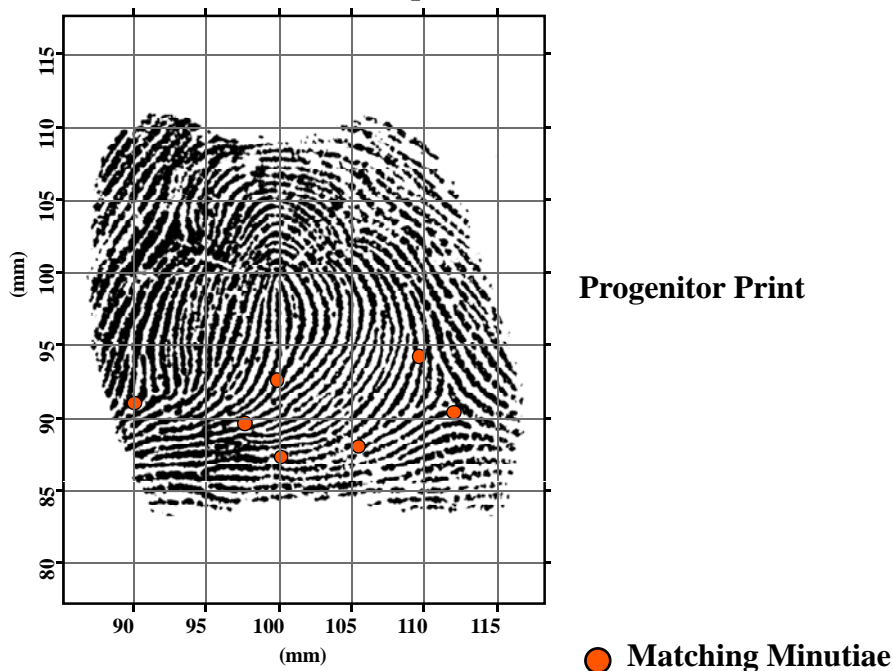


Figure 4-2. Average probabilities of a false-match for Monte Carlo simulations 1 through 6 using 3, 5, 7 and 9 minutiae

Selected Print: Left Slant Loop – Left Index



False Match: Whorl – Left Thumb

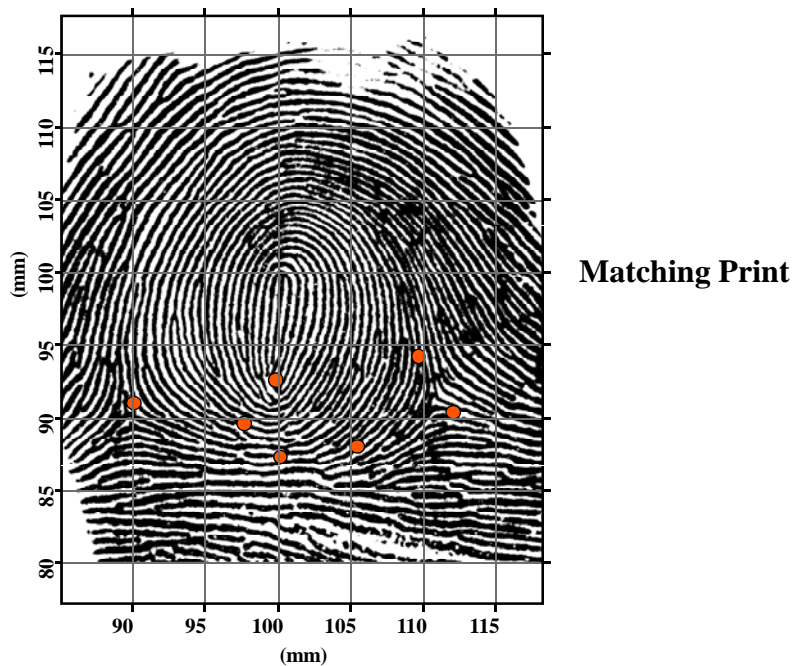


Figure 4-3. Illustration of a false match using a Monte Carlo 1 simulation of grid cell 5 having 7 minutiae located at the same X-Y coordinates.

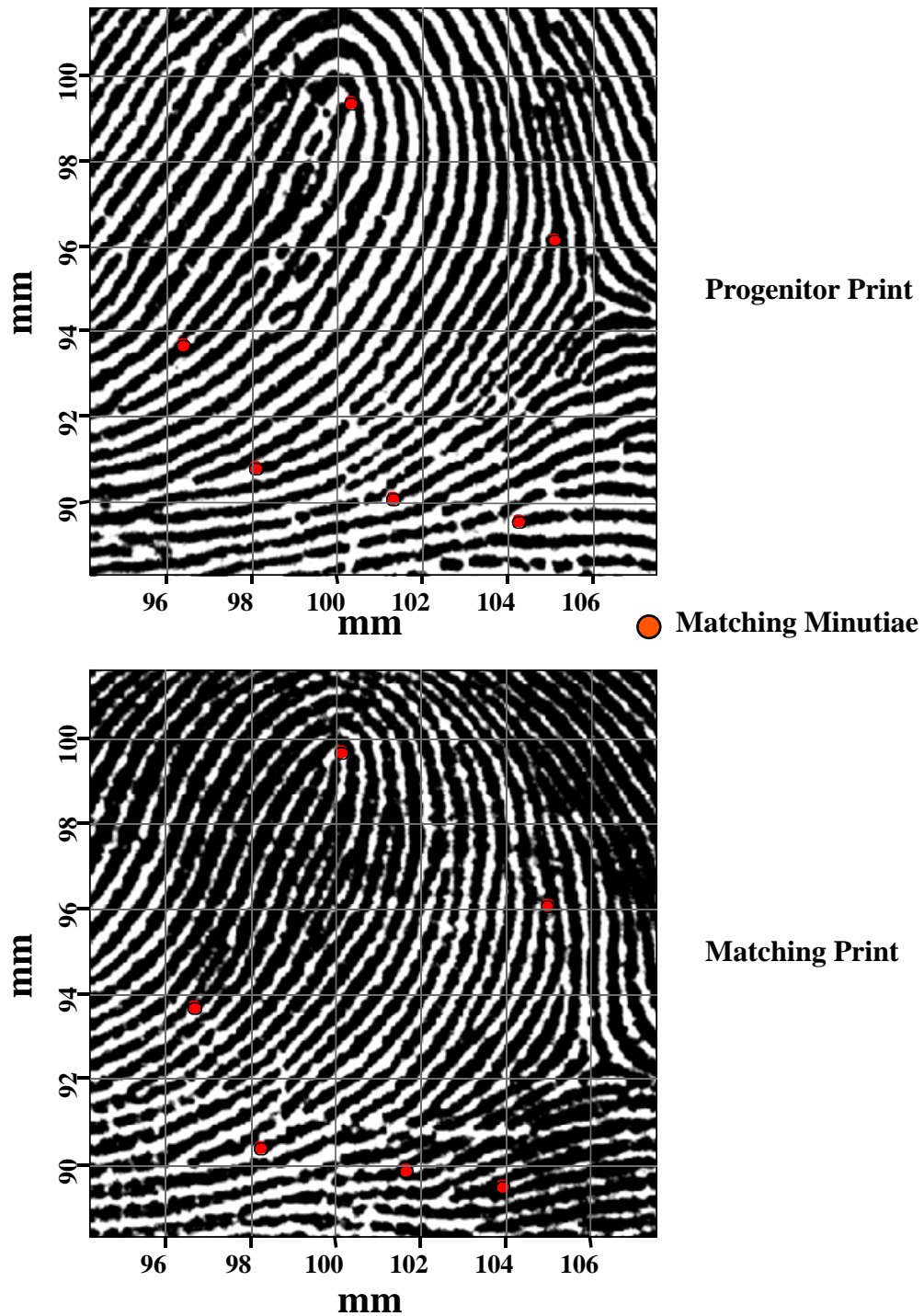


Figure 4-4. Illustration of a false match using a Monte Carlo 7 simulation of grid cell 2 with 6 minutiae with same X-Y coordinates and direction.

TABLES

Table 4-1. Parameter Combinations for Monte Carlo (MC) Minutiae Matching Simulator			
Key	Match Pattern Type	Match Minutiae Type	Match Minutiae Direction
MC1	No	No	No
MC2	No	Yes	No
MC3	Yes	No	No
MC4	Yes	Yes	No
MC5	No	Yes	Yes
MC6	Yes	Yes	Yes
MC7	No	No	Yes
MC8	Yes	No	Yes

Table 4-2. Monte Carlo Simulations 1-4 Probabilities of a False Match for Arches									
MC1 Coordinates only					MC2 Coordinates, Minutiae Type				
	3	5	7	9		3	5	7	9
Grid 1	2.38E-04	1.71E-06	1.25E-08	0	Grid 1	2.95E-05	8.68E-08	0	0
Grid 2	2.62E-04	1.67E-06	0	0	Grid 2	3.63E-05	1.21E-07	0	0
Grid 3	2.65E-04	1.66E-06	0	0	Grid 3	3.91E-05	2.43E-08	0	0
Grid 4	1.46E-04	5.18E-07	0	0	Grid 4	1.93E-05	0	0	0
Grid 5	1.61E-04	6.54E-07	0	0	Grid 5	2.24E-05	3.52E-08	0	0
Grid 6	1.74E-04	8.79E-07	0	0	Grid 6	2.53E-05	2.43E-08	0	0
Grid 7	5.46E-05	1.60E-07	0	0	Grid 7	1.05E-05	0	0	0
Grid 8	5.56E-05	1.85E-07	0	0	Grid 8	8.88E-06	1.17E-08	0	0
Grid 9	7.29E-05	7.41E-08	0	0	Grid 9	1.19E-05	0	0	0
MC3 Coordinates, Pattern Type					MC4 Coordinates, Pattern Type, Minutiae Type				
	3	5	7	9		3	5	7	9
Grid 1	2.37E-04	7.68E-06	0	0	Grid 1	3.23E-05	0	0	0
Grid 2	1.76E-04	5.31E-07	0	0	Grid 2	1.84E-05	0	0	0
Grid 3	1.40E-04	2.66E-07	0	0	Grid 3	1.47E-05	0	0	0
Grid 4	1.37E-04	7.97E-07	0	0	Grid 4	1.43E-05	0	0	0
Grid 5	1.02E-04	5.31E-07	0	0	Grid 5	1.45E-05	0	0	0
Grid 6	1.04E-04	2.61E-07	0	0	Grid 6	1.58E-05	0	0	0
Grid 7	1.67E-05	0	0	0	Grid 7	2.37E-06	0	0	0
Grid 8	3.96E-05	0	0	0	Grid 8	1.21E-05	0	0	0
Grid 9	6.00E-05	0	0	0	Grid 9	8.14E-06	0	0	0

Table 4-3. Monte Carlo Simulations 5-8									
Probabilities of a False Match for Arches									
MC5					MC6				
Coordinates, Minutiae Type & Direction					Coordinates, Pattern Type, Minutiae Type & Direction				
	3	5	7	9		3	5	7	9
Grid 1	3.68E-08	0	0	0	Grid 1	2.61E-07	0	0	0
Grid 2	2.51E-08	0	0	0	Grid 2	0	0	0	0
Grid 3	3.76E-08	0	0	0	Grid 3	0	0	0	0
Grid 4	5.71E-07	0	0	0	Grid 4	2.61E-07	0	0	0
Grid 5	1.17E-08	0	0	0	Grid 5	0	0	0	0
Grid 6	3.60E-08	0	0	0	Grid 6	0	0	0	0
Grid 7	0	0	0	0	Grid 7	0	0	0	0
Grid 8	5.01E-08	0	0	0	Grid 8	5.21E-07	0	0	0
Grid 9	0	0	0	0	Grid 9	0	0	0	0
MC7					MC8				
Coordinates, Minutiae Direction					Coordinates, Pattern Type, Minutiae Direction				
	3	5	7	9		3	5	7	9
Grid 1	4.58E-07	0	0	0	Grid 1	0	0	0	0
Grid 2	4.58E-07	0	0	0	Grid 2	9.25E-07	0	0	0
Grid 3	6.26E-07	0	0	0	Grid 3	4.63E-07	0	0	0
Grid 4	1.04E-07	0	0	0	Grid 4	4.63E-07	0	0	0
Grid 5	2.29E-07	0	0	0	Grid 5	4.63E-07	0	0	0
Grid 6	2.08E-07	0	0	0	Grid 6	4.63E-07	0	0	0
Grid 7	4.18E-08	0	0	0	Grid 7	0	0	0	0
Grid 8	6.25E-08	0	0	0	Grid 8	2.78E-06	0	0	0
Grid 9	5.43E-07	0	0	0	Grid 9	4.18E-06	0	0	0

**Table 4-4. Monte Carlo Simulations 1-4
Probabilities of a False Match for Left Slant Loops**

MC1					MC2				
Coordinates only					Coordinates, Minutiae type				
	3	5	7	9		3	5	7	9
Grid 1	2.54E-04	1.73E-06	1.73E-08	0	Grid 1	3.69E-05	2.24E-08	0	0
Grid 2	2.53E-04	1.74E-06	1.14E-08	0	Grid 2	3.75E-05	6.84E-08	0	0
Grid 3	2.47E-04	1.73E-06	5.52E-09	0	Grid 3	3.77E-05	4.53E-08	0	0
Grid 4	1.80E-04	7.65E-07	5.52E-09	0	Grid 4	2.48E-05	2.32E-08	0	0
Grid 5	1.79E-04	8.72E-07	0	0	Grid 5	2.68E-05	7.32E-08	0	0
Grid 6	1.80E-04	8.49E-07	1.69E-08	0	Grid 6	2.73E-05	5.67E-08	0	0
Grid 7	6.88E-05	2.50E-07	0	0	Grid 7	1.04E-05	1.17E-08	0	0
Grid 8	7.21E-05	2.30E-07	5.55E-09	0	Grid 8	1.08E-05	2.21E-08	0	0
Grid 9	7.93E-05	1.45E-07	0	0	Grid 9	9.86E-06	1.74E-08	0	0
MC3					MC4				
Coordinates, Pattern Type					Coordinates, Pattern Type, Minutiae Type				
	3	5	7	9		3	5	7	9
Grid 1	2.10E-04	1.25E-06	0	0	Grid 1	3.10E-05	7.91E-08	0	0
Grid 2	2.66E-04	1.78E-06	0	0	Grid 2	4.08E-05	6.00E-08	0	0
Grid 3	3.03E-04	2.52E-06	0	0	Grid 3	4.51E-05	1.16E-07	0	0
Grid 4	1.52E-04	6.58E-07	0	0	Grid 4	2.23E-05	0	0	0
Grid 5	1.89E-04	1.21E-06	2.05E-08	0	Grid 5	2.82E-05	5.71E-08	0	0
Grid 6	2.19E-04	1.35E-06	0	0	Grid 6	3.59E-05	3.95E-08	0	0
Grid 7	6.37E-05	0	0	0	Grid 7	1.44E-05	0	0	0
Grid 8	7.64E-05	2.50E-07	0	0	Grid 8	1.25E-05	1.14E-07	0	0
Grid 9	9.18E-05	4.85E-07	0	0	Grid 9	1.30E-05	5.86E-08	0	0

Table 4-5. Monte Carlo Simulations 5-8									
Probabilities of a False Match for Left Slant Loops									
MC5 Coordinates, Minutiae Type & Direction					MC6 Coordinates, Pattern Type, Minutiae Type & Direction				
	3	5	7	9		3	5	7	9
Grid 1	1.66E-07	0	0	0	Grid 1	4.04E-07	0	0	0
Grid 2	1.27E-07	0	0	0	Grid 2	1.36E-07	0	0	0
Grid 3	7.36E-08	0	0	0	Grid 3	2.55E-07	0	0	0
Grid 4	1.55E-07	0	0	0	Grid 4	2.21E-07	0	0	0
Grid 5	8.67E-08	0	0	0	Grid 5	1.58E-07	0	0	0
Grid 6	1.39E-07	0	0	0	Grid 6	1.60E-07	0	0	0
Grid 7	1.92E-07	0	0	0	Grid 7	2.69E-07	0	0	0
Grid 8	6.35E-08	0	0	0	Grid 8	3.06E-07	0	0	0
Grid 9	4.07E-08	0	0	0	Grid 9	9.94E-08	0	0	0
MC7 Coordinates, Minutiae Direction					MC8 Coordinates, Pattern Type, Minutiae Direction				
	3	5	7	9		3	5	7	9
Grid 1	6.09E-07	0	0	0	Grid 1	1.55E-06	0	0	0
Grid 2	6.50E-07	8.33E-09	0	0	Grid 2	2.38E-06	0	0	0
Grid 3	8.16E-07	0	0	0	Grid 3	1.78E-06	0	0	0
Grid 4	4.42E-07	0	0	0	Grid 4	1.06E-06	0	0	0
Grid 5	4.92E-07	0	0	0	Grid 5	1.41E-06	0	0	0
Grid 6	5.67E-07	0	0	0	Grid 6	1.69E-06	0	0	0
Grid 7	1.92E-07	0	0	0	Grid 7	5.45E-07	0	0	0
Grid 8	3.66E-07	0	0	0	Grid 8	1.00E-06	0	0	0
Grid 9	3.74E-07	0	0	0	Grid 9	1.23E-06	0	0	0

Table 4-6. Monte Carlo Simulations 1-4									
Probabilities of a False Match for Right Slant Loops									
MC1					MC2				
Coordinates only					Coordinates, Minutiae type				
	3	5	7	9		3	5	7	9
Grid 1	2.34E-04	1.58E-06	2.89E-08	0	Grid 1	3.44E-05	9.19E-08	0	0
Grid 2	2.46E-04	1.49E-06	1.15E-08	0	Grid 2	3.71E-05	6.82E-08	0	0
Grid 3	2.56E-04	1.90E-06	1.74E-08	0	Grid 3	3.95E-05	9.57E-08	0	0
Grid 4	1.68E-04	8.77E-07	3.45E-08	0	Grid 4	2.36E-05	1.15E-08	0	0
Grid 5	1.77E-04	8.51E-07	0	0	Grid 5	2.65E-05	4.63E-08	0	0
Grid 6	1.84E-04	9.06E-07	1.71E-08	0	Grid 6	2.87E-05	4.52E-08	0	0
Grid 7	7.50E-05	2.47E-07	0	0	Grid 7	8.71E-06	6.28E-08	5.99E-09	0
Grid 8	7.52E-05	2.83E-07	0	0	Grid 8	1.01E-05	0	0	0
Grid 9	6.97E-05	1.04E-06	0	0	Grid 9	1.03E-05	0	0	0
MC3					MC4				
Coordinates, Pattern Type					Coordinates, Pattern Type, Minutiae Type				
	3	5	7	9		3	5	7	9
Grid 1	2.49E-04	1.53E-06	0	0	Grid 1	3.76E-05	4.41E-08	0	0
Grid 2	2.33E-04	1.30E-06	2.16E-08	0	Grid 2	3.70E-05	4.41E-08	0	0
Grid 3	2.07E-04	1.40E-06	4.31E-08	0	Grid 3	3.59E-05	4.41E-08	0	0
Grid 4	1.77E-04	1.13E-06	2.25E-08	0	Grid 4	2.46E-05	8.82E-08	0	0
Grid 5	1.63E-04	5.58E-07	2.25E-08	0	Grid 5	2.55E-05	2.16E-08	0	0
Grid 6	1.44E-04	6.34E-07	2.25E-08	0	Grid 6	2.10E-05	0	0	0
Grid 7	6.51E-05	9.14E-08	0	0	Grid 7	8.07E-06	0	0	0
Grid 8	6.42E-05	2.21E-07	0	0	Grid 8	8.32E-06	4.51E-08	0	0
Grid 9	4.56E-05	0	0	0	Grid 9	3.55E-06	0	0	0

Table 4-7. Monte Carlo Simulations 5-8									
Probabilities of a False Match for Right Slant Loops									
MC5 Coordinates, Minutiae Type & Direction					MC6 Coordinates, Pattern Type, Minutiae Type & Direction				
	3	5	7	9		3	5	7	9
Grid 1	8.00E-08	0	0	0	Grid 1	1.35E-07	0	0	0
Grid 2	5.71E-08	0	0	0	Grid 2	1.75E-07	0	0	0
Grid 3	2.23E-07	0	0	0	Grid 3	6.37E-07	0	0	0
Grid 4	1.71E-08	0	0	0	Grid 4	4.30E-08	0	0	0
Grid 5	5.71E-08	0	0	0	Grid 5	1.54E-07	0	0	0
Grid 6	1.29E-07	0	0	0	Grid 6	1.75E-07	0	0	0
Grid 7	2.25E-08	0	0	0	Grid 7	0	0	0	0
Grid 8	5.93E-09	0	0	0	Grid 8	0	0	0	0
Grid 9	0	0	0	0	Grid 9	0	0	0	0
MC7 Coordinates, Minutiae Direction					MC8 Coordinates, Pattern Type, Minutiae Direction				
	3	5	7	9		3	5	7	9
Grid 1	5.42E-07	0	0	0	Grid 1	6.79E-07	0	0	0
Grid 2	3.08E-07	0	0	0	Grid 2	9.38E-07	0	0	0
Grid 3	1.00E-06	0	0	0	Grid 3	1.62E-06	0	0	0
Grid 4	2.75E-07	0	0	0	Grid 4	3.56E-07	0	0	0
Grid 5	3.17E-07	0	0	0	Grid 5	6.48E-07	0	0	0
Grid 6	2.92E-07	0	0	0	Grid 6	6.15E-07	0	0	0
Grid 7	2.02E-07	0	0	0	Grid 7	0	0	0	0
Grid 8	2.00E-07	0	0	0	Grid 8	1.94E-07	0	0	0
Grid 9	4.34E-08	0	0	0	Grid 9	1.01E-07	0	0	0

Table 4-8. Monte Carlo Simulations 1-4									
Probabilities of a False Match for Tented Arches									
MC1					MC2				
Coordinates only					Coordinates, Minutiae type				
	3	5	7	9		3	5	7	9
Grid 1	3.29E-04	2.30E-06	1.06E-07	1.08E-08	Grid 1	4.28E-05	5.43E-08	0	0
Grid 2	3.44E-04	2.50E-06	2.15E-08	0	Grid 2	4.67E-05	1.83E-07	0	0
Grid 3	3.56E-04	2.95E-06	9.45E-08	0	Grid 3	4.96E-05	1.28E-07	0	0
Grid 4	2.38E-04	1.63E-06	2.09E-08	0	Grid 4	3.37E-05	7.64E-08	0	0
Grid 5	2.32E-04	1.35E-06	1.04E-08	0	Grid 5	3.10E-05	5.49E-08	0	0
Grid 6	2.36E-04	1.27E-06	1.11E-08	0	Grid 6	3.13E-05	3.27E-08	0	0
Grid 7	1.05E-04	2.71E-07	0	0	Grid 7	1.57E-05	4.87E-08	0	0
Grid 8	9.06E-05	2.35E-07	0	0	Grid 8	1.31E-05	0	0	0
Grid 9	7.46E-05	2.92E-07	0	0	Grid 9	1.02E-05	0	0	0
MC3					MC4				
Coordinates, Pattern Type					Coordinates, Pattern Type, Minutiae Type				
	3	5	7	9		3	5	7	9
Grid 1	3.07E-04	1.65E-06	0	0	Grid 1	3.13E-05	0	0	0
Grid 2	3.61E-04	4.29E-06	0	0	Grid 2	4.57E-05	0	0	0
Grid 3	4.03E-04	1.97E-06	0	0	Grid 3	3.63E-05	1.90E-07	0	0
Grid 4	2.23E-04	1.81E-06	0	0	Grid 4	3.41E-05	0	0	0
Grid 5	2.17E-04	1.40E-06	0	0	Grid 5	2.74E-05	0	0	0
Grid 6	2.17E-04	1.43E-06	0	0	Grid 6	2.93E-05	0	0	0
Grid 7	1.03E-04	0	0	0	Grid 7	2.45E-05	0	0	0
Grid 8	6.11E-05	2.15E-07	0	0	Grid 8	9.34E-06	0	0	0
Grid 9	2.03E-05	0	0	0	Grid 9	0	0	0	0

Table 4-9. Monte Carlo Simulations 5-8									
Probabilities of a False Match for Tented Arched									
MC5 Coordinates, Minutiae Type & Direction					MC6 Coordinates, Pattern Type, Minutiae Type & Direction				
	3	5	7	9		3	5	7	9
Grid 1	1.70E-07	0	0	0	Grid 1	1.81E-06	0	0	0
Grid 2	8.55E-08	0	0	0	Grid 2	0	0	0	0
Grid 3	5.21E-08	0	0	0	Grid 3	0	0	0	0
Grid 4	5.49E-08	0	0	0	Grid 4	1.89E-07	0	0	0
Grid 5	5.49E-08	0	0	0	Grid 5	2.15E-07	0	0	0
Grid 6	6.39E-08	0	0	0	Grid 6	4.04E-07	0	0	0
Grid 7	0	0	0	0	Grid 7	0	0	0	0
Grid 8	2.09E-08	0	0	0	Grid 8	0	0	0	0
Grid 9	4.56E-08	0	0	0	Grid 9	0	0	0	0
MC7 Coordinates, Minutiae Direction					MC8 Coordinates, Pattern Type, Minutiae Direction				
	3	5	7	9		3	5	7	9
Grid 1	4.84E-07	0	0	0	Grid 1	9.10E-07	0	0	0
Grid 2	3.33E-07	0	0	0	Grid 2	6.06E-07	0	0	0
Grid 3	7.33E-07	0	0	0	Grid 3	2.72E-06	0	0	0
Grid 4	1.83E-07	0	0	0	Grid 4	3.04E-07	0	0	0
Grid 5	2.84E-07	0	0	0	Grid 5	3.04E-07	0	0	0
Grid 6	1.50E-07	0	0	0	Grid 6	9.10E-07	0	0	0
Grid 7	1.33E-07	0	0	0	Grid 7	0	0	0	0
Grid 8	1.67E-07	0	0	0	Grid 8	3.04E-07	0	0	0
Grid 9	2.71E-07	0	0	0	Grid 9	0	0	0	0

Table 4-10. Monte Carlo Simulations 1-4									
Probabilities of a False Match for Double Loop Whorls									
MC1					MC2				
Coordinates only					Coordinates, Minutiae type				
	3	5	7	9		3	5	7	9
Grid 1	1.84E-04	1.04E-06	5.55E-09	0	Grid 1	2.80E-05	1.05E-07	0	0
Grid 2	2.02E-04	1.07E-06	0	0	Grid 2	3.26E-05	6.26E-08	0	0
Grid 3	1.91E-04	1.26E-06	1.19E-08	0	Grid 3	2.95E-05	4.04E-08	0	0
Grid 4	1.37E-04	5.37E-07	1.74E-08	0	Grid 4	2.04E-05	2.89E-08	0	0
Grid 5	1.47E-04	6.05E-07	5.93E-09	0	Grid 5	2.28E-05	1.19E-08	0	0
Grid 6	1.41E-04	7.21E-07	0	0	Grid 6	2.20E-05	2.85E-08	0	0
Grid 7	6.69E-05	6.37E-08	0	0	Grid 7	9.91E-06	5.55E-09	0	0
Grid 8	6.39E-05	1.83E-07	5.63E-09	0	Grid 8	8.98E-06	5.93E-09	0	0
Grid 9	5.44E-05	2.13E-07	0	0	Grid 9	9.22E-06	0	0	0
MC3					MC4				
Coordinates, Pattern Type					Coordinates, Pattern Type, Minutiae Type				
	3	5	7	9		3	5	7	9
Grid 1	2.59E-04	2.08E-06	8.00E-08	0	Grid 1	4.09E-05	7.60E-08	0	0
Grid 2	2.79E-04	1.25E-06	0	0	Grid 2	4.40E-05	3.81E-08	0	0
Grid 3	2.55E-04	1.54E-06	0	0	Grid 3	3.84E-05	1.18E-07	0	0
Grid 4	1.93E-04	1.29E-06	0	0	Grid 4	2.99E-05	1.18E-07	0	0
Grid 5	2.02E-04	8.91E-07	0	0	Grid 5	3.05E-05	0	0	0
Grid 6	1.81E-04	7.01E-07	0	0	Grid 6	2.71E-05	4.01E-08	0	0
Grid 7	8.54E-05	1.56E-07	0	0	Grid 7	1.34E-05	0	0	0
Grid 8	8.45E-05	2.35E-07	0	0	Grid 8	1.27E-05	3.81E-08	0	0
Grid 9	7.80E-05	1.64E-07	0	0	Grid 9	1.24E-05	0	0	0

**Table 4-11. Monte Carlo Simulations 5-8
Probabilities of a False Match for Double Loop Whorls**

MC5					MC6				
Coordinates, Minutiae Type & Direction					Coordinates, Pattern Type, Minutiae Type & Direction				
	3	5	7	9		3	5	7	9
Grid 1	7.33E-08	0	0	0	Grid 1	1.55E-07	0	0	0
Grid 2	6.93E-08	0	0	0	Grid 2	1.54E-07	0	0	0
Grid 3	8.49E-08	0	0	0	Grid 3	1.52E-07	0	0	0
Grid 4	5.15E-08	0	0	0	Grid 4	1.57E-07	0	0	0
Grid 5	1.35E-07	0	0	0	Grid 5	7.81E-08	0	0	0
Grid 6	1.07E-07	0	0	0	Grid 6	7.70E-08	0	0	0
Grid 7	3.55E-08	0	0	0	Grid 7	0	0	0	0
Grid 8	4.04E-08	0	0	0	Grid 8	3.80E-08	0	0	0
Grid 9	1.70E-08	0	0	0	Grid 9	7.77E-08	0	0	0
MC7					MC8				
Coordinates, Minutiae Direction					Coordinates, Pattern Type, Minutiae Direction				
	3	5	7	9		3	5	7	9
Grid 1	2.00E-07	0	0	0	Grid 1	2.29E-07	0	0	0
Grid 2	2.00E-07	0	0	0	Grid 2	2.29E-07	0	0	0
Grid 3	4.17E-07	0	0	0	Grid 3	1.20E-06	0	0	0
Grid 4	1.33E-07	0	0	0	Grid 4	2.29E-07	0	0	0
Grid 5	2.17E-07	0	0	0	Grid 5	2.29E-07	0	0	0
Grid 6	3.17E-07	0	0	0	Grid 6	5.14E-07	0	0	0
Grid 7	1.00E-07	0	0	0	Grid 7	5.71E-08	0	0	0
Grid 8	3.42E-07	0	0	0	Grid 8	5.71E-07	0	0	0
Grid 9	3.96E-07	0	0	0	Grid 9	9.42E-07	0	0	0

Table 4-12. Monte Carlo Simulations 1-4									
Probabilities of a False Match for Whorls									
MC1					MC2				
Coordinates only					Coordinates, Minutiae type				
	3	5	7	9		3	5	7	9
Grid 1	2.28E-04	1.54E-06	1.69E-08	0	Grid 1	3.31E-05	5.67E-08	0	0
Grid 2	2.31E-04	1.42E-06	1.14E-08	0	Grid 2	3.49E-05	6.77E-08	0	0
Grid 3	2.39E-04	1.45E-06	1.14E-08	0	Grid 3	3.64E-05	7.87E-08	0	0
Grid 4	1.78E-04	9.17E-07	5.52E-09	0	Grid 4	2.65E-05	2.83E-08	0	0
Grid 5	1.77E-04	8.81E-07	0	0	Grid 5	2.65E-05	2.32E-08	0	0
Grid 6	1.83E-04	1.06E-06	5.52E-09	0	Grid 6	2.75E-05	3.38E-08	0	0
Grid 7	8.56E-05	1.41E-07	0	0	Grid 7	1.13E-05	0	0	0
Grid 8	8.09E-05	2.49E-07	0	0	Grid 8	1.18E-05	1.11E-08	0	0
Grid 9	8.72E-05	2.38E-07	0	0	Grid 9	1.39E-05	1.69E-08	0	0
MC3					MC4				
Coordinates, Pattern Type					Coordinates, Pattern Type, Minutiae Type				
	3	5	7	9		3	5	7	9
Grid 1	2.72E-04	2.38E-06	5.34E-08	0	Grid 1	3.81E-05	2.67E-08	0	0
Grid 2	2.89E-04	2.36E-06	0	0	Grid 2	4.45E-05	8.01E-08	0	0
Grid 3	3.08E-04	2.28E-06	0	0	Grid 3	4.71E-05	1.96E-07	0	0
Grid 4	2.14E-04	1.14E-06	0	0	Grid 4	2.93E-05	0	0	0
Grid 5	2.31E-04	1.05E-06	0	0	Grid 5	3.33E-05	5.31E-08	0	0
Grid 6	2.43E-04	1.50E-06	0	0	Grid 6	3.66E-05	2.67E-08	0	0
Grid 7	1.15E-04	6.81E-07	0	0	Grid 7	1.39E-05	2.67E-08	0	0
Grid 8	1.01E-04	3.63E-07	0	0	Grid 8	1.52E-05	5.34E-08	0	0
Grid 9	1.10E-04	5.97E-07	0	0	Grid 9	1.72E-05	5.45E-08	0	0

**Table 4-13. Monte Carlo Simulations 5-8
Probabilities of a False Match for Whorls**

MC5					MC6				
Coordinates, Minutiae Type & Direction					Coordinates, Pattern Type, Minutiae Type & Direction				
	3	5	7	9		3	5	7	9
Grid 1	1.28E-07	0	0	0	Grid 1	1.64E-07	0	0	0
Grid 2	3.38E-08	0	0	0	Grid 2	1.67E-07	0	0	0
Grid 3	8.31E-08	0	0	0	Grid 3	1.69E-07	0	0	0
Grid 4	3.90E-08	0	0	0	Grid 4	1.89E-07	0	0	0
Grid 5	3.38E-08	0	0	0	Grid 5	8.23E-08	0	0	0
Grid 6	6.15E-08	0	0	0	Grid 6	1.40E-07	0	0	0
Grid 7	1.45E-07	0	0	0	Grid 7	4.78E-07	0	0	0
Grid 8	1.05E-07	0	0	0	Grid 8	1.11E-07	0	0	0
Grid 9	5.04E-08	0	0	0	Grid 9	0	0	0	0
MC7					MC8				
Coordinates, Minutiae Direction					Coordinates, Pattern Type, Minutiae Direction				
	3	5	7	9		3	5	7	9
Grid 1	3.75E-07	0	0	0	Grid 1	8.47E-07	0	0	0
Grid 2	2.92E-07	0	0	0	Grid 2	7.66E-07	0	0	0
Grid 3	1.11E-06	0	0	0	Grid 3	7.65E-07	0	0	0
Grid 4	2.33E-07	0	0	0	Grid 4	5.65E-07	0	0	0
Grid 5	2.08E-07	0	0	0	Grid 5	3.23E-07	0	0	0
Grid 6	4.75E-07	0	0	0	Grid 6	8.06E-07	0	0	0
Grid 7	2.17E-07	0	0	0	Grid 7	1.61E-07	0	0	0
Grid 8	3.00E-07	0	0	0	Grid 8	6.05E-07	0	0	0
Grid 9	5.25E-07	0	0	0	Grid 9	3.62E-07	0	0	0

CHAPTER 5 – SUMMARY

I. PROJECT SUMMARY

The purpose of the study was to evaluate and quantify fingerprint characteristics (e.g., minutiae and ridge lines) using Geographic Information Systems (GIS) techniques to derive probabilities of a false match to describe the discriminating value of fingerprint features and to establish certainty levels for fingerprint identifications. Using GIS software as the unifying platform, many disparate analyses derived from a variety of mathematical and scientific disciplines (e.g., statistics, geometry, geology, ecology) were adapted to characterize fingerprints and create metrics to describe the distribution and frequency of fingerprints ridgeline features. These methods included geometric morphometrics, spatial statistics, Monte Carlo, and cartographic analysis. They were systematically employed to characterize fingerprint spatial patterns and ascertain the similarity of regions within and among fingerprints.

GIS allowed for the placement of fingerprints within a common georeferenced coordinate space centered about the core. Once fingers were projected in a standardized coordinate space, the aforementioned spatial analyses were conducted to characterize pattern types and minutiae distributions. Overall, there was a greater density of minutiae and ridgelines below the core compared to above the core regardless of pattern type. However, the distributions of bifurcations and ridge endings were more similar within any pattern type rather than among them. Also, pattern types with comparable ridge flow (e.g., loops and whorls) had greater similarity between them when comparing various metrics such as axis dimensions and Thiessen polygon ratios, suggesting that these patterns arise through similar biological phenomena.

As latent examiners have observed, fingerprint minutiae distributions are not uniform nor do they appear to be random. Furthermore, taking into account the greater number of ridges in the lower region as compared with the upper region of the finger does not explain the differential distribution of the minutiae across the fingerprint. It appears that the more complex the pattern type (i.e., double loop whorls are more complex than arches), the greater number of minutiae present on the finger.

The discrepancy between the upper and lower regions of the finger also implies that this minutiae differential is influenced by complexity of pattern because the lower sections are where the deltas occur along with other more frequent disruptions in ridge flow. Conversely, the upper regions of the finger (above the core) have a relatively uniform flow of ridgelines. Thus, the more complex pattern types, whorls and double loop whorls, tend to be similar to each other, are associated with larger pattern dimensions, and significantly differ from all other pattern types. The less complex pattern types, as exemplified by arches, tend to display fingerprint metrics at the other end of the scale.

Geometric morphometric techniques were successfully applied to provide an independent measure of shape variation in fingerprint features. While this type of analysis has not been widely or systematically applied to fingerprint patterns, geometric morphometrics offers promise as a tool for further refining our understanding of comparisons. Given the inherent biological assumptions regarding fingerprint features as landmarks in this analysis, it is anticipated that these results will be especially informative about the extent of variation around readily identifiable regions such as deltas and cores. This information about fingerprint features and shape variation could be used in future studies to determine and / or predict the limits of both native and depositional fingerprint distortion for any pattern type.

Along with pattern characterization and analyses, a primary goal of the study was to assess false-match probabilities associated with fingerprint minutiae patterns. The study used a naïve brute force Monte Carlo approach for empirically estimating probabilities of identical minutiae spatial patterns occurring on different fingers. The simulations demonstrated a general trend that the minutiae in the

upper region of a finger above the core have a lower probability of coincidence as compared to those below, regardless of pattern type and complexity of model parameterization. In addition, when considering only the spatial location of minutiae in standardized coordinate space, increasing the number of minutiae used in a comparison drastically decreased the probability of coincidence between fingers. Probabilities of false match decreased even further when other attribute parameters, such as minutiae type and direction, were added to the selection model. The Monte Carlo simulations indicated that our database was too small to produce probabilities for larger sets of minutiae used for comparison. This suggests that the occurrence of a false match with larger sets of minutiae is extremely rare, and to create an associated probability, the data set will need to be increased 10 to 100 fold. However, the probabilities that were produced from the current data set are quite robust, are adequate for use within the Oregon population, and they provide a baseline probability of occurrence for minutiae patterns on fingerprints.

Utilizing geometric morphometrics, in conjunction with a GIS, represents a novel approach for evaluating and quantifying spatial relationships among friction ridgeline features (i.e., minutiae). The impacts of this work include an increase in forensic science knowledge and understanding of the spatial patterns of friction skin minutiae. Additionally, there will be direct implications for quantifying another element of potential variance associated with estimating probabilities for describing the discriminating value of fingerprint features, especially when the probabilities are based on ten-print standards. This is the first empirical study that quantifies fingerprint shape variation utilizing geometric morphometric methods for latent print comparison purposes, which in turn, could have implications for the latent print comparison process and practice.

Increasingly, the forensic community is being asked to provide quantifiable metrics and statistics during testimony on latent print comparisons. The research presented herein provides information that will aid in bolstering latent print examiners' testimony with data that characterize fingerprint patterns and metrics. While not all the analyses used in the study will be directly applied within the criminal justice system, the scientific approach to pattern characterization taken here will strengthen the validity of using fingerprints for identification. The spatial analysis of fingerprints, and the consistent clustering of similar pattern types strongly suggest a biological association between fingerprint development and fingerprint pattern type.

2. IMPLICATIONS FOR POLICY AND PRACTICE

Impacts of this work include making a significant contribution toward forensic practice in the laboratory by establishing a degree of certainty and defining the limits for latent print identifications. In addition, this will strengthen the accuracy and reliability of the ACE-V methodology as called for in the National Academy of Sciences report (National Research Council, 2009). While GIS is widely used for crime pattern analysis and emergency management applications (Bodbyl-Mast, 2009; Chainey and Ratcliffe, 2005; ESRI, 2000, 2001), use as an analytical tool for fingerprint probability estimates is virtually absent from the literature. In addition, much of the statistical modeling of fingerprint patterns is being conducted in the computer science community for use in biometric verification (e.g., Maio et al., 2002; Cappelli et al., 2006; Dass and Jain, 2007) and is largely absent from latent print comparison applications. This project takes a novel approach in utilizing GIS and related tools to derive probability estimates for latent print identifications with the final deliverable involving model testing on active casework in a forensic laboratory. The final project outcomes connect the daily work of latent print examiners to science-based research; thus, directly addressing the National Academy of Sciences call for improved linkages between forensics and the academic community.

Impact on the Development of the Latent Print Discipline

There has been minimal impact on the development of the latent print discipline thus far. However, it is anticipated that the end product of this grant will have a significant impact on the latent print comparison practice and testimony provided. The project's aim was to provide a quantitative measure of the discriminating value of the various ridgeline features by estimating the probability of a false-match. The resultant probabilities are applicable for subsequent qualification of latent print comparison conclusions. The results of this study will aid latent print examiners in testimony by grounding their results in the scientific method. In addition, our use of GIS is a novel approach to fingerprint analysis. GIS software is readily available in the marketplace, with a vast community of users. Thus, a value-added outcome of this work will include the development of alternative methodologies and tools to aid latent print analysts in improving the efficacy of latent print identifications.

Impact on Other Disciplines

Because the resultant product(s) will be a pattern-based process, the use of GIS for pattern based statistical analysis can be applied to any pattern identification forensic discipline including, but not limited to, toolmarks, ballistics, and shoe and tire impressions.

3. IMPLICATIONS FOR FURTHER RESEARCH

Current project results highlight areas where additional work is needed. One area is the estimation of false-match probabilities with greater numbers of minutiae which will require a significantly larger fingerprint image dataset (one that is beyond the resources of this current work). The implementation of parallel Markov Chain Monte Carlo methods or conditional Monte Carlo methods will allow for the generation of probability simulation data and consequently greater numbers of simulation runs. Also, simulations that perform a modified Markov Chain Monte Carlo associated with a nearest neighbor approach will more closely emulate the way latent print examiners search target groups of minutiae on fingerprints. Results from geometric morphometric spatial analyses for the current study indicate that this approach is ideally suited for studying elastic skin deformation and attendant fingerprint distortion. In addition, the novel GIS approach employed here for conducting spatial analyses and deriving probability estimates can be utilized for further fingerprint characterization.

4. DISSEMINATION OF RESEARCH FINDINGS

During the review period, data were disseminated to Oregon State Police (OSP), Forensic Services Division (FSD) latent print examiners for review, consultation, and feedback. In addition we presented at the IAI conference in August and at the Pacific Northwest-IAI conference in September. We will continue to disseminate information and collaborate with OSP, FSD latent print examiners. We also anticipate submitting a paper or papers for publication in forensic journals (e.g., *Journal of Forensic Science* or *Journal of Forensic Identification*) in the upcoming months.

Publications, Conference Papers, and Presentations

1. Aldrich, P. 2010. Application of Spatial Statistics to Latent Print Identifications: Towards Improved Forensic Science Methodologies. *International Association for Identification, 95th International Educational Conference*: 66.

2. Dutton, E. K. 2010. Application of Spatial Statistics to Latent Print Identifications: Towards Improved Forensic Science Methodologies. *Flames, Craniums, and Fundamentals: Highlighting NIJ Research*. Office of Investigative and Forensic Sciences, National Institute of Justice, U.S. Department of Justice.
3. Dutton, E. K., Taylor, S.B., Aldrich, P., and Dutton, B. E. 2010a. NIJ Grant Project. AFIS Internet, Inc. *24th Annual Users Conference*: 31.
4. Dutton, E.K., Taylor, S.B., Aldrich, P., Dutton, B. E. 2010b. Application of Spatial Statistics To Latent Print Identifications. Proceedings of Northwest Association of Forensic Scientists. Portland, Oregon. Last Accessed April 2011.
<http://www.nwafs.org/Meeting/Old%20Meeting%20Info/2010_technical_abstracts.pdf>.
5. Dutton, E.K., Taylor, S.B., Aldrich, P., and Dutton, B. E. 2011. *Application of Geographic Information Systems and Spatial Statistics to Probability Estimates In Latent-Print Identification*. Abstract with Program, the 2011 International Association for Identification annual conference, Milwaukee, Wisconsin.
6. Dutton, E.K., Taylor, S.B., Aldrich, P.R., Dutton, B.E. and Stanley, R.J. 2012. *Geographic Information Systems and Spatial Analysis – Part 2: A Monte Carlo Approach to Estimating Probabilities for Latent Print Identification*. Abstract with Program, the 2012 American Academy of Forensic Sciences annual conference, Atlanta, Georgia.
7. Hidalgo, S.C., Dutton, B.E., Stanley, R.J., Aldrich, P.R., Dutton, E.K. and Taylor, S.B. 2012. *A Geometric Morphometric Approach to Fingerprint Analysis*. Abstract with Program, the 2012 American Academy of Forensic Sciences annual conference, Atlanta, Georgia.
8. Stanley, R.J., Dutton, E.K., Taylor, S.B., Aldrich, P.R. and Dutton, B.E. 2012. *Geographic Information Systems and Spatial Analysis – Part 1: Quantifying Fingerprint Patterns and Minutiae Distributions*. Abstract with Program, the 2012 American Academy of Forensic Sciences annual conference, Atlanta, Georgia.
9. Aldrich, P.R., Stanley, R.J., Hidalgo, S.C., Dutton, E.K., Dutton, B.E. and Taylor, S.B. 2012. *Geographic Information Systems and Spatial Analysis of Fingerprints: Pattern Characterization, Monte Carlo Probability Estimates and Geometric Morphometric Analysis*. Abstract with Program, the 2012 Pacific Northwest Division of the International Association for Identification annual conference, Boise, Idaho.
10. Dutton, E.K., Aldrich, P.R., Taylor, S.B., Dutton, B.E., Stanley, R.J. and Hidalgo, S.C. 2012. *Application of Spatial Statistics to Latent Print Identifications: Towards Improved Forensic Science Methodologies*. NIJ sponsored webinar: June 12, 2012 and June 21, 2012. Meeting Room: <https://rti.connectsolutions.com/r7d6kzeqqsi/>.
11. Dutton, E.K., Aldrich, P.R., Taylor, S.B., Dutton, B.E., Stanley, R.J. and Hidalgo, S.C. 2012. *Application of Spatial Statistics to Latent Print Identifications: Towards Improved Forensic Science Methodologies*. Abstract with Program, the 2012 Impression and Pattern

Evidence Symposium. *Recognize, Develop, and Implement: Building on our Foundations*. Clearwater Beach, Florida.

12. Taylor, S. B., Stanley, R.J., Dutton, E.K., Aldrich, P.R., Dutton, B.E. and Hidalgo, S.C. 2012. *Novel Use of GIS for Spatial Analysis of Fingerprint Patterns*. Presented at the 2012 Annual Meeting of the Urban and Regional Information Systems Association (URISA) GIS Pro Conference, Portland, Oregon.

Website

We developed a website for dissemination of information and research activities to the community (<http://whorl.wou.edu/>). Information posted to this website includes the original project proposal, conference presentation abstracts, and reports as well as related links to other forensic science information.